1.0
1.1
1.25
1.4
1.6
1.8
2.0
2.2
2.5
2.8
3.2
3.6
4.0
4.5
5.0
5.6
6.3
7.1
8.0
9.0

1 of 2

PNL-9000, Pt. 1
UC-408

Pacific Northwest Laboratory Annual Report for 1993 to the DOE Office of Energy Research

Part 1: Biomedical Sciences

J. F. Park and Staff

March 1994

Prepared for
the U.S. Department of Energy
under Contract DE-AC06-76RLO 1830

Pacific Northwest Laboratory
Richland, Washington 99352

Preface

This 1993 Annual Report from Pacific Northwest Laboratory (PNL) to the U.S. Department of Energy (DOE) describes research in environment and health conducted during fiscal year (FY) 1993. This year, the report consists of four parts, each in a separate volume.

The four parts of the report are oriented to particular segments of the PNL program, describing research performed for the DOE Office of Health and Environmental Research (OHER) in the Office of Energy Research. In some instances, the volumes report on research funded by other DOE components or by other governmental entities under interagency agreements. Each part consists of project reports authored by scientists from several PNL research departments, reflecting the multidisciplinary nature of the research effort.

The parts of the 1993 Annual Report are as follows:

Part 1: Biomedical Sciences	J.F. Park, Program Manager A.L. Brooks, Report Coordinator C.C. Lumetta, Editor
Part 2: Environmental Sciences	R.E. Wildung, Program Manager L.K. Grove, Editor
Part 3: Atmospheric Sciences	W.R. Barchet, Program Manager B.V. Johnston, Editor
Part 4: Physical Sciences	L.A. Braby, Program Manager S.L. Downs, Editor

Activities of the scientists whose work is described in this annual report are broader in scope than the articles indicate. PNL staff have responded to numerous requests from DOE during the year for planning, for service on various task groups, and for special assistance.

Credit for this annual report goes to the many scientists who performed the research and wrote the individual project reports, to the program managers who directed the research and coordinated the technical progress reports, to the editors who edited the individual project reports and assembled the four parts, and to Ray Baalman, editor in chief, who directed the total effort.

T. S. Tenforde
Manager, Health and Environmental Research Program

Previous Annual Reports in this series:

1951	HW-25021, HW-25709
1952	HW-27814, HW-28636
1953	HW-30437, HW-30464
1954	HW-30306, HW-33128, HW-35905, HW-35917
1955	HW-39558, HW-41315, HW-41500
1956	HW-47500
1957	HW-53500
1958	HW-59500
1959	HW-63824, HW-65500
1960	HW-69500, HW-70050
1961	HW-72500, HW-73337
1962	HW-76000, HW-77609
1963	HW-80500, HW-81746
1964	BNWL-122
1965	BNWL-280, BNWL-235, Vol. 1-4; BNWL-361
1966	BNWL-480, Vol. 1; BNWL-481, Vol. 2, Pt. 1-4
1967	BNWL-714, Vol. 1; BNWL-715, Vol. 2, Pt. 1-4
1968	BNWL-1050, Vol. 1, Pt. 1-2; BNWL-1051, Vol. 2, Pt. 1-3
1969	BNWL-1306, Vol. 1, Pt. 1-2; BNWL-1307, Vol. 2, Pt. 1-3
1970	BNWL-1550, Vol. 1, Pt. 1-2; BNWL-1551, Vol. 2, Pt. 1-2
1971	BNWL-1650, Vol. 1, Pt. 1-2; BNWL-1651, Vol. 2, Pt. 1-2
1972	BNWL-1750, Vol. 1, Pt. 1-2; BNWL-1751, Vol. 2, Pt. 1-2
1973	BNWL-1850, Pt. 1-4
1974	BNWL-1950, Pt. 1-4
1975	BNWL-2000, Pt. 1-4
1976	BNWL-2100, Pt. 1-5
1977	PNL-2500, Pt. 1-5
1978	PNL-2850, Pt. 1-5
1979	PNL-3300, Pt. 1-5
1980	PNL-3700, Pt. 1-5
1981	PNL-4100, Pt. 1-5
1982	PNL-4600, Pt. 1-5
1983	PNL-5000, Pt. 1-5
1984	PNL-5500, Pt. 1-5
1985	PNL-5750, Pt. 1-5
1986	PNL-6100, Pt. 1-5
1987	PNL-6500, Pt. 1-5
1988	PNL-6800, Pt. 1-5
1989	PNL-7200, Pt. 1-5
1990	PNL-7600, Pt. 1-5
1991	PNL-8000, Pt. 1-5
1992	PNL-8500, Pt. 1-4
1993	PNL-9000, Pt. 1-4

Foreword

This report summarizes FY 1993 progress in biological and general life sciences research programs conducted for the Department of Energy's Office of Health and Environmental Research (OHER) at Pacific Northwest Laboratory (PNL). This research provides knowledge of fundamental principles necessary to identify, understand, and anticipate the long-term health consequences of exposure to energy-related radiation and chemicals. Our emphasis is to understand the mechanisms involved in radiation- and chemically induced damage. Through this understanding, the health risks associated with exposure to effluents from energy-related technologies can be better defined, and the uncertainty associated with those risks decreased.

The sequence of this report of PNL research reflects the OHER programmatic structure. The **Biological Research** section contains reports of studies using laboratory animals, *in vitro* cell systems, and molecular biological systems. This research includes studies of the impact of radiation, radionuclides, and chemicals on biological responses at all levels of biological organization. The **General Life Sciences Research** section reports research conducted for the OHER human genome program.

Biological Research

The progress in several life-span studies in rats and dogs on the effects of inhaled radioactive materials including radon, $^{238}PuO_2$, $^{239}PuO_2$, and $^{239}Pu(NO_3)_4$ is reviewed. Recent research has produced important new information on the induction of tumors by internally deposited radiactive materials in organs other than the primary target organ (lung).

Because many of the life-span studies using experimental animals are in the late phase of completion, it is essential to ensure that we do not lose valuable data or experimental materials generated by these studies. To this end, the "National Radiobiology Archives" (NRA) project is being conducted as a comprehensive effort to gather, organize, and catalog data, documents, and tissues related to life-span radiobiology studies for future research and analyses. New developments in the NRA project also are found in this report.

The animal studies on cancer induction from radon are the core of an extensive research program. This program characterizes each step in the exposure–dose–response pathway of radon. We are combining *in vivo* and *in vitro* methods with up-to-date exposure systems and modern cytogenetic and molecular techniques to understand the mechanisms involved in each step between exposure and the induction of cancer. We also hope to reduce the uncertainty involved in extrapolating the information to risk assessment: Such improvement in basic mechanistic understanding will aid in risk assessment and extrapolation between damage produced by radon progeny in mine and home environments.

The relationship between site and type of initial DNA damage and the development of molecular changes, mutations, chromosome damage, and cell transformation contributes to an understanding of the disease process. Chemical- and radiation-effects studies are being conducted using molecular techniques to understand the sites of radiation-induced damage, the types of products produced, and the binding of carcinogenic chemicals to the DNA. The influence that primary, secondary, and tertiary DNA structure has on the induction and location of DNA damage and binding is being determined. This report includes reviews of these studies and outlines important progress as well as future directions.

General Life Sciences Research

Researchers at PNL have developed a computer information system to graphically display and manipulate the vast amounts of information in genome databases. GnomeView is an interface to data bases rather than a data repository, integrating information across databases and between different levels in the mapping hierarchy.

Laboratory-Wide Effort

Biomedical research at PNL is an interdisciplinary effort requiring scientific contributions from many research departments throughout the laboratory. Personnel in the Life Sciences Center are the principal contributors to this report.

Additional information on the PNL research efforts can be obtained by requesting reprints from the list of publications.

Contents

Biological Research

Inhaled Plutonium in Dogs

Principal Investigator: J. F. Park

Other Investigators: R. L. Buschbom, G. E. Dagle, E. S. Gilbert, G. J. Powers, C. R. Watson, and R. E. Weller

Technical Assistance: R. F. Flores, B. B. Kimsey, and B. G. Moore

These projects (Inhaled Plutonium Oxide in Dogs, Inhaled Plutonium Nitrate in Dogs) are concerned with long-term experiments to determine the life-span dose-effect relationships of inhaled $^{239}PuO_2$, $^{238}PuO_2$, and $^{239}Pu(NO_3)_4$ in beagles. This report describes dose-effect relationships in the tracheobronchial lymph nodes of beagle dogs receiving a single exposure of $^{239}PuO_2$ aerosols to obtain dose-level groups of 20 dogs with mean initial lung depositions (ILDs) of 0.12, 0.69, 2.7, 11, 41, and 213 kBq. Lung tumors were the primary plutonium-exposure-related causes of death in dogs with ILDs $\geq$ 0.82 kBq. Fifty-one of 116 plutonium exposed dogs had lung tumors; however, tumors directly attributable to plutonium deposition in the tracheobronchial lymph nodes were not observed. Although plutonium-induced tumors of the thoracic lymph nodes were not detected, marked lymph node atrophy and lymphopenia, indicating damage to the hemolymphatic system, were observed in dogs with ILDs $\geq$ 0.82 kBq as compared to control dogs. In the lowest dose-level group exhibiting lymphopenia, lymphocyte concentrations were first observed to be lower in exposed animals than those of controls 3 years after exposure, 10 years earlier than the median survival time of the group. At 3 years after exposure, the mean cumulative dose to the tracheobronchial lymph nodes of dogs with mean ILDs of 0.69 kBq was 4.8 Gy, the mean dose rate was 2.92 Gy/yr, and the concentration of plutonium in the tracheobronchial lymph nodes was 133 Bq/g. There was a direct relationship between plutonium body burden and activity in the testes, but no relationship existed between plutonium activity in the testes and the occurrence of testicular neoplasia in male dogs. At long times after inhalation, plutonium in the testes was between 0.0001% and 0.03% of projected ILD, depending on the form of plutonium. Those percentages are similar to those previously reported for dogs, primates, and human subjects.

To determine the life-span dose-effect relationships of inhaled plutonium, 18-month-old beagle dogs were exposed to aerosols of $^{239}PuO_2$, $^{238}PuO_2$, or $^{239}Pu(NO_3)_4$. The production of the aerosol, the aerosol exposures, and chemical characterization of the aerosols have been published previously (Dagle *et al.* 1993; Park *et al.* 1993). The experimental design of the studies, including the aerosol form, number of animals, and initial deposition can be found in Table 1 for $^{239}PuO_2$, Table 2 for $^{238}PuO_2$, and Table 3 for $^{239}Pu(NO_3)_4$. The *Pacific Northwest Laboratory Annual Report for 1989 to the DOE Office of Energy Research, Part 1*, summarizes the results of the $^{239}PuO_2$ study, and the results of the $^{238}PuO_2$ study are summarized in the *Annual Report for 1990*. The Appendix at the back of this volume provides mortality information for the dogs assigned to the $^{239}Pu(NO_3)_4$ study. The last dog in the $^{239}Pu(NO_3)_4$ study died in 1992. Lung tumors were the primary $^{239}PuO_2$-related cause of death in dose-level groups that had

TABLE 1. Life-Span Dose-Effect Studies with Inhaled $^{239}PuO_2$ in Beagles[a]

Exposure-Level	Number of Dogs		Initial Lung Deposition[b]		
Group	Male	Female	kBq[c]	Bq/g Lung[c]	
Control	10	10	0	0	
1	10	11	0.12 ± 0.05	0.93 ±	0.39
2	11	11	0.69 ± 0.14	6.2 ±	1.3
3	11	10	2.7 ± 0.05	23 ±	4
4	12	12	11 ± 2	95 ±	17
5	10	10	41 ± 6	349 ±	46
6	3	5	213 ± 120	2130 ±	1160
	67	69			

(a) Exposed in 1970 and 1971.
(b) Estimated from external thorax counts at 2 and 4 weeks after exposure, and from estimated lung weights (0.011 x body weight).
(c) Mean ± 95% confidence intervals around mean.

TABLE 2. Life-Span Dose-Effect Studies with Inhaled $^{238}PuO_2$ in Beagles[a]

Exposure-Level	Number of Dogs		Initial Lung Deposition[b]		
Group	Male	Female	kBq[c]	Bq/g Lung[c]	
Control	10	10	0	0	
1	10	10	0.061 ± 0.036	0.48 ±	0.28
2	11	10	0.67 ± 0.12	5.9 ±	1.2
3	12	10	2.9 ± 0.4	24 ±	3
4	10	10	13 ± 3	106 ±	21
5	10	10	51 ± 10	403 ±	68
6	7	6	192 ± 51	1651 ±	443
	70	66			

(a) Exposed in 1973 and 1974.
(b) Estimated from external thorax counts at 2 and 4 weeks after exposure, and from estimated lung weights (0.011 x body weight).
(c) Mean ± 95% confidence intervals around mean.

TABLE 3. Life-Span Dose-Effect Studies with Inhaled $^{239}PuO_2(NO_3)_4$ in Beagles[a]

Exposure-Level	Number of Dogs		Initial Lung Deposition[b]		
Group	Male	Female	kBq[c]	Bq/g Lung[c]	
Control	10	10	0	0	
1	10	10	0.062 ± 0.033	0.48 ±	0.26
2	10	10	0.32 ± 0.6	2.6 ±	0.6
3	10	10	2.2 ± 0.31	9 ±	4
4	10	10	11 ± 1	91 ±	15
5	10	10	63 ± 11	518 ±	106
6	6	3	2202 ± 84	1722 ±	747
	66	63			

(a) Exposed in 1976 and 1977.
(b) Estimated from external thorax counts at 2 and 4 weeks after exposure, and from estimated lung weights (0.011 x body weight).
(c) Mean ± 95% confidence intervals around mean.

initial lung depositions (ILDs) of 23 Bq/g of lung or greater. This year, because lymphopenia is an early deterministic effect of inhaled $^{239}PuO_2$, we focused on evaluating dose-effect relationships of inhaled $^{239}PuO_2$ deposited in the tracheobronchial lymph nodes, and on the effects of internally deposited plutonium on the risk of testicular cancer in male beagle dogs exposed to inhaled aerosols of $^{239}PuO_2$, $^{238}PuO_2$, and $^{239}Pu(NO_3)_4$.

Dose to Tracheobronchial Lymph Nodes from Inhaled $^{239}PuO_2$

Radiation doses to the thoracic lymph nodes were estimated by the following method: Plutonium content in the thoracic lymph nodes at the time of death for each dog was expressed as percent ILD, determined by *in vivo* counting to obtain a thoracic lymph node retention function fitted by nonlinear regression. The thoracic lymph node retention equation is

$$y = 42.6\,(1-e^{-0.00044t})$$

where y = percent ILD in the thoracic lymph nodes
t = days after exposure.

Cumulative radiation dose to the thoracic lymph nodes was estimated by integrating the thoracic lymph node retention function and multiplying by the appropriate factors. The equation used to calculate the cumulative radiation dose is

$$D = [(1.38 \times 10^{-5})\,(5.15)\,(L)/(W)]\{0.426[t+(e^{-0.00044t}-1)/0.00044]\}$$

where D = dose in Gy
1.38×10^{-5} = conversion factor for converting Bq to Gy
5.15 = alpha energy for ^{239}Pu in MeV
L = ILD in Bq
W = lymph node weight in grams
= (0.000098) (body weight at exposure in grams)
t = days over which the dose was accumulated.

Cumulative radiation dose to the tracheobronchial lymph nodes continued to increase throughout the lifetime of the dog.

Dose rates were estimated instantaneously after exposure when lymphopenic events were observed. Those dose rates were estimated by taking the derivative of the cumulative dose equation and evaluating this derivative at the day the increase occurred. The equation used to calculate the dose rate is

$$DR = [(1.38 \times 10^{-5})\,(5.15)\,(L)/(W)]\,[0.426(1-e^{-0.00044x})]$$

where DR = dose rate in Gy/day
1.38×10^{-5} = conversion factor for converting Bq to Gy
5.15 = alpha energy for ^{239}Pu in MeV
L = ILD in Bq
W = lymph node weight in grams
= (0.000098) (body weight at exposure in grams)
x = days when lymphopenic event was observed.

For the fit for the thoracic lymph node retention function, we used the data from 128 dogs exposed to $^{239}PuO_2$. The ILD was estimated by *in vivo* whole-body counting and the lymph node retention determined at sacrifice. In 19 cases, the final body burden was higher than ILD; in these cases, final body burden was used in place of the ILD for the calculation. Figure 1 shows the thoracic lymph node retention function and the observed values.

At the four highest exposure levels ($> \approx 23$ Bq/g), the tracheobronchial lymph nodes were essentially replaced with scar tissue in those dogs that died or were euthanatized more than one year after exposure. The lymphoid tissue was uniformly obliterated by scar tissue in each of the three tracheobronchial lymph nodes at the two highest exposure levels ($> \approx 345$ Bq/g); there were only very small foci of lymphocytes

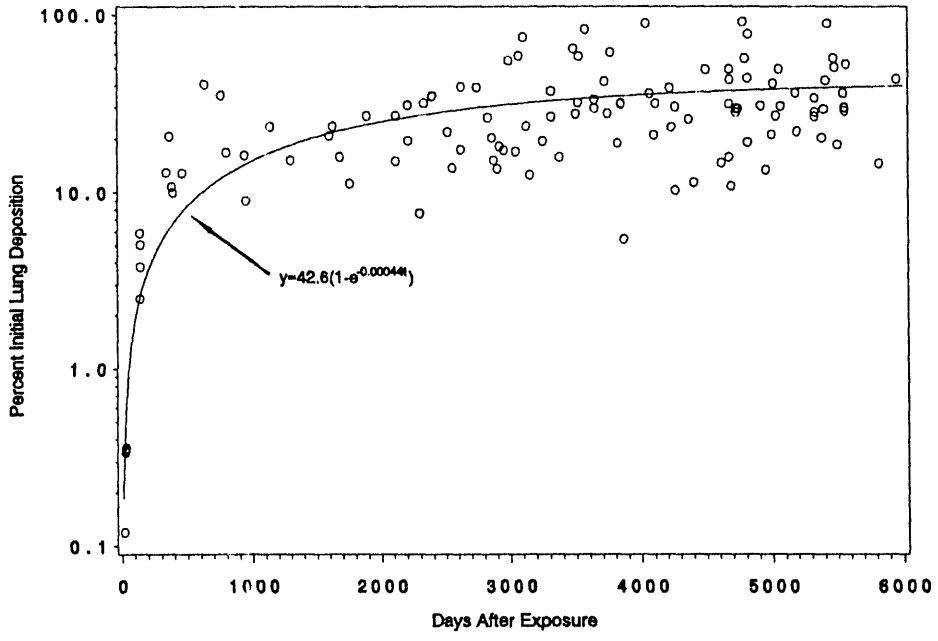

FIGURE 1. Thoracic Lymph Node Retention of Inhaled $^{239}PuO_2$ Determined by [(final lymph node burden of plutonium)/(initial lung deposition of plutonium)] x 100

in the capsular areas of a few tracheobronchial lymph nodes in dogs that died early or were assigned to an exposure level of ≈ 95 Bq/g. The center of the scar tissue tended to be hypocellular and associated with yellow pigmentation that was believed to represent a mixture of inhaled particulates (including plutonium) and hemosiderin. Autoradiographs showed heavy concentrations of alpha stars associated with yellow pigment in the center of the scar tissue.

Marked to extreme scar tissue was present in one or more tracheobronchial lymph nodes from 15 dogs with ILDs ≈ 23 Bg/g, from 4 dogs with burdens projected to be ≈ 6.2 Bq/g, and from 1 dog with ILDs < 1. The scar tissue was similar to that found at the higher exposure levels, and was associated with lympoid atrophy, pigment deposition, and autoradiographic evidence of alpha stars. Very small to moderate amounts of scar tissue were present in one or more tracheobronchial lymph nodes in the remaining dogs from the ≈ 23-Bq/g level, in all but two dogs from the ≈ 6.2-Bq/g level, and in six dogs from those with exposure levels < 1. Autoradiographs showed alpha activity in these areas of scar tissue, and a similar incidence of lymphoid atrophy. The average severity and incidence of pigment in tracheobronchial lymph nodes tended to remain constant in all exposure levels, and in the control group. No tumors were associated with any of the tracheobronchial lymph nodes in these studies.

Hematologic Effects

No deaths were associated with tracheobronchial lymph node damage, although 58% of the dogs in this study showed hematologic evidence of significant lymphopenia. Lymphopenia, indicating hemolymphatic damage, was observed in all but the lowest dose-level group.

Blood samples from fasted dogs were collected every three to four months, during the lives of the animals, from the external jugular vein using potassium EDTA as the anticoagulant. Leuko-

cyte, erythrocyte, and hemoglobin concentrations, volume of packed red cells, and red cell corpuscular indices were determined using a Coulter Counter model S. Smears for leukocyte differential cell counts were made on a Platt blood-film centrifuge, stained with Wright-Giemsa stain, and a differential count was made on the basis of a minimum of 200 leukocytes counted by two technologists.

Hematologic variables for all exposed dogs were compared to those of the cohort control group. Lymphocyte values for a lifetime blood parameter for the control dogs were determined from blood samples usually drawn at irregular time intervals; the time intervals generally varied from dog to dog. The technique of smoothing by splines was used to deal with the problem of irregular time intervals. Monthly values for each parameter were estimated by fitting a spline function to the observed data. Using these spline-smoothed values for each parameter, percentiles (5th, 10th, 25th, 50th, 75th, 90th, and 95th) were calculated for each month of age in the controls. Individual values between the 5th and 95th percentiles were defined as normal for any given age. A parameter baseline value for each control dog was determined by averaging the values of the parameters for months 17, 18, and 19. The baseline value was subtracted from the monthly values, divided by the baseline value, and multiplied by 100 to calculate the percent change for each month. Percent-change percentiles were calculated for each month of age. For control dogs, any percent change in blood lymphocytes between the 5th and 95th percentiles was defined as normal (Figure 2).

The normal range of percent changes was used to determine when a blood lymphocyte parameter for an exposed dog was abnormal. The percent change in a parameter value was calculated at each age that a blood sample was taken from an exposed dog. Percent changes in a parameter for an exposed dog were calculated by subtracting the dog's parameter baseline value

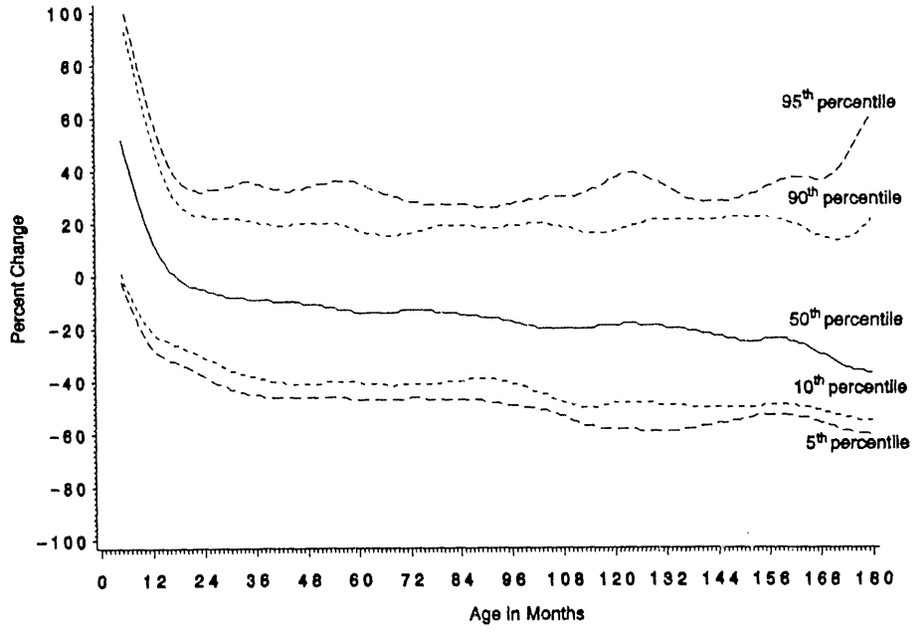

FIGURE 2. Graph Showing Smoothed Percentiles of Lymphocytes by Age in Control Dogs

from the dog's parameter value, dividing by the dog's parameter baseline value, and multiplying by 100. Parameter baseline value for an exposed dog was calculated by averaging the values of the parameter one month before exposure, at exposure, and one month after exposure. The percent change at each age was compared to the normal percent-change range at that age. If the percent change was outside the normal range for two consecutive measurements, then the parameter was classified as abnormal at the age of the first abnormal value. The representative pattern of intermittent lymphopenia in a dog exposed to $^{239}PuO_2$ illustrated in Figure 3 shows that an abnormal parameter was classified as normal again when two consecutive values were within the normal range. Using this method, we were able to determine the time after exposure when values for a parameter became abnormal with respect to the control dogs, and when, if at all, the values returned to normal.

Significant hematologic manifestations of the dose from inhaled $^{239}PuO_2$ were restricted primarily to such effects on lymphocytes, with the exception of the highest dose-level dogs, which demonstrated a modest neutropenia. Sixty-seven of 116 dogs (58%) enrolled in this study exhibited some degree of significant lymphopenia during their lives. Although there was considerable individual-to-individual variability, when examined on a case-by-case basis, exposed dogs could be assigned to one of three groups: 1) dogs that never showed lymphopenia; 2) dogs that showed intermittent lymphopenia; and 3) dogs that consistently showed lymphopenia. Forty-nine dogs never showed lymphopenia, 38 dogs showed intermittent lymphopenia, and 29 dogs were classified as consistently lymphopenic. Dogs categorized as consistently lymphopenic were characterized by percent changes outside the normal range for two consecutive measurements and failure to achieve two consecutive values

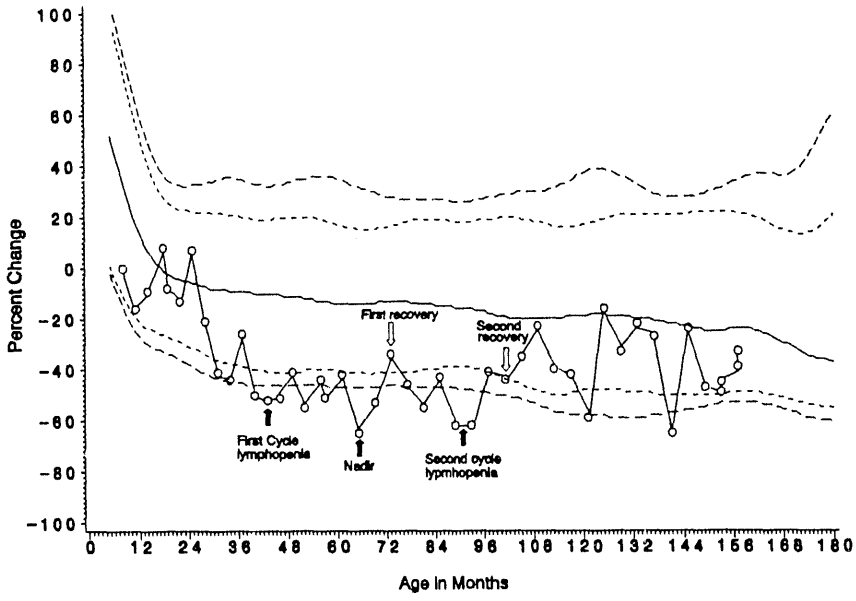

FIGURE 3. Representative Pattern of Intermittent Lymphopenia in a Dog Exposed to $^{239}PuO_2$

within the normal range for the remainder of their lives. Animals with intermittent lymphopenia showed irregular cycles of percent change outside the normal range for two consecutive measurements, followed by a return to normal characterized by two consecutive values within the normal range. Nonlymphopenic dogs did not exhibit percent changes outside the normal range for two consecutive measurements at any time during their lives. Summary statistics for the three groups of dogs are presented in Table 4. The nonparametric Wilcoxon Two-Sample Test indicated that significant differences existed between lymphopenic dogs and intermittently lymphopenic dogs with regard to ILD, time-to-effect, time-to-nadir, and degree of lymphopenia. Linear regression analysis revealed moderate correlation between reduction in lymphocyte values and ILD, both in magnitude and time of appearance after exposure (Table 5). Summary statistics for dose and dose rates for dogs with lymphopenia and intermittent lymphopenia are given in Table 6. Application of the nonparametric Wilcoxon Two-Sample Test to these dose and dose-rate data showed that significant differences existed between the two groups of lymphopenic dogs.

Lymphopenia was observed in dose-level groups with a cumulative dose to the tracheobronchial lymph nodes of 4.8 Gy and higher (Table 7). Cumulative radiation dose to the tracheobronchial lymph nodes for the mean ILD for each dose-level group with lymphopenia was calculated to the time after exposure for each dose-level group when the median lymphocyte values were first observed to fall outside the reference range of the control group at the same time after exposure (Table 7). At a dose level of

TABLE 4. Summary Statistics of Lymphopenia Data for 119 Beagles Exposed to $^{239}PuO_2$ By Inhalation

Variable	Nonlymphopenic (n = 49) Mean ± SE	Intermittently Lymphopenic[a] (n = 38) Mean ± SE	Lymphopenic[b] (n = 29) Mean ± SE
ILD	0.8 ± 0.15	12.6 ± 2.15	74.4 ± 20.15
T_1 (months)	no	21.9 ± 2.9	10.8 ± 1.6
L_1 (cells μl)	no	1.58 ± 0.05	1.33 ± 0.06
T_N (months)	no	41.7 ± 3.6	29.5 ± 3.6
L_N (cells μl)	no	1.21 ± 0.05	0.81 ± 0.04
C_N (%)	no	62.3 ± 1.3	69.3 ± 1.7
T_2 (months)	no	73.6 ± 4.7	no
L_2 (cells/μl)	no	1.29 ± 0.05	no

(a, b) Means for all parameters are significantly different at $P \leq 0.05$.
No No observation.
ILD Initial lung deposition.
T_1 Time to first effect (months post-exposure).
L_1 Lymphocyte count at time of first effect (cells x $10^3/\mu l$).
T_N Time to lowest lymphocyte count (nadir).
L_N Lymphocyte count at nadir (cells x $10^3/\mu l$).
C_N Percent change in lymphocyte count at nadir.
T_2 Time to second cycle of lymphopenia.
L_2 Lymphocyte count at time of second cycle (cells x $10^3/\mu l$).

TABLE 5. Correlation Coefficients of Initial Lung Burden on Time-Course and Lymphocyte Concentrations in Beagles Exposed to $^{239}PuO_2$ by Inhalation

	Lymphopenic Dogs			Intermittently Lymphopenic Dogs		
Variable	T_1	T_N	L_N	T_1	T_N	T_2
LILD	-0.63	-0.79	-0.43	-0.56	-0.60	-0.36

LILD = log - initial lung deposition (nCi)
T_1 = time to first effect
T_N = time to lowest lymphocyte count (nadir)
L_N = lymphocyte count at nadir (cells x $10^3/\mu$)
T_2 = time to second cycle of lymphopenia.

TABLE 6. Summary Statistics of Dose and Dose-Rate Data for 66 Beagles with Lymphopenia Due to Inhaled $^{239}PuO_2$

	Lymphopenic (n = 28)				Intermittently Lymphopenic (n = 38)			
Variable	Mean	±	SE	Median	Mean	±	SE	Median
D_1 (Gy)	23.9	±	6.8[a]	16.4	19.6	±	4.6	9.4
DR_1 (Gy/day)	0.16	±	0.03[a]	0.15	0.06	±	0.01	0.05
D_N (Gy)	149.1	±	20.3[a]	112.0	79.5	±	19.4	50.5
DR_N (Gy/day)	0.42	±	0.07[a]	0.34	0.12	±	0.02	0.09
D_2 (Gy)		no			230.0	±	41.7	133.4
DR_2 (Gy/day)		no			0.19	±	0.04	0.13

(a) Means significantly different, $P \leq 0.05$.
no = no observation.
D_1 = cumulative radiation dose at first effect.
DR_1 = dose rate at first effect.
D_N = cumulative dose at nadir.
DR_N = dose rate at nadir.
D_2 = cumulative dose at second cycle.
DR_2 = dose rate at second cycle.

≈ 0.69 kBq, lymphopenia was not observed until 3 years after exposure, 10 years earlier than the mean survival time of the group. The dose rate to the tracheobronchial lymph nodes when lymphocyte concentrations first decreased was 2.92 Gy/yr or higher for all dose-level groups but the lowest (see Table 7). The mean plutonium concentration in the tracheobronchial lymph nodes at time of death for these dose-level groups was ≥ 133 Bq/g per lymph node; these animals developed lymphopenia at some point in their lives.

Testicular Neoplasia

Plutonium Activity in the Testes

The amount of plutonium translocated to the testes was determined radiochemically by liquid-scintillation alpha counting using a previously described method. There was a direct correlation between ILD (Bq) and the amount of plutonium in the testes (Bq/g) (Figure 4). The slope of the relationship was 0.35, 0.89, and 0.91 for $^{239}PuO_2$, $^{238}PuO_2$, and $^{239}Pu(NO_3)_4$,

TABLE 7. Frequency of Lymphopenia in Dogs Exposed to $^{239}PuO_2$

Exposure Group	No. Dogs	kBq	Mos. PE[a]	L[b]	I[c]	N[d]	Total L[e]	Total N	Cum. Dose (Gy)	Dose Rate (Gy/day)
1	21	0.12	149	-	-	21	-	21	8.8	0.003
2	22	0.69	153	-	5	17	5	17	54.9	0.018
3	21	2.73	16	3	8	10	11	10	3.8	0.015
4	24	11.50	13	4	19	1	23	1	10.7	0.053
5	20	40.88	7	14	6	-	20	-	11.4	0.106
6	8	213.30	4	8	-	-	8	-	21.8	0.356
Total	116			29	38	49	67	49		

(a) Post exposure.
(b) Lymphopenic.
(c) Intermittently lymphopenic.
(d) Nonlymphopenic.
(e) Includes lymphopenic and intermittently lymphopenic.

respectively. At long times after inhalation, plutonium in the testes was between 0.0001% and 0.03% of projected ILD, depending on the physicochemical form of plutonium (Figure 5). Those percentages are similar to those previously reported in dogs, primates, and human subjects.

Biological Effects

Male dogs, both control and plutonium-exposed, that were evaluated for the risk of testicular cancer had neoplasms diagnosed either before death by histologic examination of testes that were surgically removed due to the presence of a palpable mass, or following death or euthanasia of the animal for humane reasons. Prior to surgical extirpation of affected testes or euthanasia, a blood sample was obtained from animals, following an overnight fast, for measurement of testosterone and estradiol 17-beta concentrations. The dogs were euthanatized by exsanguination via carotid artery catheterization following anesthesia with pentobarbital sodium given intravenously. The prostate, testes, and some other organs were removed, and the excess tissue was trimmed away and examined, measured, weighed, and fixed in 10% neutral buffered formalin. Tumor volumes were calculated using the following formula:

$$V = 4.18\ r^3$$

where V = volume in cm^3
r = radius of the lesion.

Five-micrometer sections of both neoplastic and adjacent testicular tissue were cut and stained with hematoxylin and eosin according to standard histologic techniques. All tissues utilized in this study were examined by one pathologist. The criteria for histopathologic diagnosis were adapted from Nielsen and Lein (1974) and Moulton (1978).

One hundred sixty-six cases of testicular neoplasia occurred among 105 dogs that were from 7.5 to 17.7 years of age at the time of diagnosis. There was no relationship between plutonium body burden or activity in the testes and the occurrence of testicular neoplasia. The 166 testicular neoplasias comprised 113 interstitial

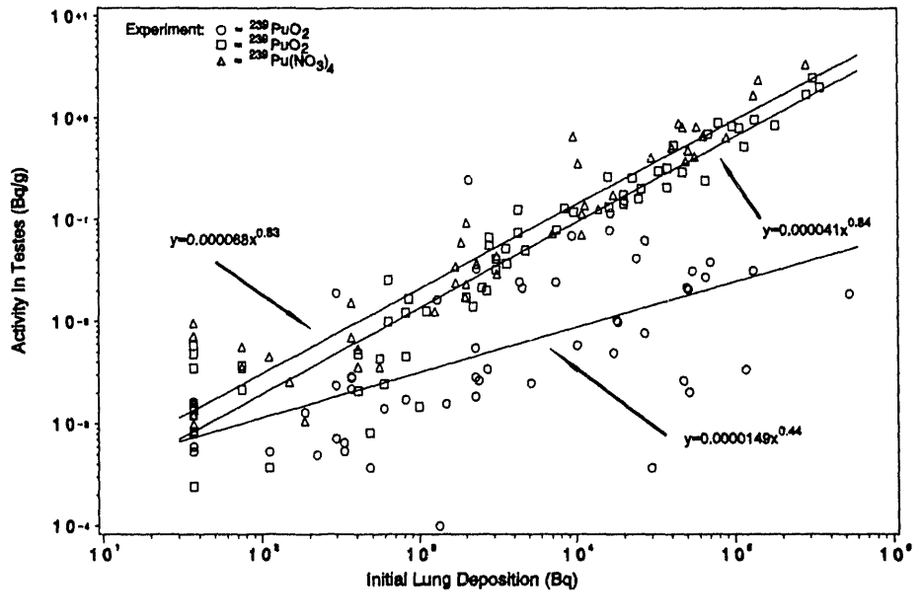

FIGURE 4. Relationship Between Plutonium Activity in the Testes (Bq/g testes) and Initial Lung Deposition (Bq)

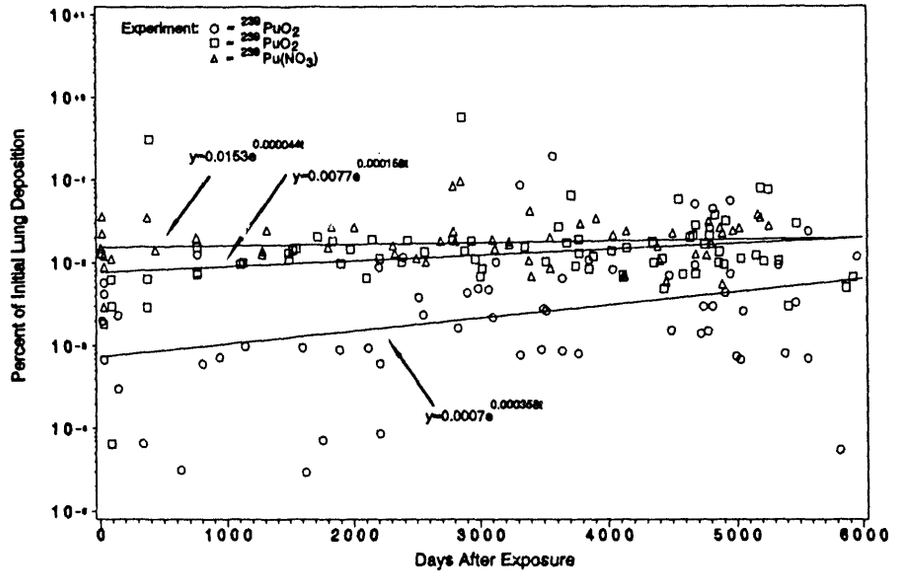

FIGURE 5. Testicular Retention of Inhaled Plutonium, Determined by [(final testes burden of plutonium)/(initial lung deposition of plutonium)] x 100, as a Function of Time After Inhalation

beta concentrations, and serum testosterone-to-estradiol ratio were evaluated in 39 dogs with testicular neoplasms and in 5 clinically normal, sexually intact, age-matched cohorts. Serum hormone concentrations did not differ significantly among tumor types or between dogs with neoplasms and age-matched cohorts, implying that androgen production by the testes is not reduced by prolonged exposure to alpha-particle irradiation.

Although the incidence of testicular neoplasia is higher in the dog than in any other species, this study failed to demonstrate any statistically meaningful association between internal deposition of plutonium and testicular neoplasia over the life span of these animals. Based on these observations in an animal model, it could be inferred that, in human subjects, the risk of testicular cancer or genetic damage from internally deposited plutonium is negligible, despite the long retention periods for plutonium in the testes.

References

Dagle, G.E., R.R. Adee, R.L. Buschbom, K.M. Gideon, E.S. Gilbert, G.J. Powers, H.A. Ragan, C.O. Romsos, S.K. Smith, C.R. Watson, and R.E. Weller. 1993. Inhaled plutonium nitrate in dogs. In: *Pacific Northwest Laboratory Annual Report for 1992 to the DOE Office of Energy Research, Part 1, Biomedical Sciences,* pp. 9-15. PNL-8500 Pt. 1, Pacific Northwest Laboratory, Richland, Washington.

Moulton, J.E. 1978. Tumors of the genital system. In: *Tumors in Domestic Animals*, 2nd edition, J.E. Moulton, ed., pp. 311-345. University of California Press, Berkeley, California.

Nielsen, S.W., and D.H. Lein. 1974. Tumors of the testis. *Bull. WHO* 50:71-78.

Park, J.F., R.L. Buschbom, G.E. Dagle, E.S. Gilbert, G.J. Powers, C.R. Watson, and R.E. Weller. 1993. Inhaled plutonium oxide in dogs. In: *Pacific Northwest Laboratory Annual Report for 1992 to the DOE Office of Energy Research, Part 1, Biomedical Sciences,* pp. 1-7. PNL-8500 Pt. 1, Pacific Northwest Laboratory, Richland, Washington.

National Radiobiology Archives

Principal Investigator: C. R. Watson

Other Investigators: S. K. Smith, E. K. Ligotke, J. C. Prather, L.G. Smith, and M. T. Karagianes

The National Radiobiology Archives (NRA) project is a comprehensive effort to gather, organize, and catalog data, documents, and tissues related to completed radiobiology studies. This archiving activity will provide future researchers with information for statistical analyses to compare results of these and other studies. The NRA also will provide materials for application of advanced molecular biology techniques to address questions, such as those related to DNA modification, that could not have been considered when these studies were performed.

Many investigations have been conducted into the biological effects of ionizing radiation. The focus has been on understanding the nature of human health effects and on quantifying dose-response relationships. When acute effects of large doses had been adequately characterized, attention shifted to effects of lower doses and lower dose rates. This focus led to initiation of life-span studies of experimental animals in several laboratories supported by the US Atomic Energy Commission (AEC), now the Department of Energy (DOE). As DOE radiobiology studies are completed, the National Radiobiology Archives (NRA) will continue to integrate and preserve this unique body of information and materials, and will continue to encourage and simplify its use.

The NRA project concentrated initially on studies of beagle dogs exposed to ionizing radiation at five DOE-supported laboratories. The project now includes similar studies using other species and at other laboratories. Three major activities are associated with this project:

1. NRA implements an interlaboratory computerized *information system* containing a summarized dose-and-effects database, a collection inventory database, and a bibliographic database. During the past year, database structures were redesigned to utilize an upgrade in database management system software. The information system now includes records from nine laboratories on approximately 7000 beagle dogs (Table 1), 30,000 mice, and more than 200 nonhuman primates. An introduction to the system is available on DOS diskette.

2. NRA establishes a *document archives* of research materials such as logbooks, clinical notes, radiographic films, and pathologists' observations. The first major collection of documents and radiographs was donated by the University of California at Davis (UC Davis).

3. NRA establishes a *specimen archives* for research materials such as tissue samples or histopathology blocks and slides. Tissue specimens, histopathology blocks and slides, serial radiographs, and extensive clinical records from more than 1000 dogs from UC Davis are organized and available. In addition, two groups of investigators have harvested brain specimens from selected aged dogs to analyze for indicators of Alzheimer's disease.

TABLE 1. Major Life-Span Beagle Studies Being Incorporated into the National Radiobiology Archives

NRA Study ID[a]	Dates of Exposures	Description of Study	Number of Life-Span Animals
1-1	1951-1974	^{239}Pu, IV injection	285
1-2	1953-1970	^{226}Ra, IV injection	164
1-3	1954-1963	^{228}Ra, IV injection	89
1-4	1954-1963	^{228}Th, IV injection	94
1-5	1955-1966	^{90}Sr, IV injection	99
1-6	1966-1975	^{241}Am, IV injection	117
1-7	1971-1974	^{249}Cf, IV injection	38
1-8	1971-1973	^{252}Cf, IV injection	35
1-9	1972-1978	^{239}Pu, IV injection (juvenile)	75
1-10	1973	^{253}Es, IV injection	5
1-11	1975-1978	^{239}Pu, IV injection (aged)	34
1-12	1975-1978	^{226}Ra, IV injection (juvenile)	53
1-13	1975-1980	^{226}Ra, IV injection (aged)	33
1-14	1977-1979	^{224}Ra, IV injection (multiple)	128
2-1	1952-1958	X ray, whole body (fractionated)	360
2-2	1961-1969	^{90}Sr, ingested (*in utero* to 540 days)	483
2-3	1964-1969	^{90}Sr, IV injection	45
2-4	1964-1969	^{226}Ra, IV injection (multiple)	336
3-1	1956	^{90}Sr, Transplacental	53
3-2	1957	^{90}Sr, SC injection (multiple, various ages)	98
3-3	1960-1964	^{144}Ce, IV injection	49
3-4	1961-1963	^{137}Cs, IV injection	65
3-5	1968-1978	Gamma ray, whole body (continuous to death)	311
3-6	1968-1977	Gamma ray, whole body (continuous to predetermined dose)	343
4-1	1959-1962	$^{239}PuO_2$, Inhalation	35
4-2	1967	$^{238}PuO_2$, Inhalation	22
4-3	1970-1972	$^{239}PuO_2$, Inhalation	136
4-4	1972-1975	$^{238}PuO_2$, Inhalation	136
4-5	1975-1977	$^{239}Pu(NO_3)_4$, Inhalation	148
5-1	1965-1967	$^{90}SrCl_2$, Inhalation	63
5-2	1966-1967	$^{144}CeCl_3$, Inhalation	70
5-3	1966-1967	$^{91}YCl_3$, Inhalation	54
5-4	1967-1971	^{144}Ce (FAP)[b], Inhalation	126
5-5	1968-1969	$^{137}CsCl$, IV injection	66
5-6	1969-1971	^{90}Y (FAP), Inhalation	101
5-7	1970-1971	^{91}Y (FAP), Inhalation	108
5-8	1970-1974	^{90}Sr (FAP), Inhalation	124
5-9	1972-1978	^{144}Ce (FAP), Inhalation (juvenile)	54
5-10	1972-1975	^{144}Ce (FAP), Inhalation (aged)	54
5-11	1972-1975	^{144}Ce (FAP), Inhalation (multiple)	36
5-12	1973-1976	$^{238}PuO_2$, Inhalation (3.0 μm)	84
5-13	1974-1976	$^{238}PuO_2$, Inhalation (1.5 μm)	84
5-14	1977-1979	$^{239}PuO_2$, Inhalation (0.75 μm)	60
5-15	1977-1979	$^{239}PuO_2$, Inhalation (1.5 μm)	108
5-16	1977-1979	$^{239}PuO_2$, Inhalation (3.0 μm)	83
5-17	1977-1978	$^{239}PuO_2$, Inhalation (multiple, 0.75 μm)	72
5-18	1979-1983	$^{239}PuO_2$, Inhalation (juvenile, 1.5 μm)	108
5-19	1979-1982	$^{239}PuO_2$, Inhalation (aged, 1.5 μm)	60
8-3	1967-1973	Gamma ray, whole body, F_3 and F_4 generations	1680
Total	1952-1983		7061

(a) Code designations indicate laboratory and study numbers; 3-5, for example, is a code that indicates laboratory 3 (ANL), study 5. Laboratory codes: 1, U of Utah; 2, UC Davis; 3, ANL; 4, PNL; 5, ITRI; 8 CSU. Study numbers: arbitrarily assigned by NRA.

(b) FAP: radionuclide was adsorbed to an insoluble fused aluminosilicate vector aerosol.

Radiobiology Studies

Nearly 40 years ago, the US AEC began life-span radiation-effect studies in beagles; these closely related experiments are now coming to fruition. The studies, conducted at the University of Utah (U of Utah), UC Davis, Argonne National Laboratory (ANL), Pacific Northwest Laboratory (PNL), and the Inhalation Toxicology Research Institute (ITRI) were summarized by Roy Thompson (1989). His book, *Life-Span Effects of Ionizing Radiation in the Beagle Dog*, became the initial focus of NRA activities. Another multigeneration study in beagle dogs was conducted by the Food and Drug Administration at Colorado State University (CSU). Information from CSU about effects of gamma rays also is being included in the NRA. There also have been many life-span studies of rodents, notably those conducted at Oak Ridge National Laboratory (ORNL), ANL, Brookhaven National Laboratory (BNL), and PNL. In addition, a series of long-term metabolism studies in nonhuman primates were initiated at the University of Rochester (UR) and continued at Lawrence Berkeley Laboratory (LBL).

The beagle experiments currently available from NRA are listed in Table 1, showing the NRA laboratory-study code, the dates of animal exposure, the nature of exposures (including duration and frequency), and the number of animals held for life-span observation. Table 2 summarizes similar information about rodent and nonhuman primate studies. Information is available on 7061 life-span beagles, 32,226 mice, and 236 nonhuman primates.

As previously noted, three tasks are associated with integrating and preserving information from these studies. The computerized

TABLE 2. Major Life-Span Studies Being Incorporated into the National Radiobiology Archives

NRA Study ID[a]	Dates of Exposures	Description of Study	Number of Life-Span Animals
Mice:			
7-1	1977	Gamma ray, single exposure at 10 wk, BALB/c & RFM *females*	4,728
7-2	1987	Gamma ray, single exposure at 10 wk, C3Hf & C57LB/6, both sexes	6,037
7-3	<1979	^{137}Cs, gamma rays, *single exposure* at 10 wk, RFM, both sexes	19,200
9-1	1982-1987	X or gamma rays, fractionated, various ages, C57BL/6 & CBA/Ca males	3,261
9-2	1986-1989	Low dose neutron leukemogenesis	
Total	1977-1987		32,226
Nonhuman Primates:			
6-0		Controls	43
6-1	1964-1982	^{90}Sr	89
6-2	1973-1986	^{238}Pu	27
6-3	1980-1982	^{241}Am	30
6-4	1986-1986	^{237}Np	2
6-5	1976	^{237}Pu	1
Total	1964-1986		192

(a) Laboratory codes: 6, LBL; 7, ORNL; 9, BNL. Study numbers: *arbitrarily* assigned by NRA.

information system provides electronic access to summary data on each animal, to document and specimen collection catalogs, and to bibliographic citations about the studies; the *document archives* house and preserve nonbiological materials; and the *specimen archives* house and preserve biological materials.

Advisory Committee

The NRA is guided by the National Radiobiology Archives Advisory Committee (NRAAC) consisting of five external advisors: Stephen A. Benjamin, CSU (dog studies); J. A. Louis Dubeau, University of Southern California (molecular biology); Kenneth L. Jackson, University of Washington (radiobiology); Elizabeth Sandager, Peabody Museum (archivist); and Philip R. Watson, Oregon State University (databases).

The committee also includes the following nine participating (or internal) advisors: Bruce B. Boecker, ITRI; Ronald E. Filipy, Washington State University, Tri-Cities; David Thomassen, DOE; Thomas E. Fritz, ANL; Scott C. Miller, U of Utah; James F. Park, PNL; Otto G. Raabe, UC Davis; Roy C. Thompson, PNL, and Michael J. Fry, ORNL.

Information System

Computer database technology is essential to integrating this broad and diverse collection of information. The NRA is developing several interrelated databases, each of which follows the relational model. There are three major databases: the dose-effects summary, the collection inventory, and the bibliography. These systems are on IBM-compatible PC systems at PNL using the Paradox database management system.

Dose-Effects Summary. The computerized summary database contains dose to and effect on each significant tissue in each animal. The summary database has six major tables:

LAB:	describing each laboratory
STUDY:	describing each study (as shown in Tables 1 and 2)
GROUP:	describing groups of animals within each study
ANIMAL:	summarizing each animal
TEFFECT:	effect (and diagnosis dates) observed in each significant tissue category
TDOSE:	dose to each significant tissue category at diagnosis dates in TEFFECT.

The summary database also includes laboratory-specific supporting tables for information such as serial hematological determinations or clinical observations. Progress toward populating the summary database is shown in Table 3.

The TEFFECT summary table is based on standardization of clinicians' and pathologists' terminology through SNODOG, an adaptation of the Systematized Nomenclature of Medicine (SNOMED). This year, two documents were published describing the SNODOG glossary and the frequency of usage of its terms in the beagle studies (Watson 1993a, 1993b).

Collection Inventory. The collection inventory database contains information about each bar-code label affixed to materials (or containers of materials) in NRA collections. The database defines materials and tracks location of items for rapid retrieval. More than 15,000 items related to 4500 animals currently are managed by this system.

Bibliography. The bibliographic database uses the collection inventory database's bar-code label system to identify reference materials. Location information about materials is stored in the collection inventory database, and bibliographic citations are stored in the bibliography system. The bibliography system includes more than 2000 items of a supporting nature, including animal-specific documents.

TABLE 3. Progress Toward Populating the Summary Database

NRA Lab and Study ID[a]	Status of NRA Database Tables[b]						
	LAB	STUDY	GROUP	ANIMAL	TEFFECT	TDOSE	LAB SPECIFIC
1-1 to 1-14	F	C	C	C	C	C	C
2-1	F	C	C	P			
2-2 to 2-04	F	C	C	C	C	C	C
3-1 to 3-03	F	C	C	P			
3-4	F	C	C	C	C		C
3-5, 3-06	F	C	C	P			
4-1, 4-02	F	C	C	P		P	
4-3 to 4-05	F	C	C	C	P	P	P
5-1 to 5-19	F	C	C	C			
6-1 to 6-3	F	C	C				
6-4 to 6-5	F	C	P				
7-1, 7-2	F	C	C	C	C	C	C
7-3	F	C	C	I			
8-3	F	P	P	I	I		
9-1	F	C	C	P			
9-2	F	C					
10-1 to 10-51	I	I	(Detailed information was *discarded* by University of Rochester; NRA has reprints of results and study definition records only.)				
Number of Records:	9	126	545	19,883	63,318	7,911	>250,000

(a) Laboratory Codes: 1, U of Utah; 2, UC Davis; 3, ANL; 4, PNL; 5, ITRI; 6, LBL; 7, ORNL; 8, CSU; 9, BNL; 10, University of Rochester. Study numbers are defined in Tables 1 and 2.

(b) Status Codes:
C, Complete: database records are complete; all significant fields have complete information.
F, Final: database records are complete and reviewed by investigator.
I, Incomplete: database tables are partially filled with representative rows.
P, Partial: database records are partially complete; some fields have no information.

An introduction to the NRA information system is available as a standalone application that can be self-loaded from diskette onto a DOS-based microcomputer. The documentation accompanying the application, "National Radiobiology Archives Distributed Access User's Manual," explains usage and extensively describes fields (Watson *et al.* 1991; Smith *et al.* 1992). This document and software are an important summary of the meta-data (information-describing data) collected. The introductory subset diskettes are distributed in response to requests for information about the NRA.

Document Archives

The research document archives collects detailed research findings associated with each study. Materials include handwritten "raw" data such as exposure logbooks, clinical notes, laboratory analysis forms, hematological profiles, and animal-care observations. A significant class of research documents from these studies comprises photographic film, autoradiographs, radiographs, and photographs. "Summarized" data, usually reduced to computer files or publication reprints, also are included. Each document (or document container such as a folder) is given a bar-coded

accession-number label and stored in a controlled environment. Material is catalogued in the bibliographic database for rapid selection and retrieval.

The first contribution to the document archives is the extensive collection of supportive documentation that provided the basis for *Radioactivity and Health: A History*, by J. Newell Stannard (1988); about 60 boxes have been accessioned. In addition, clinical and radiographic records were donated by the UC Davis in June 1992. In 1990, documents from the U of Utah such as clinical records, radiographs, photographs, and autoradiography preparations, as well as specimens such as organs, histology blocks, and slides, were accessioned; these materials will remain in Utah pending completion of the studies.

Specimen Archives

The biological specimen archives contain collected research materials such as tissues preserved in formalin or alcohol, tissue samples embedded in paraffin or plastic for histopathological analysis, microscope slides, and radiographic films. Many materials are radioactive and associated with hazardous materials such as formalin, alcohol, or paraffin. A building has been renovated to serve as the repository of these specimens. The building contains a specimen-manipulation laboratory, storage bays, and an automatic fire-suppression system. Materials are nominated for donation to the NRA by an institution which recognizes that specific completed studies are worthy of consideration for archival preservation.

Collaborations and Retrievals

Cooperation of participating institutions and investigators is essential to achieve goals of the NRA project. Collaboration has been excellent with the nine institutions that have donated information and materials. NRA staff have participated in, or have been invited to participate in, several site visits; collaborative projects were initiated, and these laboratory directors serve on the NRAAC.

The NRA encourages analysis of studies that examine previous information from a new perspective by applying different analytical approaches, or by comparing results of studies performed at different institutions. The NRA collaborated with investigators at UC Davis to obtain brain specimens of dogs whose clinical records indicated Alzheimer-like symptoms. NRA staff retrieved tissues and provided laboratory facilities, and the UC Davis team prepared histopathology slides for staining and interpretation. In addition, the NRA specimen archives supplied histopathology slides of control beagle stomach to the veterinary school at UC Davis and brain specimens to the University of Tennessee. The information system responded to several requests for detailed data subsets.

A subcommittee of the NRAAC met in December 1991 to plan a collaborative database combining information from 1096 control beagles. The NRA is coordinating publication of this reference set to provide baseline information for comparison with experimental groups. A consortium of biostatisticians from ANL, ITRI, and PNL will analyze this control beagle subset.

Collaboration with the Europeans

A similar archiving task has been initiated by the Commission of European Communities (CEC). The European Radiation Biology Archive (ERAD) is being developed for the European Late Effects Program (EULEP) by Dr. Georg Gerber. The NRA is actively cooperating with Dr. Gerber to coordinate database design with the goal of eventual integration. Agreement on computer hardware and database management software was reached, and the database structures are being merged. Exchange of typical data files and merger of descriptive information is planned for spring of 1994.

Rodent Workshop

The NRA conducted a workshop focused on long-term radiobiology studies in rodents. Representatives of ANL, BNL, ITRI, ORNL,

and PNL met in August along with NRAAC members to review the scope of the studies and discuss availability of information and specimens for archiving. The synopsis of the workshop will include tables defining the major studies.

Future Activities

The NRA will continue the orderly accessioning of life-span beagle-study information, and shipment of selected specimens and documents to PNL. While these studies are being completed, NRA will play an increasing role in facilitating analyses that cut across studies and species. For example, NRA will compile and publish a combined data set of control beagles. Because most rodent-based radiobiology studies involved thousands of animals, access to original, unpublished data from them is limited. Therefore, the NRA will continue to solicit details about additional rodent studies, initially those conducted at ANL, BNL, ORNL, and PNL. The NRA will work closely with the interlaboratory consortium of statisticians developing techniques for comparing and combining information from the beagle studies.

References

Smith, S. K., J. C. Prather, E. K. Ligotke, and C. R. Watson. 1992. *National Radiobiology Archives Distributed Access User's Manual Version 1.1.* PNL-7877, Rev. 1, Pacific Northwest Laboratory, Richland, Washington.

Stannard, N. J. 1988. *Radioactivity and Health: A History*, R. W. Baalman, ed. DOE/RL/10830-T59 (DE88013791), Office of Scientific and Technical Information, Springfield, Virginia.

Thompson, R. C. 1989. *Life-Span Effects of Ionizing Radiation in the Beagle Dog: A Summary Account of Four Decades of Research by the U.S. Department of Energy and Its Predecessor Agencies.* PNL-6822, Pacific Northwest Laboratory, Richland, Washington.

Watson, C. R., J. C. Prather, and S. K. Smith. 1991. *National Radiobiology Archives Distributed Access User's Manual.* PNL-7877, Pacific Northwest Laboratory, Richland, Washington.

Watson, C. R. 1993. *SNODOG Glossary: Part 1, Introduction.* PNL-8650, Part 1, Pacific Northwest Laboratory, Richland, Washington.

Watson, C. R. 1993. *SNODOG Glossary: Part 2, Usage of Terms.* PNL-8650, Part 2, Pacific Northwest Laboratory, Richland, Washington.

Low-Level $^{239}PuO_2$ Life-Span Studies

Principal Investigator: C. L. Sanders

Other Investigators: K. E. Lauhala, B. G. Moore

This report concentrates on the influence of sex and strain on the frequency of $^{239}PuO_2$-induced lung cancer in rats. The data illustrate that there are sex and strain differences reflected in the induction of adenomatous and squamous metaplasia and lung cancer. Male Wistar rats have a higher incidence of adenomatous metaplasia than female rats. When exposed to similar total radiation doses, the absolute risk for the induction of lung tumors in male Wistar rats (730 lung tumors/10^4 rat-Gy) was again much higher than observed in females (81 lung tumors/10^4 rat-Gy). This result contrasts markedly to the induction of squamous metaplasia; the male Wistar rat is much less sensitive than female rats for this endpoint. Wistar rats (both male and female) were less sensitive for $^{239}PuO_2$-induced cancer than were F344 or Long-Evans rats. We also are reporting on formation of cancers in the nose following $^{239}PuO_2$ inhalation. The crude incidence of nasal cancers in exposed female Wistar rats was low, but showed that there were 7 tumors in 2515 animal exposed to $^{239}PuO_2$ and a single tumor in the 1232 control animals. These studies illustrate the importance of considering tissues at risk, l[illegible]ional factors, and genetic background in evaluation of risk from lung cancer from inhaled $^{239}PuO_2$.

Gender and Strain Comparison of Pulmonary Carcinogenesis

The following mix of exposed and sham-exposed young adult rats were examined for lung and nasal tumors in the upper respiratory tract after inhalation of high-fired $^{239}PuO_2$: 3157 female and 198 male Wistar rats, 200 female F344 rats, and 192 female Long-Evans rats. Lung-cancer incidence and type in these rodents were compared in similar dose groups (Table 1).

Table 1 illustrates that all the strains and sexes had similar initial $^{239}PuO_2$ lung depositions (ILDs). Female Long-Evans rats had the lowest calculated lung doses observed in this study (low-dose group: 0.57 ± 0.17 Gy; high-dose group: 26.1 ± 7.7 Gy). These lung doses were, however, within a factor of two of the highest doses observed for female F344 rats, with a low dose of 0.98 ± 0.20 and high of 37.1 ± 6.7.

Crude incidences of adenomatous metaplasia are shown in Table 2. This table provides evidence of a sex difference in sensitivity for the induction of adenomatous metaplasia; the male animals showed a higher incidence than observed in females. Table 3 contains data on the influence of gender and strain on the induction of squamous metaplasia. Tables 4, 5, and 6 all are related to the induction of lung cancer; in Table 4, the crude-incidence data is presented. These data are converted to relative risk in Table 5 by using the observed background for female Wistar and female F344 rats and assigning an indicence of 0.1 to the remaining animals that had no observed lung tumors in the controls. The high background level observed in the F344 rats resulted in a low relative risk value for these animals, especially at the high total doses. In Table 6, the data is expressed as absolute risk for lung-tumor induction by inhaled $^{239}PuO_2$.

TABLE 1. Dosimetric Data for Gender and Strain of Life-Span Rat Following Inhalation of $^{239}PuO_2$. Values are means ± standard deviation (number of animals).

	Female F344	Female Long-Evans	Female Wistar	Male Wistar
ILD, kBq				
Low-Dose Group	0.23 ± 0.04 (80)	0.21 ± 0.05 (72)	0.26 ± 0.06 (111)	0.28 ± 0.12 (78)
High-Dose Group	3.59 ± 0.38 (60)	3.67 ± 0.78 (60)	4.87 ± 1.35 (65)	4.49 ± 1.01 (60)
Lung Dose, Gy				
Low-Dose Group	0.98 ± 0.20	0.57 ± 0.17	0.75 ± 0.18	0.70 ± 0.33
High-Dose Group	37.1 ± 6.7	26.1 ± 7.7	34.4 ± 7.3	28.2 ± 7.3
Lung Weight as % Body Weight	0.62	0.74	0.60	0.50

TABLE 2. Incidence of Adenomatous Metaplasia in the Lung for Gender and Strain of Rat Following Inhalation of $^{239}PuO_2$

	Crude Incidence of Adenomatous Metaplasia, %			
Mean Lung Dose Range, Gy	Female F344	Female Long-Evans	Female Wistar	Male Wistar
0	3.3	0	0.095	0
0.57-0.98	25.0	11.1	2.7	12.8
25-37	60.0	63.3	58.5	80.0

TABLE 3. Incidence of Squamous Metaplasia in the Lung for Gender and Strain of Rat Following Inhalation of $^{239}PuO_2$

	Crude Incidence of Squamous Metaplasia, %			
Mean Lung Dose Range, Gy	Female F344	Female Long-Evans	Female Wistar	Male Wistar
0	0	0	0	0
0.57-0.98	0	0	0	1.3
25-37	61.7	28.3	64.6	18.3

TABLE 4. Incidence of Lung Tumors for Gender and Strain of Rat Following Inhalation of $^{239}PuO_2$. Each tumor was evaluated separately in rats with multiple lung tumors.

	Crude Incidence of Lung Tumors, %			
Mean Lung Dose Range, Gy	Female F344	Female Long-Evans	Female Wistar	Male Wistar
0	1.7	0	0.095	0
0.57-0.98	20.0	8.3	0.46	6.4
25-37	118.3	81.7	70.7	118.3

TABLE 5. Relative Risk of Lung Tumors for Gender and Strain of Rat Following Inhalation of $^{239}PuO_2$. Each tumor was evaluated separately in rats with multiple lung tumors. Spontaneous lung tumors were assumed to be 0.1% for the determination of relative risk in those groups with nil lung tumors in controls.

	Relative Risk			
Mean Lung Dose Range, Gy	Female F344	Female Long-Evans	Female Wistar	Male Wistar
0	1	1	1	1
0.57-0.98	12	110	4.6	51
25-37	48	550	750	830

TABLE 6. Absolute Risk of Lung Tumors for Gender and Strain of Rat Following Inhalation of $^{239}PuO_2$. Each tumor was evaluated separately in rats with multiple lung tumors. Spontaneous lung tumors were assumed to be 0.1% for the determination of relative risk in those groups with nil lung tumors in controls.

	Absolute Risk (Lung Tumors per 10^4 Rat-Gy)			
Mean Lung Dose Range, Gy	Female F344	Female Long-Evans	Female Wistar	Male Wistar
0	0	0	0	0
0.57-0.98	1900	1900	81	730
25-37	220	210	210	300

Survival times were similar in control, low-dose, and high-dose groups for both genders and all strains. Differences in epithelial metaplasias and lung-tumor responses were seen among both genders and all strains. Adenomatous metaplasia was considerably higher in control and low-dose groups of F344 rats than in Wistar rats. In male Wistar and female Long-Evans rats, adenomatous metaplasia was not found in control rats; it was, however, found at a higher incidence in the low-dose groups of F344, Long-Evans, and male Wistar rats than in female Wistar rats (Table 2). The sex differences are demonstrated by the fact that the male Wistar rat appeared much more sensitive to the induction of squamous metaplasia than the female Wistar rat. A strain difference also is evidenced by the female Long-Evans rat being less sensitive to the induction of squamous metaplasia than either female F344 or the Wistar rats.

Squamous metaplasia was not found in control or low-dose groups of any strain or gender, except in one male Wistar rat. Squamous metaplasia was found in 62% to 65% of high-dose female F344 and Wistar rats, but only in 18% to 28% of high-dose female Long-Evans and male Wistar rats (Table 3). The incidence of lung tumors in F344 rats was 1.7% in controls, 20% in the low-dose group, and 118.3% in the high-dose group. The incidence of lung tumors in female Wistar rats was 0.095% in controls, 0.46% in the low-dose group, and 71% in the high-dose group. About half of all lung tumors in both genders and all strains were considered to be the primary cause of death.

Because of the differences in sample size, and the small number of tumors observed in most control groups and the single tumor observed in the small sample (60 animals) of F344 female controls (Table 4), it is difficult to draw many conclusions concerning the relative risk for lung-cancer induction as a function of gender or strain. By assigning the same spontaneous lung-tumor incidence to all groups that had zero lung tumors, relative risk values were determined (Table 5) which suggest that the

male Wistar rat is more sensitive to the induction of tumors than the female, and that the Long-Evans rats are the most sensitive among the different strains.

Absolute risk of lung tumors (Table 6) was similar in the low-dose group for female F344 and female Long-Evans rats, both being much greater than for female Wistar rats. As was observed for relative risk, the absolute risk for male Wistar rats in the low-dose group was nearly tenfold higher than for female Wistar rats. Absolute risk of lung tumors in the high-dose group was similar for all genders and strains. The adenomatous tumor phenotype predominated in the F344 strain, while the squamous tumor phenotype predominated in the Wistar strain. Risk of squamous tumors was similar for both strains. Overall, the female F344 rat appears more than tenfold more sensitive than the female Wistar rat to lung-tumor formation at low to moderate doses from inhaled $^{239}PuO_2$, evidenced by an increased incidence of adenomatous phenotype tumors.

The variability in lung-tumor response among the strains and genders of the rat following inhalation of $^{239}PuO_2$ complicates the use of the rat lung model in applying and/or projecting risk of lung cancer to humans. The cause for differences in lung-tumor response among strains and genders requires additional research, but may be due to such factors as genetic susceptibility, hormones, and diet.

Nasal and Oral Carcinoma

Nine oral squamous cell carcinomas were distributed proportionately among control and exposed Wistar rats of both genders; these tumors all appeared to be associated with malocclusion of incisor teeth. No oral carcinomas were found in F344 or Long-Evans rats.

A small number of inhaled $^{239}PuO_2$ particles were retained in subepithelial regions of the larynx and nasal cavity. No tumors were found originating from the trachea or larynx. One nasal-cavity tumor was found in a control female Wistar rat (0.095%) while five tumors were found in exposed female Wistar rats (0.24%) (Table 7). Two nasal-cavity tumors were found in exposed female Long-Evans rats (1.5%), while no nasal cavity tumors were found in control Long-Evans rats, or in control or exposed female F344 or male Wistar rats. Thus, in 2515 exposed rates, there were 7 nasal tumors, and in the 1232 control animals, only a single tumor was observed. The association found between inhaled $^{239}PuO^2$ radiation dose and tumor formation in the upper respiratory tract, especially in the nose, requires additional research.

TABLE 7. Tumor Incidence in the Nasal Cavity of the Rat Following Inhalation of $^{239}PuO_2$

	Gender/Strain	Number of Rats	Crude Incidence of Tumors, %	Total Tumors
Exposed	Female Wistar	2105	0.24	5
	Male Wistar	138	0	0
	Female F344	140	0	0
	Female Long-Evans	132	1.5	2
		2515	0.28	7
Controls	Female Wistar	1052	0.095	1
	Male Wistar	60	0	0
	Female F344	60	0	0
	Female Long-Evans	60	0	0
		1232	0.08	1

Genotoxicity of Inhaled Energy Effluents

Principal Investigator: A. L. Brooks

Other Investigators: K. M. Groch, J. D. Saffer, and G. E. Dagle

The interaction of cellular and genetic damage induced by low- and high-LET radiation with damage induced by chemicals is being studied to identify health risks associated with the nuclear industry and nuclear waste sites. This project has three objectives: 1) to provide cellular and molecular techniques that can be used to help understand the risks associated with inhalation of complex mixtures; 2) to conduct mechanistic studies using chromosome aberrations; and 3) to understand the molecular mechanisms which result in interaction between damage induced by radiation and that from exposure to chemicals. To evaluate the risk from inhaled complex mixtures, we have developed a model to expose cells directly to vapor-phase materials associated with the nuclear waste tanks. To continue the mechanistic studies associated with chromosome aberrations, it was necessary to develop probes with which to "paint" the chromosomes of rat cells by using fluorescent *in situ* hybridization (FISH) techniques. With these probes in hand, we now hope to determine the relationship between the frequency and type of chromosome aberrations measured in respiratory tract cells at early times after clastogenic exposure and the development of lung cancer. To understand the interaction between radiation and chemicals, it is necessary to define the changes induced by the radiation and determine how these changes in gene expression influence the processing of damage induced by chemical exposure.

Methods

Model Exposure Systems for Airway Epithelium

The model we developed was similar to that developed to expose cells to vapor-phase materials (Zamora *et al.* 1983); we at Pacific Northwest Laboratory will work with Westinghouse Hanford Company to obtain vapor-phase samples from waste tanks to test for biological activity. The criteria for the model system were 1) the ability to use normal lung epithelial cells; 2) the capacity to develop dose–response relationships either as a function of concentration or time of exposure; and 3) the capacity to measure a variety of cellular endpoints, including cell membrane disruption, chromosomal aberrations, cell survival, and neoplastic transformation. Biological data from the vapor-phase materials will be combined with chemical evaluation to generate a first cut at determining the potential for long-term risk from vapor-phase exposure. We will determine which chemical or chemical class in the mixture has the most cellular and genetic toxicology information. We will conduct short-term tests on this chemical, comparing the results to those determined for the complex mixture. Such studies will provide preliminary data that will be important in long-term worker protection during the waste cleanup efforts.

Mechanisms Involved in Chromosome Aberration Production

During 1993, we worked with Drs. Jim Tucker and John Breneman of Lawrence Liver-

more National Laboratory (LLNL), Livermore, California, to develop molecular probes to "paint" the chromosomes of selected rat chromosomes using a method previously developed for mouse chromosomes (Breneman *et al.* 1993). These probes were designed to include the following traits: to label enough of the rat genome to be useful in dosimetry and translocation studies needed to follow the development of tumors; to identify the X and Y chromosomes to enable gender identification of rat cells in tumor models; and to be able to locate important oncogenes and tumor-suppressor genes in the rat karyotype (Szpirer *et al.* 1985, 1988). Now that we have the probes, we will use them to track radiation- or chemically induced chromosome translocations in rat cells.

Interactions Between Radiation and Chemicals

Identification of the gene activation and protein induction by small radiation doses is essential to understand the interactions between radiation and chemical damage. This objective is a major goal in this portion of the study. We are using radiation and other clastogenic agents to determine if radiation can induce genes to produce RNA that results in new proteins, if these proteins are related to DNA repair, and which if any of these proteins are involved in repair of DNA damage. Studies have been initiated to identify the genes that change their expression after low doses of radiation. We are using the differential display method (Liang and Pardee 1992), which screens hundreds of RNAs at once to identify genes that change expression after radiation exposure.

Results and Discussion

Model Exposure Systems for Airway Epithelium

Preliminary experiments were required for developing the model system. These experiments involved a Fischer rat lung epithelial cell (LEC) line (Li *et al.* 1983) cultured on polymerized rat tail collagen. The studies had three goals: 1) to determine how long the cells could live on collagen gels without culture medium; 2) to determine the rate of growth during medium deprivation; and 3) to determine if the cells would return to normal growth patterns after being removed and plated under normal culture conditions.

To assess the effects of withdrawing the culture medium (Ham's F-12 containing 10% FBS) from the LEC, 5 x 10^5 cells were plated onto collagen gels in T-75 flasks and incubated overnight at 37° C in a humidified incubator with 5% CO_2. Twenty-four hours after plating, the tissue culture medium was removed and the cultures returned to the incubator. At 4 and 24 hours later, the collagen matrix was dissolved in collagenase (200 units/ml) and total cell yield and intact cells (as judged by trypan blue exclusion) quantified. In two separate experiments, withdrawing medium for up to 24 hours had little effect on cell numbers or morphologic viability (Figure 1). It was observed, however, that plating LEC onto collagen gels down-regulated the proliferation of these cells as compared to similar cells cultured on a tissue culture substrate (Figure 2).

To assess whether the collagen-induced cellular quiescence was reversible, 5 x 10^5 cells were plated onto either collagen gels or tissue culture plastic and incubated as described previously. Twelve hours later, the cells on the collagen gels were removed with collagenase, pelleted, and transferred to plastic tissue culture dishes. Subsequent cell counts indicated that the collagen-induced quiescent was reversible (Figure 3). The system seems to be adequate for studies involving cell survival, micronuclei induction, and chromosome aberrations. The cells will be exposed to organic vapors and these endpoints measured.

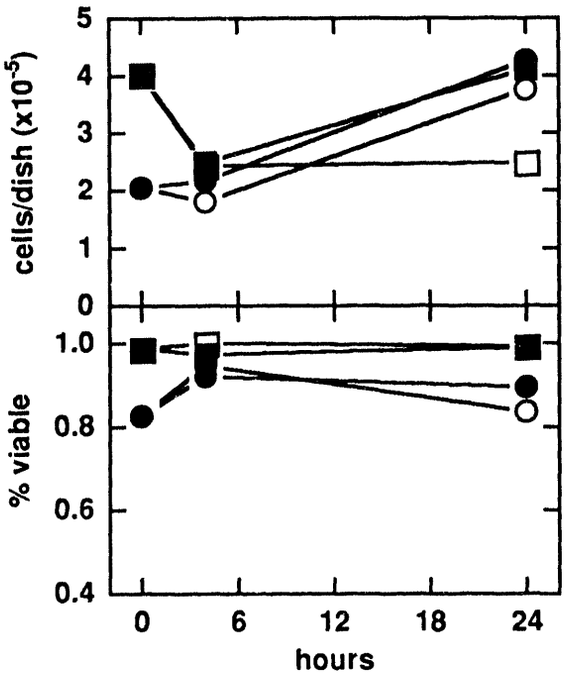

FIGURE 1. Effect of Withdrawing Medium on the Growth and Viability as Measured by Trypan Blue Exclusion of LEC Cells Cultured on Collagen Gels (closed symbols: with medium; open symbols: without medium; squares: experiment 1; circles: experiment 2)

Mechanisms Involved in Chromosome Aberration Production

To develop chromosome-specific probes for fluorescent *in situ* hybridization (FISH) "painting" techniques, it is necessary to have a large source of primary cells in culture; therefore, we established primary cultures of rat skin fibroblasts. The cells were harvested after four passages and 2.4 x 10^8 cells were mailed to Dr. Tucker at LLNL. Dr. Tucker's team treated the cells with colcemid to accumulate metaphase cells, isolated chromosomes from the dividing cells, and sorted individual chromosomes on a flow cytometer. The methods that were used for developing these chromosome-specific DNA probes have been published previously (Breneman *et al.* 1993). Briefly, small pools of each chromosome were denatured, then hybridized with degenerate oligonucleotide primers (DOP); next, a polymerase chain reaction (PCR) was conducted. Using these methods, it was possible to develop probes for rat chromosomes 1, 2, 4, 10, X, and Y. The identification of the chromosomes that

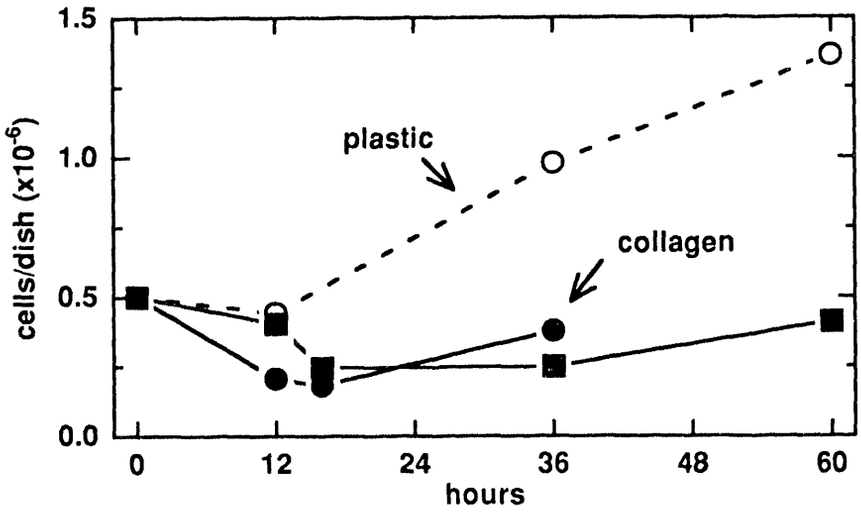

FIGURE 2. Changes in Cell Population Numbers as a Function of Time After Plating LEC Cells on Either Plastic with Medium or Collagen Without Medium (open circle: cells cultured on tissue culture-treated plastic; closed symbols: cells cultured on collagen gels; circles: experiment 1; squares: experiment 2)

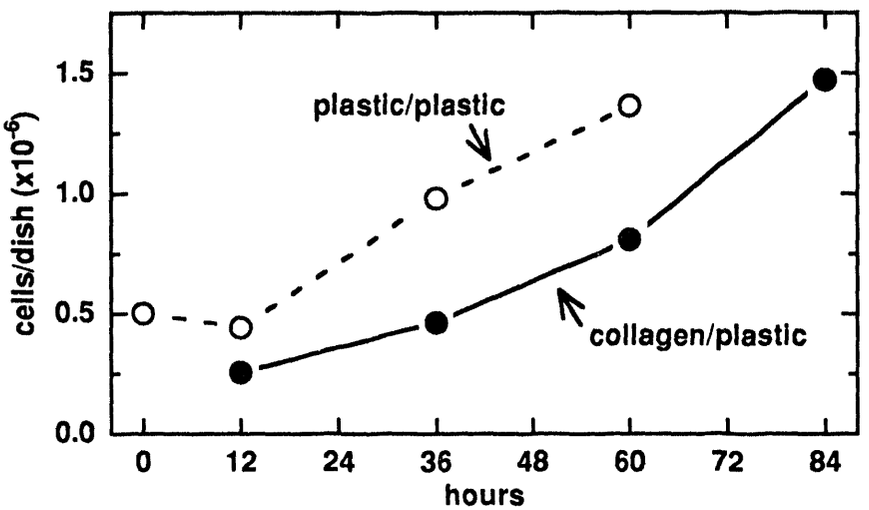

FIGURE 3. Growth of Cells that Were Cultured with Medium on Plastic or Collagen Without Medium, then Transferred to Plastic with Medium (solid line: precultured on collagen gels; dashed line: precultured on tissue culture-treated plastic). The figure shows that the cells are delayed in their growth but resume normal growth after being returned to normal culture conditions.

are painted is still tentative, because G-banding has not yet been done. Examples of cells stained with and without the FISH technique are shown in Figure 4. The chromosome stained in Figure 4A was tentatively identified as chromosome 1; Figure 4B shows the X chromosome. These chromosome probes will be very useful in studying cancer induction in rats, and will provide tools that can be used to better understand the role that chromosome aberrations play during the induction and progression phases of cancer development.

Interactions Between Radiation and Chemicals

Changes in gene expression can be sensitive indicators of cellular responses. In most analyses of RNA expression, a particular gene product is detected using a gene-specific molecular probe. Methods such as northern blots and RNA protection studies are very powerful, but are limited to the one gene (or sometimes a few) for which probes are used within one assay. Examining other genes requires preparing separate probes and performing additional assays.

In order to perform a comprehensive analysis of radiation-induced cellular changes at the RNA level, we have begun to use the differential display PCR (ddPCR) method (Liang and Pardee 1992). In brief, a subset of mRNAs are reverse-transcribed to cDNA using a primer that anneals to the poly(A) tail plus two additional bases (e.g., 5'-T_{12}CC would define those RNAs that end with GGA_n). These cDNAs are then amplified by PCR using a short arbitrary upstream primer resulting in a distinctly sized fragment from each cDNA. In comparing exposed and control cells, a change in the amount of any resulting band would indicate that the mRNA represented by that band has altered expression.

Exponentially growing Chinese hamster ovary (CHO-K1) cells were exposed to ^{60}Co gamma rays, resulting in doses of 0, 0.01, 0.1, and 1.0 Gy. The RNA isolated from these cells has been screened for differential expression. Approximately one-quarter of the

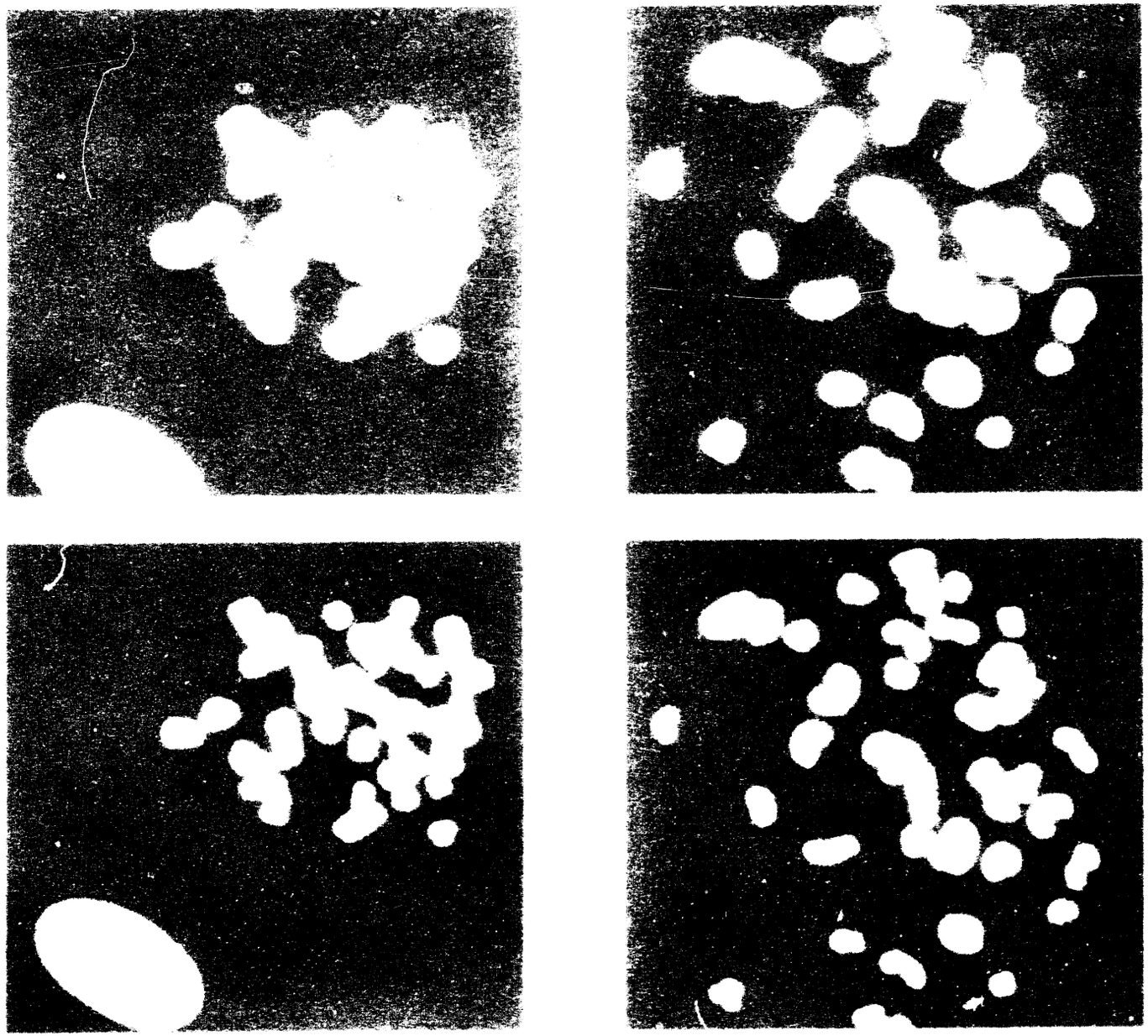

mRNAs within the cell have been examined, revealing two candidates with altered expression. Both of these candidates are affected by doses as low as 0.01 Gy. We have shown that genes identified by ddPCR can rapidly be confirmed by northern analysis or by ribonuclease protection assay. Furthermore, we have demonstrated that these genes can be cloned and sequenced easily. This characterization is now in progress for the candidate genes identified in this work. As these genes are identified then, we can characterize the role they play in altering the response of chromosomes and DNA to priming doses and subsequent challenge doses of radiation or chemicals. With this characterization, it will be possible to determine which if any of these genes are involved in DNA repair, and if overexpression of these genes alters the response to radiation and chemicals given alone and in combination.

References

Breneman, J.W., J.D. Tucker, G.G. Eveleth, D.A. Lee, J.L. Minkler, M.J. Ramsey, and R.R. Swiger. 1993. The development of chromosome-specific DNA probes for the mouse. *Environ. Mol. Mutagen. Suppl.* 22:8 (abstract).

Li, A.P., F.F. Hahn, P.O. Zamora, R.N. Shimizu, R.F. Henderson, A.L. Brooks, and R. Richards. 1983. Characterization of a lung epithelial cell strain with potential application in toxicological studies. *Toxicology* 27: 257-272.

Liang, P., and A.B. Pardee. 1992. Differential display of eukaryotic messenger RNA by means of the polymerase chain reaction. *Science* 257: 967-971.

Szpirer, J. D. Defeo-Jones, R.W. Ellis, G. Levan, and C. Szpirer. 1985. Assignment of three rat cellular *ras* oncogenes to chromosomes 1, 4, and X. *Somatic Cell Mol. Genet.* 11:93-97.

Szpirer, C., J. Szpirer, M.Q. Islam, and G. Levan. 1988. The rat gene map. *Curr. Top. Microbiol. Immunol.* 137:33-38.

Zamora, P.O., J.M. Benson, T.C. Marshall, B.V. Mokler, A.P. Li, A.R. Dahl, A.L. Brooks, and R.O. McClellan. 1983. Cytotoxicity and mutagenicity of vapor-phase pollutants in rat lung epithelial cells and Chinese hamster ovary cells grown on collagen gels. *J.Toxicol. Environ. Health* 12:27-38.

Molecular Events During Tumor Initiation

Principal Investigator: D. L. Springer

Other Investigators: B. D. Thrall, D. B. Mann, and A. O. Murad

This project's primary objective is to test the hypothesis that chromatin structure influences the sites of adduction by carcinogens. These studies will contribute to our understanding of adduct-induced structural changes, and determine whether structural changes influence expression of genes associated with tumorigenesis. For this research, we have studied the binding of benzo[a]pyrene diolepoxide (BPDE) to DNA reconstituted with histone octamers to determine the effect that nucleosome structure has on covalent adduct formation. Reconstitution of a plasmid containing the somatic 5S rRNA gene from *Xenopus borealis* resulted in characteristic nucleosome structure as determined by micrococcal nuclease digestion, shifted migration on agarose gels, and hydroxyl radical footprinting. Formation of covalent adducts by BPDE occurred initially at a slower rate in nucleosomal DNA than in naked plasmid, but after 120 min, the total adduction levels (adducts/plasmid) were equal. Analysis of adduction at the sequence level by primer extension indicated that after a 120-min BPDE reaction, the degree of adduction within the 5S rRNA nucleosome was suppressed by approximately 50% compared to naked DNA. Additionally, sequences near the dyad of the nucleosome, where known modulations in minor groove width occur, were the least susceptible to adduction. Comparison of the rotational setting and BPDE binding indicated that guanines near the histone core were as susceptible to adduction as guanines on the outer nucleosome surface. These results indicate that the structural features of DNA assembled into nucleosomes contribute to the susceptibility of the DNA to modification by BPDE.

Benzo[a]pyrene-7,8-diol-9,10-epoxide (BPDE), the ultimate carcinogenic metabolite of benzo[a]pyrene, covalently binds to DNA predominantly at guanine residues. Covalent adduct formation by BPDE interferes with a number of cellular processes, including DNA replication and transcription, and is thought to be a critical event in tumor initiation. The primary target of covalent modification is through trans addition of (+)-anti-BPDE to the exocyclic amine group of guanines.

Because most DNA in eukaryotic cells is closely associated with histones, an accurate understanding of carcinogen binding to DNA must consider the role of nucleosome structure. In the nucleosome, contact points exist between the DNA and histone cores approximately every 10 base pairs (bp), and histones H3 and H4 make contact with the DNA within 30 bp of either side of the center (dyad) of the nucleosome. In addition, the helical periodicity of DNA varies throughout the nucleosome, with the central three turns of the helix having a periodicity of 10.7 bp and the outer turns having a 10.0-bp periodicity (Thoma 1992). It is conceivable that the DNA-histone contact points due to periodicity of nucleosomal DNA would alter the susceptibility of particular bases to carcinogen damage. Indeed, in a study by Gale *et al.* (1987), ultraviolet (UV)-induced pyrimidine dimer formation in nucleosomes was not uniform, but was maximal at bases

farthest from the histone core, resulting in an average 10.3-bp repeat pattern of damage. Studies with the bulky aflatoxin-derived adduct also demonstrated that binding was suppressed up to 2.4 times in nucleosomal DNA compared with naked DNA, again setting a precedent for examining the influence of nucleosome structure on covalent binding by bulky carcinogens (Moyer *et al.* 1989).

Naked and nucleosomal DNA from genomic sources were bound, to similar degrees, by BPDE (MacLeod *et al.* 1989); however, both the rate of adduction and types of adducts produced varied. Binding of BPDE to DNA also was influenced by DNA sequence (Thrall *et al.* 1992), with preference for modification of guanines flanked by 3′ guanines. However, the influence of the nucleosome on the sequence specificity of BPDE binding is unknown. To explore sequence specificity, we used a plasmid containing the 5S rRNA gene, which forms a highly positioned nucleosome *in vitro*, and examined the effect of nucleosome assembly on the sequence-related patterns of BPDE modification.

Methods and Results

For these studies, we prepared the plasmid pGEM-5S, which contains the 5S rRNA gene, in large quantities. Core histones were isolated from chick erythrocytes using hydroxyapatite and, in a stepwise salt dialysis method, reconstituted with pGEM-5S to form nucleosomes. Micrococcal digestion, restriction enzyme digestion, and gel retardation assays all substantiated that the nucleosome formed as expected; polyacrylamide gel electrophoresis demonstrated that the core histones were intact as octamers. Naked and reconstituted plasmid DNA were incubated with ^{3}H-(±)-*anti*-BPDE under conditions that yielded approximately three adducts/plasmid. After extensive cleanup of the DNA, the adduction levels were calculated based on radioactivity measurements and UV estimates of DNA concentration.

The influence of nucleosome structure on the rate of total covalent adduct formation by BPDE indicated that the initial rate (5- to 30-min reaction time) of covalent adduct formation in the reconstituted sample was suppressed (by 22% to 30%) compared to the naked DNA; however, after the reaction was complete (120 min), the total adduction levels for both naked and reconstituted samples were approximately equal.

To determine the effect of nucleosome structure on the sequence-specific binding patterns of BPDE within the 5S nucleosome, we used blockage of a DNA polymerase (Sequenase) during primer extension as an indication of adduction patterns. Nonadducted DNA did not produce polymerase blockage; however, a comparison of dideoxy sequencing ladders and the bands produced by primer extension of the 120-min adducted samples demonstrated that polymerase blockage occurred one base prior to modified guanines. Densitometric analysis of these bands revealed that, in regions outside of the 3′ edge of the nucleosome, the relative degree and pattern of polymerase blockage were similar in both naked and nucleosomal DNA.

Within the 5S nucleosome, however, the degree of polymerase blockage, and thus the amount of adduction, was suppressed in the reconstituted sample by approximately 50% (Figure 1). This pattern of BPDE binding was consistent with the position of the 5S nucleosome, because the positions in which adduct formation were suppressed corresponded with the 3′ portion of the nucleosome. These results demonstrate that nucleosome structure inhibits BPDE binding, and provide additional evidence for the presence of a positioned 5S nucleosome in the plasmid.

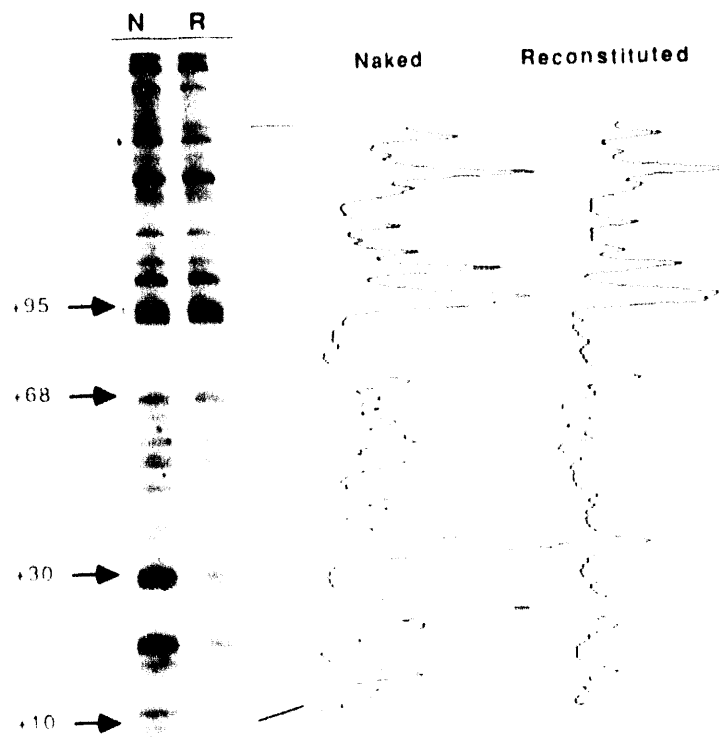

FIGURE 1. Analysis of Binding Within the 5S Nucleosome by Primer Extension. Adduct formation by BPDE after a 120-min reaction with either naked (N) or reconstituted (R) DNA was determined by primer extension. The numbering refers to guanine position relative to the start of the 5S gene (+1). Densitometric scans of the lanes are shown to the right of the figure. The 3′ end of the nucleosome begins at approximately base +78.

To determine whether there were differences in susceptibility to BPDE modification within the nucleosome, we conducted primer extension on naked and reconstituted samples reacted with BPDE for varying times. The degree of protection by the nucleosome (expressed as percent of adduction for the equivalent sites in naked DNA) relative to the position of the guanine (distance from the nucleosome dyad) is shown in Figure 2. Samples reacted for 120 min with BPDE showed a 50% to 60% decrease in binding throughout the nucleosome; the binding level at the edge of the nucleosome (see arrow in Figure 2) approached that of naked DNA.

In the 15- and 30-min reaction samples, adduct formation in the reconstituted sample also was suppressed. However, the amount of suppression of binding in these samples was progressively greater near the dyad of the nucleosome compared to the binding at the fringes. Surprisingly, the adduction levels on the fringes of, and immediately outside, the nucleosome were enhanced relative to those of the naked DNA; in future studies, we will explore the factors responsible for these differences in distribution of binding.

In addition to sequence-specific adduct locations, it was important to determine the rotational setting–the position of the guanines

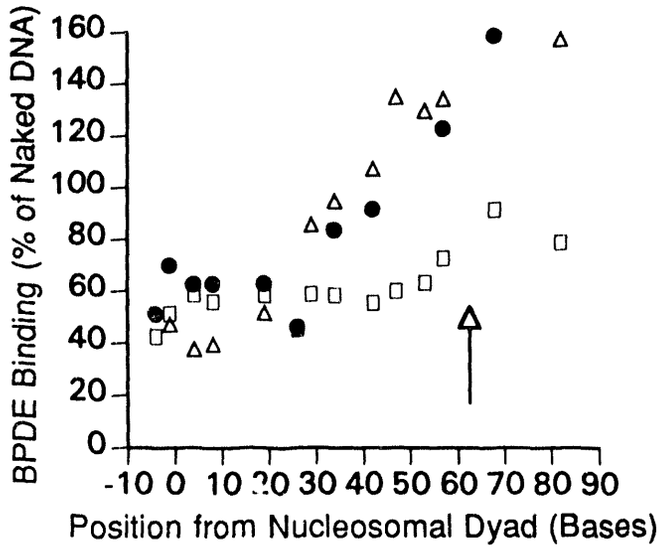

FIGURE 2. Relationship Between Reaction Time and Region of the Nucleosome. Samples that were reacted with BPDE for varying times were analyzed by primer extension. The degree of inhibition of binding at individual guanines within the nucleosome, expressed as a percentage of the corresponding site in naked DNA, is plotted versus the position of the guanine in samples reacted with BPDE for 15 min (circles), 30 min (triangles) or 120 min (squares). The arrow indicates the approximate position of the 3' edge of the nucleosome.

on the DNA helix within the nucleosome. For this determination, we performed hydroxyl radical footprinting on a 300-bp restriction fragment containing the 5S rRNA gene. Cleavage of nucleosomal DNA by hydroxyl radicals is known to occur more intensely in regions where the minor groove of the DNA is facing away from the histone octamer. In these experiments, hydroxyl radical cleavage of nucleosomal DNA resulted in a characteristic pattern of protection approximately every 10 bp, while cleavage of the naked DNA sample was random. Analysis of the positions of most intense cleavage revealed a strong cut site at about the start of the 5S gene in both the naked and reconstituted samples; we interpret this to be a native structural characteristic of the DNA. Within the approximately two-base resolution of these experiments, these results reveal that both the translational position and rotational setting of the 5S nucleosome concur with peak intensities corresponding to bases -15, -5, +6, +17, +27, +37, +47, and +57 surrounding the presumed position of the nucleosomal dyad (base +10).

We hypothesized that the guanines closest to the histone cores would have the least potential for adduction because of steric hindrance. Therefore, we compared the positions of the guanines on the DNA helix within the nucleosome with the relative BPDE binding (Figure 3). The positions of the guanines were deduced from the intensity of cleavage by hydroxyl radicals; the relative degree of BPDE binding was determined by primer extension. Within the resolution of the data from hydroxyl radical footprinting, we did not find a correlation between the average adduction of guanines and the sensitivity of the guanines to cleavage by hydroxyl radicals. For example, a region of

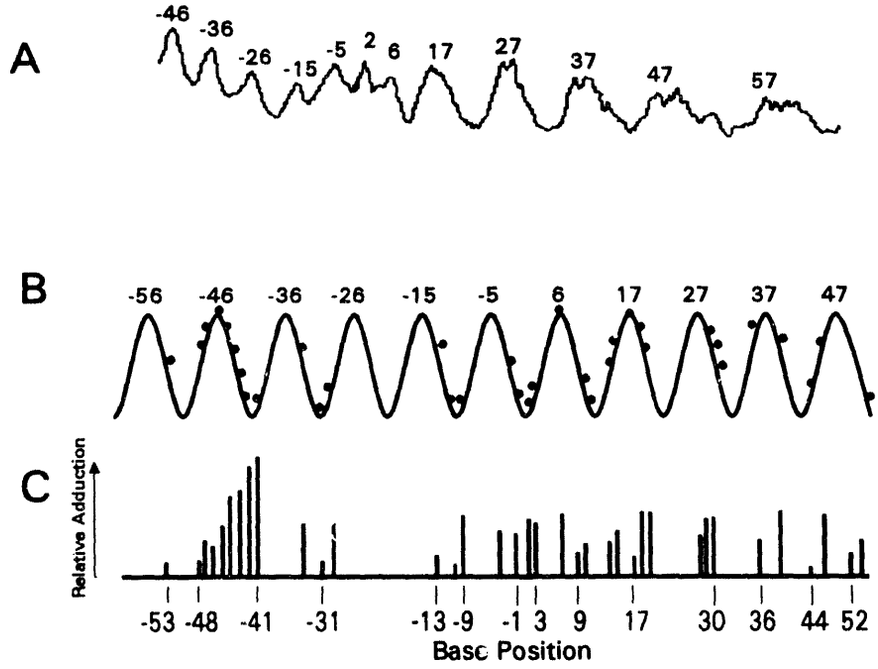

FIGURE 3. Comparison of Rotational Setting and BPDE Binding in Reconstituted pGEM-5S. The rotational setting of the guanines and its relationship to adduct formation within the 5S nucleosome was deduced using hydroxyl radical footprinting and primer extension analysis. Panel A shows adensitometric scan of the hydroxyl radical footprint of the reconstituted 5S gene. Panel B is a graphic depiction of the position of the guanines (indicated by dots) relative to the DNA helix on the noncoding strand. The position of the dyad corresponds to that reported by Pruss and Wolffe (1993). The peaks of the helix in panel B represent where the minor groove is facing away from the histone cores, whereas the valleys are positions nearest the histone cores. Panel C shows the adduction by BPDE (after a 120-min reaction) at the individual guanines represented in Panel B, relative to the first guanine in the 5S gene (base 2). Note that the X axis in panel C corresponds to the position of the guanines in panel B.

eight consecutive guanines (Figure 3C, bases -41 to -48) showed a bias for greater adduction of the 5′ guanines, yet these guanines appeared to be nearest the histone cores. Similar inconsistencies between adduction level and rotational setting occurred throughout the 5S nucleosome; in general no apparent correlation exists between the position of the guanine relative to the histone cores and the frequency for covalent adduct formation.

Within a local sequence context, however, covalent binding of BPDE to a particular guanine is influenced significantly by flanking bases. For example, the potential for a particular guanine to be modified by BPDE is enhanced by the presence of 3′ flanking guanines (Thrall *et al.* 1992). The patterns of adduction in the poly dG8 region (Figure 3C, bases -41 to -48) observed in nucleosomal DNA in this study also demonstrate this nearest-neighbor

effect, and is nearly identical to patterns we have reported previously for this same sequence in naked DNA (Thrall *et al.* 1992). Thus, on a local sequence scale, the nearest-neighbor effects on BPDE binding are not significantly altered within the nucleosome.

Discussion

By examining the pattern of binding at early time points during the reaction with BPDE, it became apparent that sequences surrounding the dyad of the 5S nucleosome were less susceptible to covalent binding than either naked DNA or fringe regions of the nucleosome. Because most BPDE adducts are thought to lie within the minor groove, these results suggest that the minor groove is less accessible near the dyad than on the fringe of the nucleosome. Aflatoxin binding to nucleosomal DNA is restricted to within the central 100 bases of the nucleosome; similarly, the formation of pyrimidine dimers from UV irradiation is lowest in the region of the nucleosome dyad. Studies using hydroxyl radical footprinting have shown that the average helical repeat of DNA in the 5S nucleosome is 10.18 bp; however, the central 30 bp of DNA in the 5S nucleosome is overwound to a periodicity of 10.7 bp while the DNA outside this region has a 10.0-bp periodicity (Thoma 1992). This overwinding is consistent with a narrowing of the minor groove of the DNA around the nucleosomal dyad, which may be important to the formation of BPDE adducts.

The sequences surrounding the dyad of the nucleosome are also thought to contain bends that contribute to the positioning of the histone octamer, and these structural elements also may be important to DNA adduct formation. Interestingly, we found enhanced BPDE binding after early reaction times in regions immediately outside the 5S nucleosome. Although further studies are needed to explain this pattern, nucleosomes can induce bending of linker DNA even in the absence of histone H1, a phenomenon that may affect the level of BPDE binding (Yao *et al.* 1991).

Comparison of the degree of BPDE binding by primer extension and the binding results obtained by hydroxyl radical footprinting showed that the degree of binding did not correlate with the position of the guanines on the DNA helix (Thrall *et al.* in press). For yet unknown reasons, this finding contrasts results found for pyrimidine dimers in genomic nucleosomes (Gale and Smerdon 1988). Damage to nucleosomes by UV shows a 10.3-bp periodicity, possibly because of preferential modification of bases farthest from the histone core. Formation of pyrimidine dimers requires significant perturbation of the DNA helix, unlike the major adduct formed by BPDE, which results in minimal perturbation in the helix (Cosman *et al.* 1992). Thus, damage to bases near the histone-DNA interface may be energetically more favorable with BPDE than with UV. However, NMR and energy-minimization studies (Cosman *et al.* 1992) suggest that the major adduct structure from BPDE does require a widening of the minor groove. For this widening to occur without significant energy input, it may be that normal thermodynamic fluctuations in minor groove widths are required for formation of an initial BPDE-DNA complex. Possibly, histone cores do not limit access of BPDE to the minor groove of the DNA, but rather restrict the thermodynamic flexibility of the minor groove, and therefore inhibit the formation of the initial BPDE-DNA complex that leads to covalent binding.

Although additional studies are required to discern the mechanisms involved, the patterns of adduction observed in this study correlate with known structural variations of the DNA within the 5S nucleosome, and with the proposed mechanisms of BPDE binding. Further studies to determine the sites of adduction and enzymatic processing, as well as the role of

nucleosome structure of critical genes involved in tumor initiation, will be particularly important in the future.

References

Cosman, M., C. de los Santos, R. Fiala, B.E. Hingerty, S.B. Singh, V. Ibanez, L.A. Margulis, D. Live, N.E. Geacintov, S. Broyde, and D.J. Patel. 1992. Solution conformation of the major adduct between the carcinogen (+)-*anti*-benzo[a]pyrene dio epoxide and DNA. *Proc. Natl. Acad. Sci. U.S.A.* 89:1914-1918.

Gale, J.M., K.A. Nissen, and M.J. Smerdon. 1987. UV-induced formation of pyrimidine dimers in nucleosome core DNA is strongly modulated with a period of 10.3 bases. *Proc. Natl. Acad. Sci. U.S.A.* 84:6644-6648.

Gale, J.M., and M.J. Smerdon. 1988. UV-induced pyrmidine dimers and trimethylpsoralen cross-links do not alter chromatin folding in vitro. *Biochemistry* 27:7197-7205.

MacLeod, M.C., B. Smith, and L. Kao Lew. 1989. Interaction of an ultimate carcinogen, benzo[*a*]pyrene diol epoxide, with nucleosomal core particles: Apparent lack of protection of DNA by histone proteins. *Mol. Carcinogenesis* 1:245-252.

Moyer, R., K. Mariën, K. van Holde, and G. Bailey. 1989. Site-specific aflatoxin B_1 adduction of sequence-positioned nucleosome core particles. *J. Biol. Chem.* 264(21):12226-12231.

Pruss, D., and A.P. Wolffe. 1993. Histone-DNA contacts in a nucleosome core containing a *Xenopus* 5S rRNA gene. *Biochemistry* 32:-6810-6814.

Thoma, F. 1992. Review: Nucleosome positioning. *Biochimica et Biophysica Acta* 1130:1-19.

Thrall, B.D., D.B. Mann, M.J. Smerdon, and D.L. Springer. 1992. DNA polymerase, RNA polymerase, and exonuclease activities on a DNA sequence modified by benzo[a]pyrene diol epoxide. *Carcinogenesis* 13(9):1529-1534.

Thrall, B.D., Mann, D.B., Smerdon, M.J., and Springer, D.L. 1994. Nucleosome structure modulates benzo[a]pyrene diol epoxide adduct formation. *Biochemistry* (in press).

Yao, J., P.T. Lowary, and J. Widom. 1991. Linker DNA bending induced by the core histones of chromatin. *Biochemistry* 30:8408-8414.

Biochemistry of Free Radical-Induced DNA Damage

Principal Investigator: A. F. Fuciarelli

Other Investigators: E. C. Sisk and J. D. Zimbrick

Exposure of DNA to free radical-generating agents, such as ionizing radiation and selected chemicals, results in a multiplicity of molecular damage that can also be characterized in terms of its spatial distribution along the DNA molecule. We are using specific free radical-induced purine and pyrimidine products as molecular probes of DNA damage in an effort to increase our understanding of the mechanisms underlying free radical damage to cells and the impact of these lesions on biochemical processes. We have examined electron migration along DNA as a potential mechanism by which radiation-induced damage can be manifested distal to the sites of initial energy deposition. Our data suggest that electron migration along DNA is significantly influenced by the DNA base sequence and that migration can occur preferentially in the 5′ to 3′ direction along DNA. Migration along 7 base pairs in oligonucleotides containing guanine bases was observed for oligonucleotides irradiated in solution, which compares to average migration distances of 6 to 10 bases for *Escherichia coli* DNA irradiated in solution and 5.5 base pairs for *Escherichia coli* DNA irradiated in cells. Our continued efforts will provide information regarding the contribution of electron transfer along DNA to formation of locally multiply damaged sites created in DNA by exposure to ionizing radiation. These studies contribute to basic knowledge regarding mechanisms underlying DNA damage, and complement studies in repair, mutagenesis, transformation, and cell death.

Electrons in Radiation-Induced DNA Damage

Absorption of energy following exposure of aqueous solutions to ionizing radiation initiates a cascade of events involving ionization and energy exchange between excess electrons and molecules within the solvent. The electrons produced during these events evolve through several intermediate states, from the quasi-free, unsolvated electrons ejected on the time scale of 10^{-16} s, to solvated electrons present at 10^{-6} s after energy absorption. Solvated and unsolvated electrons can be captured by purine and pyrimidine bases in DNA and these electrons can subsequently "tunnel" along DNA in the overlapping pi-electron system created by the stacked bases. Migration of electrons along DNA is an important, but not well understood, mechanism underlying the distribution of radiation damage.

Migration of unsolvated electrons, generated by direct ionization of DNA, has been examined using several spectroscopic methods (reviewed by Fuciarelli *et al.* 1993b; Beach *et al.* 1993a). Measurements of long-range migration distances following irradiation range from 33,000 base pairs in hydrated DNA samples to 100 to 300 base pairs in dry or frozen samples of DNA. Intermediate migration distances of 17 base pairs and 25 base pairs also have been reported in irradiated dry DNA preparations and irradiated frozen DNA solutions, respectively. Radiation-induced short-range migration over 1 to 3 base pairs and 2 to 6 base pairs also have been reported in frozen preparations of hydrated DNA.

In aqueous samples of DNA, electron migration is technically more difficult to study compared with DNA in the solid state, and it is the solvated electron, captured by DNA bases from solution, that is the species under investigation. An electron trap of sufficient reduction potential must be located in close proximity to DNA to facilitate measurement of migration distances. Both the low capture efficiency (electron affinity) and the inability to attain high concentrations of the electron traps in the vicinity of DNA bases have compromised accurate measurement of electron migration distances. These limitations were partially solved in studies which used intercalators of sufficiently high reduction potential (i.e., nitracrine and related basic nitroacridines) to successfully reveal average electron migration distances of 3 base pairs in aqueous DNA solutions (Anderson *et al.* 1991). However, electron transfer to other sites on DNA, instead of transfer to the electron trap in solution, can be a potential limitation in this approach.

5-Bromouracil as an Indicator of Electron Interactions in DNA

To overcome the practical limitations of techniques utilizing electron-affinic compounds as traps to assess electron migration in aqueous DNA solutions, 5-bromouracil (5-BrU) incorporated directly into DNA has been proposed as a molecular indicator of electron migration (Beach *et al.* in press; Fuciarelli *et al.* in press). In aqueous solution, interaction of 5-BrU with solvated electrons results in release of bromide ions and formation of a highly reactive 5-uracilyl radical capable of capturing hydrogen atoms from substrates in the irradiated solution. In irradiated solutions of 5-BrU, release of bromide ion (Zimbrick *et al.* 1969) and formation of uracil (Fuciarelli *et al.* submitted[b]) occur in a quantitative manner; that is, within experimental error all solvated electrons formed during water radiolysis yield bromide ions and uracil. In a series of experiments in which we used deuterated water and deuterated t-butanol (t-butanol is used to scavenge hydroxyl radicals formed during water radiolysis), we demonstrated that hydrogen atom donation can occur from different sources depending upon whether 5-BrU is irradiated as a monomer in solution or as another base incorporated into DNA (Fuciarelli *et al.* submitted[b]). When irradiated as a monomer, 5-BrU captures a hydrogen atom from t-butanol. This was observed by irradiating solutions of 5-BrU containing deuterated t-butanol and using gas chromatography-mass spectrometry methods to demonstrate the presence of a deuterated uracil derivative with a molecular mass 1 a.m.u. greater than that observed for uracil due to the presence of a deuteron (Figure 1).

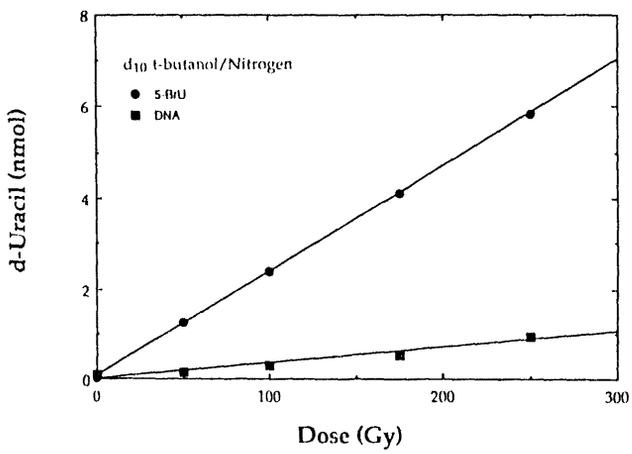

FIGURE 1. 5-Bromouracil as an Indicator of Electron Interactions. Yields of uracil from solutions of 5-BrU (1 mM) or an oligonucleotide [5'-(BrUAAA)$_3$-3'] (200 μg/ml) saturated with nitrogen containing 0.4 M deuterated t-butanol are plotted as a function of radiation dose. The radiation chemical yield of uracil in solutions containing 5-BrU is 0.28 μmol J^{-1}, which corresponds to that of the solvated electron. Yields of uracil are lower in oligonucleotides. Using deuterated t-butanol, we demonstrated that the proton captured by the uracilyl radical intermediate comes from t-butanol in solutions of 5-BrU and from other components of the oligonucleotide, such as the deoxyribose sugar, in irradiated oligonucleotide solutions.

However, when 5-BrU-containing oligonucleotides are irradiated in their double-stranded forms, the hydrogen atom is captured from the DNA molecule because solutions containing deuterated t-butanol resulted in low levels of deuterated uracil (Fuciarelli *et al.* submitted[b]). This latter observation is consistent with the hypothesis that hydrogen atom donation may occur from the 2′ carbon of the 5′ deoxynucleoside in DNA rather than from other substrates in solution. Molecular models of the orientation of the bromine atom on the 5-BrU moiety in DNA and the hydrogen atom on the 2′ carbon of the 5′-adjacent deoxyribose indicate that these atoms are very close to each other in DNA, thereby facilitating hydrogen atom donation. In a more general sense, these data reveal that radiation chemistry occurring in DNA can be quite different than the chemistry that one might expect based upon data from monomers.

Radiation chemical studies utilizing DNA bases or nucleosides homogeneously distributed in aqueous solution revealed quantitative reaction of 5-BrU with hydrated electrons (Fuciarelli *et al.* submitted[b]). On the other hand, 5-BrU incorporated into DNA using automated syn- thesis techniques (Fuciarelli *et al.* in press), or by substituting 5-BrU for thymine in growth medium (Beach *et al.* in press; Beach *et al.* submitted), led to substantially lower radiation chemical yields. For example, the concentration of hydrated electrons generated from water radiolysis in aqueous solution exposed to 500 Gy is 135 μm, assuming a radiation chemical yield of 0.27 μmol J^{-1} for the solvated electron. The yield of bromide from DNA extracted from cells grown in medium in which 5-BrU was substituted for thymine and irradiated to 500 Gy in aqueous solution was 27 μm, which represents 20% of the total yield of electrons (Beach *et al.* in press). Radiation chemical yields for uracil formation in aqueous samples of 5-BrU-containing oligonucleotides range from 0.206 μmol J^{-1} (representing approximately 78% of the electrons generated from water radiolysis) for double-stranded oligonucleotides containing guanine base spacers between 5-BrU molecules down to 0.0099 μmol J^{-1} for double-stranded oligonucleotides containing adenine base spacers between 5-BrU molecules (Fuciarelli *et al.* in press). Decreased product yields in DNA parallel data revealing that measured rate constants for the reaction of hydrated electrons with polynucleotides are approximately an order of magnitude lower than those measured for the free bases (Shragge *et al.* 1971). This decrease in reaction rates could reflect a combination of charge repulsion of the hydrated electron by the negatively charged phosphate groups on DNA, decreased collisional frequency of electrons with DNA, decreased fraction of electrons interacting in each collision, and increased structural shielding due to base stacking in duplex DNA.

Effects of DNA Base Sequence on Electron Migration

DNA base sequence potentially can have a significant influence on the maximum distance over which electrons can migrate along DNA, and reactions involving mixtures of DNA bases with solvated electrons provide some preliminary insights in this regard. Additionally, in native DNA, it was hypothesized that the transfer of an electron along the helix axis competes with proton transfer processes, including both intra-base pair transfer occurring in the direction perpendicular to the helix axis and extra-base pair transfer from bulk water (Steenken 1992). These insights provide some indication that DNA base sequence could have a significant influence on the ability of the electron to migration along DNA.

To examine the effects of base sequence and DNA conformation on electron migration, a set of oligonucleotides containing 5-BrU at selected positions with 3 base (guanine, cytosine,

thymine, or adenine) spacers (e.g., [BrU-$(GGG)_3]_3$) were exposed to ionizing radiation in their single-stranded form, or alternatively, in their double-stranded form following annealing with appropriate complementary sequences. Differences in uracil yields, as measured by gas chromatography-mass spectrometry, suggested that electron migration occurred to different extents, in oligonucleotides containing different base sequences. In irradiated single-stranded oligonucleotides, the yield of uracil decreased in the following order: $A > T > > C \approx G$ (Figure 2A). However, in irradiated double-stranded oligonucleotides, the yield of uracil decreased in the following order: $G > C \approx T > A$ (Figure 2B). The mechanisms underlying these results may be due to electron transfer-induced changes in the acidity/basicity, which leads to corresponding changes in the protonation and charge state of the molecules (Steenken 1992). In addition to differences in the chemical reactivity of a molecule (or radical) for its various protonation states, the source of the proton is also an important consideration. For example, in aqueous solutions of nucleobases, the proton exchange partner is bulk water. However, in DNA, extra-pair hydrogen bonds between the O and N heteroatoms are involved with water molecules in the hydration shell of the DNA and, in the case of double-stranded segments of DNA, the complementary base in the opposite strand can be an important source for intra-pair proton transfer reactions (Steenken 1992). Electron migration along DNA can therefore be influenced by competing proton transfer reactions occurring within DNA base pairs and between DNA and bulk solvent.

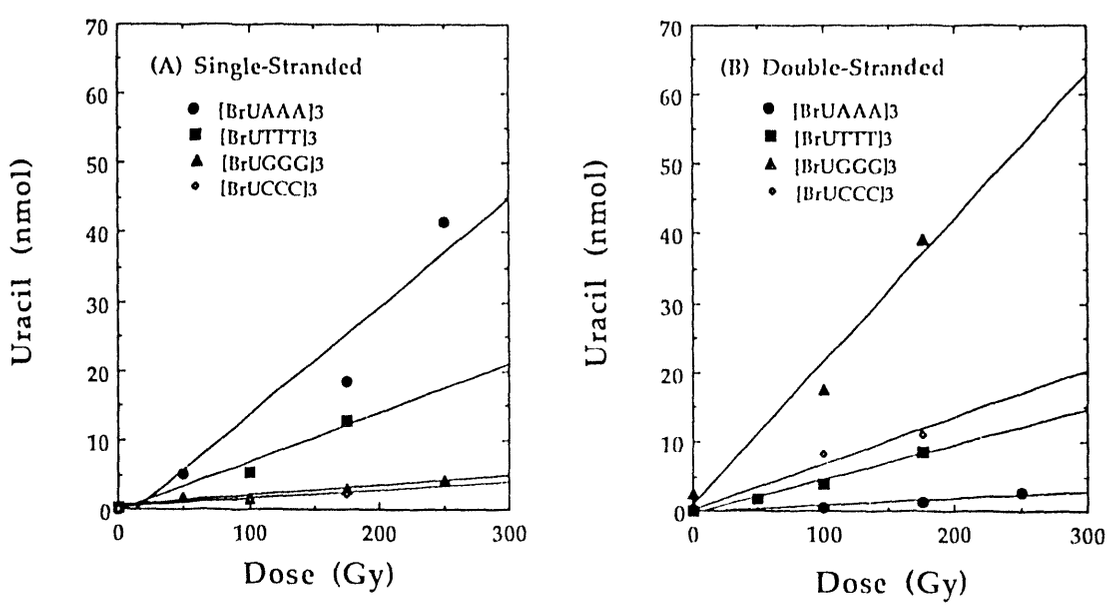

FIGURE 2. Effects of DNA Base Sequence on Electron Migration. Yields of uracil from samples of oligonucleotides 5′-[BrU$(X)_3]_3$-3′ (where X = adenine, guanine, thymine, or cytosine) saturated with nitrogen and irradiated with ^{60}Co gamma rays in aqueous solution containing 0.4 M t-butanol are plotted as a function of radiation dose in the single-stranded (A) or double-stranded (B) conformation. Oligonucleotides containing 5-BrU were constructed using solid phase synthesis. Yields are identified by symbols labeled with the 5-BrU-containing strand.

Migration Distances Along DNA in Irradiated Solutions

The distance over which the electron would migrate was determined using a series of oligonucleotides containing 5-BrU at selected positions with guanine spacers (i.e., $[BrU(G)_n]_3$, where n=3, 5, 7, 9). Oligonucleotides containing only guanine were used in accordance with data illustrated in Figure 2B, which reveal that these samples, annealed with their complements, had the greatest uracil yield for double-stranded oligonucleotides. Gas chromatography-mass spectrometry was used to measure 5-BrU destruction as a function of radiation dose, and linear regression analysis was used to calculate the radiation chemical yield of 5-BrU destruction. Slopes of the regression lines then were plotted as a function of the number of guanine bases in the spacer region separating the 5-BrU moieties. A significantly lower amount of 5-BrU destruction was evident for oligonucleotides with 9 base spacers compared to oligonucleotides having 3, 5, or 7 base spacers (Figure 3). This observation suggested that the average distance for migration does not extend beyond 3 to 4 bases assuming that migration occurs as efficiently in either direction along the DNA molecule. The migration distance could increase to 7 bases if migration proceeds in only one direction.

In another series of experiments, different amounts of 5-BrU were substituted for thymine in medium used to grow *Escherichia coli* cells, and average electron migration distances were assessed in *Escherichia coli* DNA extracted and irradiated in solution, or irradiated in cells (Beach *et al.* in press). Bromide ion release was assayed using x-ray fluorescence spectrometry (which actually measures bromine atoms) following irradiation. By varying the amount of 5-BrU in the medium, hence the amount incorporated into the DNA, the average distance between 5-BrU molecules was systematically changed and, because the number of 5-BrU/electron reactions was monitored by the amount of bromine released, the maximum average electron migration distance along the 5-BrU-DNA could be estimated. Using this approach, the maximum average electron migration distance in aqueous solutions of 5-BrU-substituted DNA was 6.5 to 10 base pairs. Similar methods revealed charge migration in 5-BrU-substituted DNA in irradiated *Escherichia coli* cells and the maximum average migration distance was 5 to 6 base pairs (Figure 4).

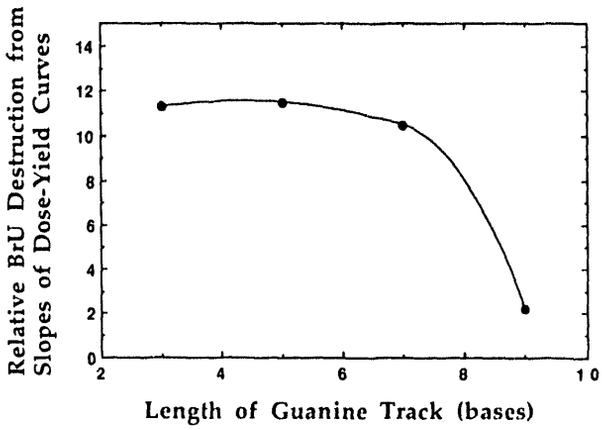

FIGURE 3. Migration Distance for Electrons in a Sequence Containing Guanine Residues in 5-BrU-Substituted Oligonucleotides. Relative destruction of 5-BrU in double-stranded oligonucleotides 5′-$[BrU(G)_n]_3$-3′ (where n=3, 5, 7, or 9) is plotted as a function of the number of guanines between 5-BrU molecules. Samples were irradiated in aqueous solution containing 0.4 M t-butanol. Data represent relative slopes of dose-yield curves.

Preferential Migration of Electrons in the 5′ to 3′ Direction Along DNA

Analysis of the extent of radiolytic destruction of 5-BrU revealed that electron migration occurred efficiently over a distance of 3 to 4 guanine bases assuming that migration could occur as efficiently in the 5′ to 3′ direction as in the 3′ to 5′ direction. The migration distance could increase to 7 bases if migration

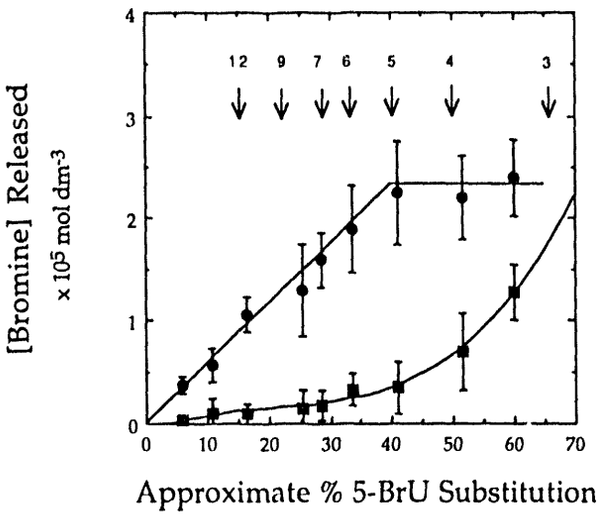

FIGURE 4. Average Migration Distance of Electrons in 5-BrU-Substituted DNA Irradiated in *Escherichia coli* Cells. Radiation-induced release of bromide as a function of approximate 5-BrU substitution for *Escherichia coli* cells irradiated under nitrogen in aqueous solutions containing 0.1 M t-butanol. The lower curve contains the control data and the upper curve is control-subtracted. The arrows running through the upper part of the graph mark the maximum number of base distances an electron would have to travel in order to reach a 5-BrU molecule, assuming only intrastrand electron migration and assuming that the electron could migrate in either direction.

proceeded preferentially in only one direction. To determine whether electron migration could occur preferentially in one direction along DNA, we synthesized oligonucleotides in which electrons were permitted to move only in one direction. Cytosine acts as an electron sink (Figure 2), therefore, electrons would be unable to migrate past them. Oligonucleotides of the following sequence were synthesized: 5′-CCC(G)$_7$BrUC-3′ and 5′-CBrU(G)$_7$CCC-3′, which permit electrons to migrate only in the 5′ to 3′, or 3′ to 5′ direction, respectively. Appropriate complimentary oligonucleotides were synthesized, annealed to create double-stranded DNA, and used for irradiations. Subsequent gas chromatography-mass spectrometric analysis for uracil formation revealed a significant radiation chemical yield of uracil in 5′-CCC(G)$_7$BrUC-3′, but very little uracil was formed in 5′-CBrU(G)$_7$CCC-3′ (Figure 5). Greater uracil yields in 5′-CCC(G)$_7$BrUC-3′ suggested that electrons are capable of preferential migration along DNA containing a segment of guanine bases in the 5′ to 3′ direction. Computer simulation of the relationship between the guanine base immediately adjacent to 5-BrU and the 5-BrU molecule indicates that this preferential migration occurs because of greater overlap of the pi-electron clouds of the DNA bases (Figure 6). This simulation implies that solvated electrons resulting from water radiolysis, once captured by the purines and pyrimidines in DNA, can move along the DNA in the pi-electron cloud created by the stacked DNA bases.

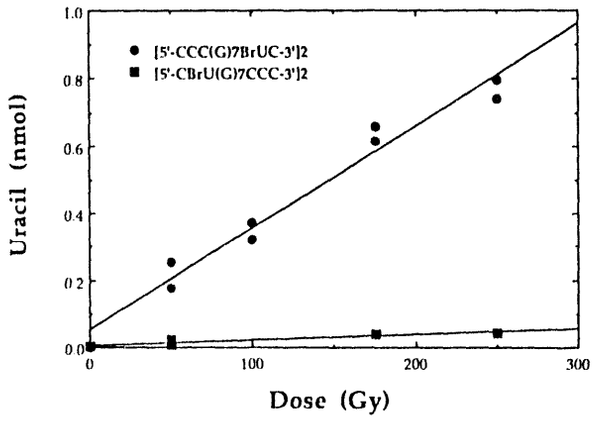

FIGURE 5. Preferential Migration Direction for Electrons in DNA. Oligonucleotides 5′-CCC(G)$_7$BrUC-3′ and 5′-CBrU(G)$_7$CCC-3′, specifically designed to permit electron migration in the 5′ to 3′ or 3′ to 5′ direction, respectively, were annealed to appropriate complementary DNA strands, saturated with nitrogen, and irradiated in aqueous solution containing 0.4 M t-butanol. Uracil yields, as measured by gas chromatography-mass spectrometry methodology, are greater for the oligonucleotide containing 5-BrU 3′ to the guanine tract, suggesting a 5′ to 3′ direction for migration of the electron along DNA.

Consequences of Electron Migration as a Component of Radiation-Induced DNA Damage

Electron migration is an important process underlying the distribution of radiation damage in DNA, and could help to explain how a non-random distribution of DNA damage occurs following energy deposition by stochastic processes. The contribution of solvated electrons to free radical-induced damage to DNA represents a uniquely different mechanism leading to oxidative DNA damage than that of other physical agents such as ultrasonic cavitation (Fuciarelli *et al.* submitted*) or chemical agents such as hydrogen peroxide (Blakely *et al.* 1990). Additionally, the distribution of DNA damage is considerably different with these agents; ionizing radiation creates locally multiply damaged sites and hydrogen peroxide exposure leads to formation of singly damaged sites along the DNA. In cells, singly damaged sites on DNA would be much easier to repair by enzymatic processes than multiply damaged sites, such as those generated by exposure to ionizing radiation. Multiply damage sites in DNA demand a significantly more complex form of enzymatic processing for repair. Increased radiosensitivity of cells containing 5-BrU-substituted DNA (Kinsella *et al.* 1984) could be a consequence of electron migration along the DNA. Increased radiosensitivity potentially could result from increased production of double-strand breaks as a result of migration of radiation damage along one strand of DNA to a position located opposite a single-strand break in the complementary strand within a locally multiply damaged site. However, alternative mechanisms leading to production of

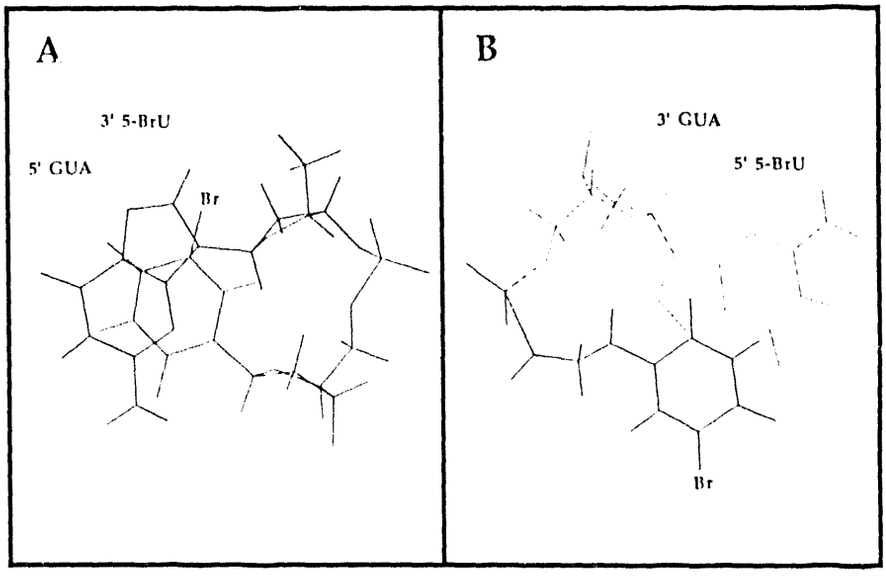

FIGURE 6. Differential Overlap of pi-Electron Clouds in DNA. The orientation of guanine and 5-BrU were simulated using computer techniques depending upon whether the guanine is 5′ (A) or 3′ (B) to the 5-BrU. If the guanine moiety is 5′ to the 5-BrU, then more overlap of the pi-electron cloud occurs. This may explain why the radiation-induced yield of uracil is greater in 5′-CCC(G)$_7$BrUC-3′ than in 5′-CBrU(G)$_7$CCC-3′ as illustrated in Figure 5.

a single-strand break on the opposite strand to that containing 5-BrU involving a radical transfer reaction of the reactive uracilyl radical cannot be discounted.

References

Anderson, R. F., K. B. Patel, and W. R. Wilson. 1991. Pulse radiolysis studies of electron migration in DNA from DNA base-radical anions to nitroacridine intercalators in aqueous solution. *J. Chem. Soc. Faraday Trans.* 87: 3739-3746.

Beach, C., A. F. Fuciarelli, and J. D. Zimbrick. Electron migration along 5-bromouracil-substituted DNA irradiated in solution and in cells. *Radiat. Res.* (in press).

Beach, C., A. F. Fuciarelli, and J. D. Zimbrick. Radiolysis of 5-bromouracil-substituted *E. coli* DNA: Quantitation of released bromide by an ion specific electrode. PNL-SA-23236, Pacific Northwest Laboratory, Richland, Washington. *Radiat. Environ. Biophys.* (submitted).

Blakely, W. F., A. F. Fuciarelli, B. J. Wegher, and M. Dizdaroglu. 1990. Hydrogen peroxide-induced base damage in deoxyribonucleic acid. *Radiat. Res.* 121:338-343.

Fuciarelli, A. F., E. C. Sisk, R. J. Thomas, and D. L. Miller. DNA base damage induced by ultrasonic cavitation. PNL-SA-23113, Pacific Northwest Laboratory, Richland, Washington. *Free Radical Biol. & Med.* (submitted[a]).

Fuciarelli, A. F., E. C. Sisk and J. D. Zimbrick. Electron migration in gamma-irradiated solutions of DNA. *Int. J. Radiat. Biol.* (in press).

Fuciarelli, A. F., D. A. Jett, J. L. Grady, E. C. Sisk, M. K. Bowman, and J. D. Zimbrick. Hydrogen atom donation in irradiated solutions containing 5-bromouracil and in 5-bromouracil-substituted oligonucleotides. PNL-SA-23655, Pacific Northwest Laboratory, Richland, Washington. *Radiat. Res.* (submitted[b]).

Kinsella, T. J., J. B. Mitchell, A. Russo, C. Morstyn, and E. Glatstein. 1984. The use of halogenated thymidine analogs as clinical radiosensitizers: Rationale, current status and future prospects. *Int. J. Radiat. Oncol. Biol. Phys.* 10:1399-1406.

Shragge, P. C., H. D. Michaels, and J. W. Hunt. 1971. Factors affecting the rate of hydrated electron attack on polynucleotides. *Radiat. Res.* 47:598-611.

Steenken, S. 1992. Electron-transfer-induced acidity/basicity and reactivity changes of purine and pyrimidine bases. Consequences of redox processes for DNA base pairs. *Free Radical Res. Com.* 16:349-379.

Zimbrick, J. D., J. F. Ward, and L. S. Myers. 1969. Studies on the chemical basis of cellular radiosensitization by 5-bromouracil substitution in DNA. II. Pulse- and steady state radiolysis of bromouracil and thymine. *Int. J. Radiat. Biol.* 16:505-523.

Radon Hazards in Homes

Principal Investigator: F. T. Cross

Other Investigators: R. L. Buschbom, G. E. Dagle, K. M. Gideon, R. A. Gies, and G. Singh[a]

Technical Assistance: C. R. Petty

Histopathological data have been compiled on rats exposed to 80 working-level months (WLM; see footnote d, Table 1) of radon progeny, at 10- and 100-working-level (WL; see footnote d, Table 1) concentrations, in combination with uranium ore dust. The possibility that risks are diminished with protracted low-level radon exposures is not evident in the raw tumor data at 80 WLM and at 10- and 100-WL concentrations. Histopathological data on rats exposed to 80 WLM at 10-WL concentrations show a significant ($P < 0.05$) increase in lung tumor incidence (3%) from that of control rats (approximately zero); no significant exposure-related changes occurred in the nose, larynx, or trachea when rats were tracked throughout their lives. Statistical risk and carcinogenesis modeling comparisons with histopathological data for 80-WLM exposures at 100-WL concentrations are currently underway. Collaborative studies were initiated with Dr. G. Singh[a] to clarify the histogenesis of radon-induced lung tumors. Preliminary findings suggest that there are differences in the histogenesis of radon- vs. plutonium-induced rat lung tumors.

Lung cancer incidence and deaths from degenerative lung disease are significant among uranium miners, but the cause-effect relationships for these diseases are based on data insufficient to determine risks of environmental radon exposures. More recent data on humans suggest that radon also is implicated in other organ diseases, although confirmatory data are lacking in animal systems. This project previously identified agents or combinations of agents (both chemical and radiological), and their exposure levels, that produced respiratory tract and other organ lesions in mine-simulation experiments. The project's current emphasis is on the development of lung carcinoma and collaborative mechanistic data for environmental exposures.

Wistar Rat Exposure Protocols

The 6000 Series (1000-working-level, WL) and 7000 Series (100-WL) mine-simulation experiments (Table 1) were designed to develop the relationships between response and exposure to radon progeny (at two rates of exposure), and to carnotite uranium ore dust. The 8000 Series (100-WL) mine-simulation experiments (Table 2) were designed to extend the exposure-response relationships to cumulative exposure levels comparable to current conditions in uranium mines, and to lifetime environmental exposures. The 9000 Series mine-simulation experiments (Table 3) continued the "low-dose" studies at exposure rates comparable to former occupational working levels (10 WL). These experiments

(a) Department of Veterans Affairs Medical Center (DVAMC), Pittsburgh, Pennsylvania

TABLE 1. Exposure-Response Relationship Study for Radon-Progeny Carcinogenesis in Rats (6000 and 7000 Series Experiments)

Number of Animals[a]			
6000 Series	7000 Series	Exposure Regimen[b,c]	Total Exposure, WLM[d]
64	0	1000 WL radon progeny 15 mg/m^3 uranium ore dust	10,240
56	32	1000 WL radon progeny 15 mg/m^3 uranium ore dust	5120
56	32	1000 WL radon progeny 15 mg/m^3 uranium ore dust	2560
56	32	1000 WL radon progeny 15 mg/m^3 uranium ore dust	1280
88	64	1000 WL radon progeny 15 mg/m^3 uranium ore dust	640
152	128	1000 WL radon progeny 15 mg/m^3 uranium ore dust	320
64	96	Controls	

(a) Number of animals is sufficient to detect the predicted incidence of lung tumors at the 0.05 to 0.1 level of significance, assuming linearity of response between 0 and 9200 WLM (see footnote d) and 0.13% spontaneous incidence.

(b) Exposure rate, 90 hr/wk; planned periodic sacrifice.

(c) Study is repeated at 100-WL (see footnote d) rate (without periodic sacrifice) to augment previous limited exposure-rate data (7000 Series experiments).

(d) Working level (WL) is defined as any combination of the short-lived radon progeny in 1 liter of air that will result in the ultimate emission of 1.3 x 10^5 MeV of potential alpha energy. Working-level month (WLM) is an exposure equivalent to 170 hours at a 1-WL concentration. Previous exposure at 900 WL for 84 hr/wk to 9200 WLM produced an 80% incidence of carcinoma.

help to evaluate the hypothesis that sublinear risk relationships exist at low exposure levels and low exposure rates. In addition, concurrent exposures to varying levels of uranium ore dust also test the hypothesis that irritants (both specific and nonspecific) act synergistically with radiation exposures. The exposures of 6000, 7000, and 8000 Series animals are complete. Exposures of 9000 Series animals were suspended with the 80-WLM and 15-mg/m^3 ore-dust exposures to allow analyses of existing data.

Exposures of rats to uranium ore dust alone (10,000 Series experiments, Table 4) are complete. The ore-dust studies reported last year (Cross *et al.* 1993) addressed the potential link of silica exposures to lung cancer. Exposures of rats to radon progeny, uranium ore dust, and cigarette-smoke mixtures (initiation-promotion-initiation [IPI; 11,000 Series, Table 5] experiments) are complete. This study continues with an investigation of the IPI relationships of radon and cigarette-smoke exposures. Exposures of female rats (12,000 Series experiments, Table 6) are also complete. This study continues with a comparison to risk data obtained from exposures of male animals using mine-simulation aerosols. Tables 1 through 6 present the actual numbers of animals (including serially sacrificed animals) used at each exposure level.

TABLE 2. Low Exposure-Response Relationship Study for Radon Progeny Carcinogenesis in Rats (8000 Series Experiments)

Number of Animals[a]	Exposure Regimen[b]	Total Exposure, WLM[c]
96	100 WL radon progeny, 15 mg/m^3 uranium ore dust	640[d]
396	100 WL radon progeny, 15 mg/m^3 uranium ore dust	320[d]
192	100 WL radon progeny, 15 mg/m^3 uranium ore dust	160
384	100 WL radon progeny, 15 mg/m^3 uranium ore dust	80
480	100 WL radon progeny, 15 mg/m^3 uranium ore dust	40
544	100 WL radon progeny, 15 mg/m^3 uranium ore dust	20
192	Controls	

(a) Number of animals is sufficient to detect lung tumors at the 0.05 to 0.1 level of significance, assuming linearity of response between 0 and 640 WLM (see footnote c) and 0.13% spontaneous incidence.
(b) Exposure rate, 90 hr/wk; planned periodic sacrifice.
(c) Previous exposures indicated a tumor incidence of 16% at 640 WLM. Working level (WL) is defined as any combination of the short-lived radon progeny in 1 liter of air that will result in the ultimate emission of 1.3×10^5 MeV of potential alpha energy. Working-level month (WLM) is an exposure equivalent to 170 hours at a 1-WL concentration.
(d) Repeat exposure is for normalization with Table 1 data.

TABLE 3. Ultralow Exposure-Rate Study for Radon Progeny Carcinogenesis in Rats (9000 Series Experiments)

Number of Animals[a]	Exposure Regimen[b]	Total Exposure, WLM[c]
64	10 WL radon progeny, 15 mg/m^3 uranium ore dust	320
64	10 WL radon progeny, 3 mg/m^3 uranium ore dust	320
384	10 WL radon progeny, 15 mg/m^3 uranium ore dust	80
384	10 WL radon progeny, 3 mg/m^3 uranium ore dust	80
512	10 WL radon progeny, 15 mg/m^3 uranium ore dust	20
512	10 WL radon progeny, 3 mg/m^3 uranium ore dust	20
192	Controls	

(a) Number of animals is sufficient to detect lung tumors at the 0.05 to 0.1 level of significance, assuming linearity of response between 0 and 640 WLM (WLM, see footnote c; tumor incidence is approximately 16% at 640 WLM) and 0.13% spontaneous incidence.
(b) Exposure rate, 90 hr/wk; planned periodic sacrifice.
(c) Working level (WL) is defined as any combination of the short-lived radon progeny in 1 liter of air that will result in the ultimate emission of 1.3×10^5 MeV of potential alpha energy. Working-level month (WLM) is an exposure equivalent to 170 hours at a 1-WL concentration.

TABLE 4. Control Study for Uranium-Ore-Dust Carcinogenesis in Rats (10,000 Series Experiments)

Number of Animals	Exposure Regimen[a]
96	15 mg/m^3 uranium ore dust
64	Sham-exposed controls

(a) Exposures, 12 to 18 months at 72 hr/wk; planned periodic sacrifice

Rat Respiratory Tract Pathology

Histopathology was completed on 9000-Series life-span rats exposed to 80 WLM and 15 mg/m^3 of uranium ore dust. Changes related to radon-progeny exposure included a 3% incidence of primary lung tumors; no primary lung tumors were found in control rats (Table 7). There were no significant exposure-related changes in the nose, larynx, or trachea. It is unclear whether the minimal increases in the incidence of tumors of the skin, kidneys, adrenals, and intestines were also related to exposure.

The lungs of the radon-progeny-exposed rats had small disseminated foci of alveolar macrophages with phagocytosed uranium ore dust. Focal interstitial reaction, with increased prominence of alveolar epithelium and thickened alveolar septa, was present in 106 (29%) of the exposed rats compared with 14 (18%) of the control rats; the group average severity in exposed and control rats was 0.2 and 0.1[a], respectively. An increased incidence of adenomatosis, composed of a focal proliferation of alveolar epithelial cells without disruption of normal architecture, was present in 36 (10%) of the exposed rats compared with one in the control group rats. A very small nodule of squamous

TABLE 5. Initiation-Promotion-Initiation (IPI) Protocol for Radon (R), Dust (D), and Cigarette-Smoke (S) Inhalation Exposure of Rats (11,000 Series Experiments)[a]

	Duration of Exposure, weeks					
Group	0	4	8	17	21	25
1	R + D---------- >					
2	R + D----- >					R + D- >
3	R + D---- > S---------- >					R + D- >
4	R + D---------- > S---------- >					
5	S---------- >				R + D---------- >	
6	D---------- > S---------- >					

(a) Moderately low concentrations of uranium ore dust (D) accompany radon exposures as the carrier aerosol for radon progeny; sham-exposed control animals (not shown) are included in each exposure group. Ten animals from each exposed or sham-exposed group of 64 rats are killed at 25, 52, and 78 weeks to evaluate developing lesions. Radon-progeny exposures: 100 WL (see footnote b), 320 cumulative WLM; uranium-ore-dust concentration: 5 mg/m^3; cigarette smoke exposures from Kentucky 1R4F cigarettes: 1 hr/day, 5 days/week, for 17 weeks.

(b) Working level (WL) is defined as any combination of the short-lived radon progeny in 1 liter of air that will result in the ultimate emission of 1.3 x 10^5 MeVof potential alpha energy. Working-level month (WLM) is an exposure equivalent to 170 hours at a 1-WL concentration.

(a) Lesions were graded on a scale of 1 through 5: 1 = very slight; 2 = slight; 3 = moderate; 4 = marked; and 5 = extreme.

TABLE 6. Exposure of Female Rats to Radon Progeny and Uranium Ore Dust (12,000 Series Experiments)

Number of Animals	Exposure Regimen[a]
96	100 WL radon progeny; 640 WLM 5 mg/m^3 uranium ore dust
96	Sham-exposed controls

(a) Exposure rate, 72 hr/wk; planned periodic sacrifice. Working level (WL) is defined as any combination of the short-lived radon progeny in 1 liter of air that will result in the ultimate emission of 1.3 x 10^5 MeV of potential alpha energy. Working-level month (WLM) is an exposure equivalent to 170 hours at a 1-WL concentration.

metaplasia also was present in the periphery of a lung lobe from an exposed rat. One exposed rat had two separate primary tumors, and of the five adenocarcinomas, one was fatal (a papillary adenocarcinoma). Two of the three epidermoid carcinomas also were fatal; however, none of the lung tumors had metastasized to regional lymph nodes or systemic organs.

Mediastinal lymph nodes had an accumulation of phagocytosed uranium ore dust that generally replaced medullary areas of the node and was associated with a diffuse hyperplasia of the cortex, with small lymphocytes. Macrophages with phagocytosed uranium ore dust and hyperplastic lymphocytes were present in perinodal areas in the more severely affected lymph nodes; fibrosis, composed of strands of mature collagen fibers, was present in the medullary areas. Cystic degeneration and hemorrhage generally occurred in lymph nodes without heavy dust accumulation, and presumably in nodes not draining the lungs. A primary hemangiosarcoma in a mediastinal lymph node of an exposed rat was not associated with a heavy deposition of uranium ore dust.

The nose, larynx, and trachea had no lesions clearly related to radon-progeny exposure. Focal chronic infiltration, composed of lymphocytes beneath the surface epithelium, was frequently observed in both exposed and control rats. Very small amounts of focal squamous metaplasia was observed in the larynx of one rat, and in the trachea of three exposed rats. Epithelial hyperplasia was present in the larynx of three exposed rats and one control rat, as well as the trachea of one exposed and one control rat. Metastatic calcification was common in the tracheal mucosa of both exposed and control rats, and generally correlated with metastatic calcification in the lung, and with chronic nephropathy. A nasal adenocarcinoma was present in one exposed rat; a squamous carcinoma was present in the nose of a control rat.

TABLE 7. Summary of Primary Tumors of the Respiratory Tract in Life-Span Animals (9000 Series Experiments).

		Extrathoracic Tumors[a]			Lung Tumors							
Nominal Exposure, WLM	Nominal Ore Dust Concen., mg/m^3	Nasal	Laryngeal	Tracheal	No. Animals Examined	No. of Animals to be Examined	Adenoma	Adenocarcinoma	Epidermoid Carcinoma	Adenosquamous Carcinoma	Sarcoma[a]	Animals with Lung Tumors %
80	15	1/348[b]	0/203	0/333	365	0	3	5	3	0	0	3.0
320[c]	3	0/50	0/36	0/48	51	0	0	8	1	0	1	16
320	15	0/50	0/41	0/46	52	0	1	4	4	1	0	19
Controls		1/108	0/80	0/99	110	0	0	0	0	0	0	0

(a) One mesothelioma in mediastinum, considered a primary tumor of the lung.
(b) Number tumors/number examined.
(c) One oropharyngeal squamous carcinoma, considered related to radon-progeny exposure; found in tissue not routinely sectioned for histopathology.

Statistical risk and carcinogenesis modeling comparisons with histopathological data for 80-WLM exposures at 100-WL concentrations (Table 8) currently are underway.

Collaborative Studies

The histopathologic features of radon-induced lung tumors in rats were discussed at the Joint BETG/EULEP Workshop on Lung Pathology in Paris, October 12-13, 1992. This workshop was organized jointly by the Biological Effects Task Group (BETG; G.E. Dagle, PNL co-chair) and by the European Late Effects Projects group (EULEP; R. Masse, COGEMA[a] co-chair). The purposes of the workshop were to compare histopathologic features of lung tumors in the rat following exposure to ionizing radiation, and to review future research priorities for radiation-induced carcinogenesis. (Dagle *et al.* 1993).

Although the diagnostic criteria currently in use were agreed upon by the participants of the workshop, it was uncertain whether alpha-irradiation from radon and from actinides affect the same target cells or regions in the rat lung. Current evidence indicated that alveolar epithelial Type II cells were the most frequent target cells for the long-lived actinides; target cells were not specifically identified for radon exposure. Other possible target cells listed in the workshop report included cells arising from bronchi, bronchioles, the bronchiolar-alveolar junction, endothelium, mesenchyme, and mesothelium.

Because a high priority was given at the workshop for research needs to identify the target cells of alpha irradiation, collaborative studies were initiated with Dr. G. Singh to study the histogenesis of radon-induced lung tumors. It should be noted that the dose distribution from radon exposure in the respiratory tract is different from that produced by the long-lived actinides. This difference could possibly lead to a different histogenesis of the lung tumors.

In preliminary studies with Dr. Singh, lung sections from eight rats with radon-induced lung tumors were stained with monoclonal antibodies against Clara cell antigen or anti-rat surfactant antibodies for alveolar epithelial Type II cells. Surfactant was the principal antigen stained in cells forming lung tumors, suggesting that alveolar epithelial cells may be the principal cell type in lung tumors induced with radon as well as

TABLE 8. Current Summary of Primary Tumors of the Respiratory Tract in Life-Span Animals (8000 Series Experiments)

		Extrathoracic Tumors[a]			Lung Tumors							
Nominal Exposure, WLM	Nominal Ore Dust Concen., mg/m^3	Nasal	Laryngeal	Tracheal	No. Animals Examined	No. of Animals to be Examined	Adenoma	Adeno carcinoma	Epidermoid Carcinoma	Adeno-squamous Carcinoma	Sarcoma[a]	Animals with Lung Tumors %
20	15	0/238[b]	0/158	0/230	246	280	1	1	1	0	0	1.2
40[c]	15	0/289	0/167	0/276	306	156	0	4	1	1	1	2.3
80	15	2/344	0/211	0/327	362	0	0	7	7	0	1	4.1
160	15	0/161	0/97	0/158	171	0	4	5	1	0	1	6.4
320	15	0/74	0/56	0/69	77	0	0	1	0	0	1	2.6
640	15	0/72	0/44	0/71	78	0	5	3	2	1	0	13
Controls		0/122	0/88	0/116	127	45	0	0	1	0	0	0.8

(a) One malignant hemangiopericytoma, one malignant fibrous histiocytoma, and two malignant mesotheliomas considered radon progeny-exposure related.
(b) Number tumors/number examined.
(c) One malignant oropharyngeal hemangiosarcoma, considered radon progeny-exposure related; found in tissue not routinely sectioned for histopathology.

(a) Compagnie Générale des Matières Nucléaires (COGEMA) in France.

with the long-lived actinides. In contrast to described changes in the long-lived actinide-induced lesions, however, there were prominent areas of Clara cell proliferation in the radon-exposed rats, and some evidence of Clara cell antigen expression in lung tumors. These preliminary findings support the hypothesis that rat lung tumors, which can have a varied phenotypic expression that could include bronchiolar as well as alveolar epithelium, arise from indifferent epithelial cells at the bronchiolar-alveolar junction.

References

Cross, F.T., R.L. Buschbom, G.E. Dagle, K.M. Gideon, and R.A. Gies. 1993. Radon hazards in homes. In: *Pacific Northwest Laboratory Annual Report for 1992 to the DOE Office of Energy Research, Part 1, Biomedical Sciences,* pp. 31-37. PNL-8500 Pt. 1, Pacific Northwest Laboratory, Richland, Washington.

Dagle, G.E., P. Fritsch, F.F. Hahn, J.R. Maisin, R. Masse, M. Morin, G. Patrick, and C.L. Sanders. 1993. Report of joint U.S. Department of Energy Biological Effects Task Group and European Late Effects Project Group (BETG/EULEP) Workshop on Lung Pathology, October 12-13, 1992. In: European Late Effects Project Group Newsletter 73, pp. 24-30.

Mechanisms of Radon Injury

Principal Investigator: F. T. Cross

Other Investigators: E. W. Fleck,[a] R. A. Gies, R. F. Jostes, L. H. Lutze,[b] R. P. Schneider, G. L. Stiegler, and L. C. Stillwell

Technical Assistance: C. R. Petty

In this project, we collaboratively conduct dosimetric, molecular, cellular, and whole-animal research relevant to understanding the mechanisms of radon and radon-progeny injury to the respiratory tract. The work in FY 1993 specifically addressed the role of suppressor genes in radon-induced cancers, and the molecular basis of radon-induced mutations in Chinese hamster ovary (CHO) cells and the Big Blue™ transgenic mouse system. Mutations of the p53 tumor suppressor gene in archived radon-induced rat lung adenocarcinomas were lower then suspected based on the frequency of altered p53 protein in human lung cancer. Southern blot and polymerase chain reaction (PCR) exon analysis of radon-induced CHO-hypoxanthine guanine phosphoribosyl transferase (HPRT) mutations were completed. The gross molecular spectrum of radon-induced mutations showed a marked increase in the frequency of deletions relative to that observed in the spontaneous spectrum, but no difference between radon and that obtained with 300-cGy x rays. Twelve *lacI* mutations, which are currently undergoing sequence analysis, were isolated from lung tissue of a Big Blue™ transgenic mouse following inhalation exposures to 960 working-level months (WLM; see footnote a, Table 3) of radon progeny.

Suppressor Gene Studies

In collaboration with Dr. R.P. Schneider at Pacific Northwest Laboratory (PNL), we examined the mutations and expression of the p53 tumor suppressor gene in radon-induced lung adenocarcinomas in rats from previous life-span radon-exposure experiments at PNL. Mutations of p53 were investigated because they are the most commonly observed genetic alterations in human cancers (Levin *et al.* 1991) and because they have been generally observed in chemically induced rodent tumors.

Tissues available for this study were formalin-fixed for varying lengths of time (weeks or months) and embedded in paraffin. DNA was extracted from 25-μm sections of the tissue, and individual exons were amplified and then analyzed for mutations with polymerase chain reaction (PCR) and DNA sequence analysis. As a prelude to this work, we first ascertained the structure of the rat p53 gene and the base sequence of introns near the splice junction sites. This enabled us to synthesize PCR primers with intron sequences for amplification of specific exon sequences. We previously reported that rat p53 lacks intron 6 found in the mouse, human, and *Xenopus* genes (Schneider *et al.* 1993).

Exons 4 through 9 were amplified and screened for mutations with single-strand conformational polymorphism (SSCP) analysis using RNA transcripts of the amplicons. This screening revealed seven potential mutants in exons 5 through 7, the most frequently mutated

(a) Whitman College, Walla Walla, Washington.
(b) University of California, San Francisco, California.

region in the human gene. However, analysis of the base sequence of these exons revealed only one mutation (Table 1), an A-to-T transversion in codon 290 in exon 7, which corresponds to exon 8 in humans and mice. The frequency of mutations was lower than expected; therefore, we are also directly analyzing the sequence of amplicons of exons 5, 6, and 7 from 10 of the tumors in case the SSCP analysis did not detect some mutations. The analysis of exon 6 is not complete, but we have found no additional mutations in exons 5 and 7 from 10 tumors. We have learned that direct sequencing of PCR products by cycle sequencing and automated methods is more efficient than screening by SSCP and then sequencing. This lower-than-expected incidence of p53 mutations agrees with another study on plutonium-induced lung carcinomas in rats at the Inhalation Toxicology Research Institute, Albuquerque, New Mexico (G. Kelly, personal communication). Unlike in humans, mutations of p53 may, therefore, occur only rarely in rats except in some forms of chemically induced cancer.

In Vitro Radon Studies

The PNL *in vitro* radon cell-exposure system was extensively employed in PNL experiments as well as in several collaborative experiments with other laboratories. The collaboration with Dr. E. W. Fleck, Whitman College (Walla Walla, Washington), on molecular analysis of radon-induced CHO-HPRT mutations using Southern blot and PCR exon analysis was completed; all exons except the first were evaluated. Our preliminary work was published in 1992 (Jostes *et al.* 1992); the completed study will be published soon (Jostes *et al.* in press).

The gross molecular spectrum of radon-induced mutations evaluated by these two methodologies indicated a marked difference from the spontaneous spectrum, but no significant differences from that obtained with 300 cGy of x rays. A clustering of deletion breakpoints was noted in the 3′ half of the *hprt* gene. Figure 1 represents the deletion breakpoint locations determined in our study. It is unknown whether the skewed distributions observed in our laboratory and elsewhere represent differential sensitivity of gene regions resulting from the conformational structure of the chromatin, impaired regional repair, increased misrepair, or other factors not considered.

To relate cellular damage to radon exposure, it is necessary to determine hit probabilities for

TABLE 1. Preliminary Results from Analyzing Rat Lung Adenocarcinomas for p53 Mutation[a]

Exons	4	5	6	7	8	9
Number of Tumors Analyzed	19	19	15	21	16	15
Number of Mutants	0	0	0	1[b]	0	0

(a) The exons were individually amplified by PCR and analyzed by SSCP, the mutation was verified by DNA sequence analysis.
(b) Codon 290, AAA → ATA.

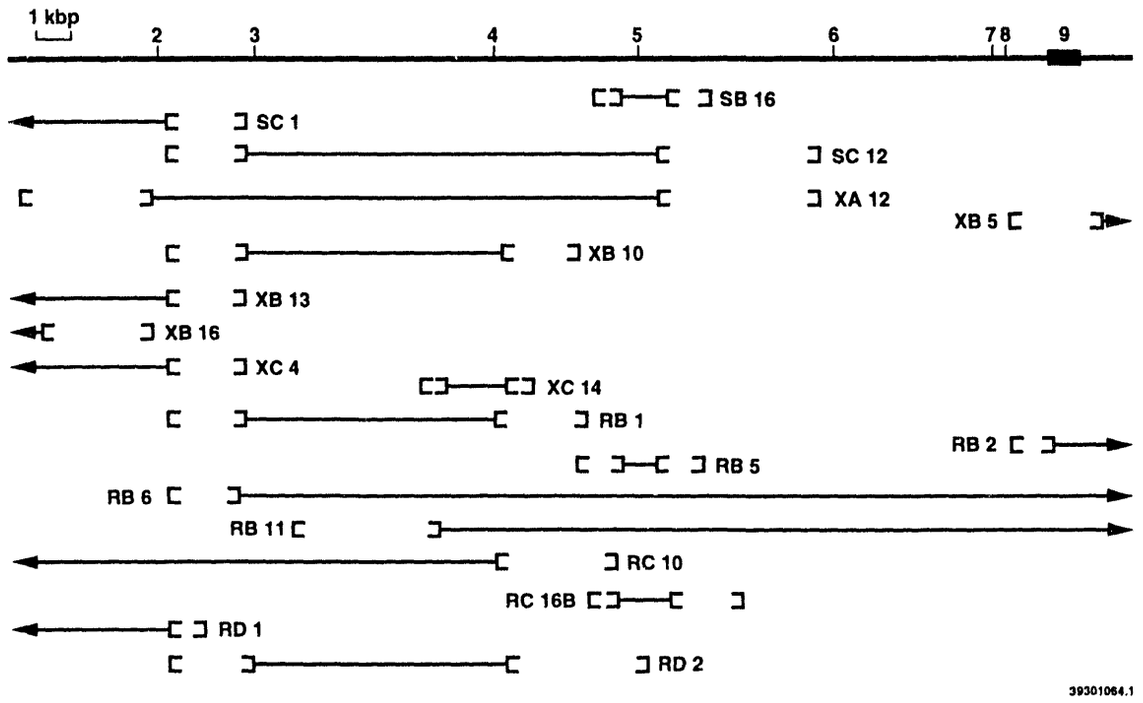

FIGURE 1. Deletion Breakpoint Locations in Radon-Induced CHO-HPRT Mutants with Altered Southern Blot Banding Patterns. The upper line represents 30 kbp of hamster *hprt* gene containing exons 2 through 9. The use of PCR and Southern blot analysis allows the placement of the deletion extent and endpoints on a genetic map of the hamster *hprt*. The alphanumerics next to each deletion represent the strain designation. The brackets represent the uncertainty of location of the endpoint; the dark line represents the extent of the deletion. A left or right arrow represents a deletion that extends outside the *hprt* or into the poorly defined region between exons 1 and 2.

alpha particles to the cell nucleus. Table 2 presents these calculations for alpha traversals of CHO cell nuclei irradiated in PNL's *in vitro* radon suspension system. At the dose (Do) of 0.61 Gy (the dose at which 37% of the cells survive), the average number of traversals was 1.5. This value is closer to that observed with other cells alpha-irradiated in suspension at the Oak Ridge National Laboratory (Ford and Terzaghi-Howe 1993; average number of traversals = ~1.0), and is in contrast with that observed with planar alpha sources and plated cells at the Los Alamos National Laboratory (Raju *et al.* 1991; range = 2.1 to 6.1 traversals). These data *in toto* support the perception that cell geometry is an important consideration in alpha-particle toxicity.

In Vivo Radon Studies

Radon mutation studies in animals included inhalation exposures of Big Blue™ transgenic mice to mixtures of radon progeny and uranium ore dust per the protocol of Table 3. We initiated mutation frequency determination and molecular analysis of the transgenic target sequence in collaboration with Drs. L. H. Lutze (University of California, San Francisco [UCSF]) and R. Winegar (Stanford Research Institute [SRI]), and Drs. R. F. Jostes and G. L. Stiegler (PNL). We have isolated 12 *lacI* mutations, which are currently undergoing sequence analysis, from the lung tissues of a mouse exposed to 960 WLM. Mutation frequency information will provide the relative mutational damage incurred in the various

TABLE 2. Hit Probabilities for Alpha Traversals of CHO Cell Nuclei irradiated in PNL's Radon Suspension System[a]

Number of Hits	Probability
0	23%
1	34%
2	25%
3	12%
≥4	6%
Average number of hits = 1.5	

(a) Calculations are for a Do = 0.61 Gy, cell diameter = 12.8 μm, and nucleus diameter = 6.5 μm; radon decay product activity attached to cells is included in the calculations.

tissues after *in vivo* radon exposure. Sequence analysis of mutations from the different tissues will provide information on whether the initial lesions are processed differently, resulting in different spectra of damage at the base-pair level, and whether the process of nonhomologous recombination, which we have found is used to rejoin radon-induced double-strand breaks in cells in culture, also is observed in cells in intact tissues.

References

Ford, J.R., and M. Terzaghi-Howe. 1993. Effects of ^{210}Po alpha particles on survival and preneoplastic transformation of primary rat tracheal epithelial cells irradiated while in suspension or in the intact tissue. *Radiat. Res.* 136:89-96.

Jostes, R.F., E.W. Fleck, R.A. Gies, T.E. Hui, T.L. Morgan, J.L. Schwartz, J.K. Wiencke, and F.T. Cross. 1992. Cytotoxic, clastogenic, and mutagenic response of mammalian cells exposed *in vitro* to radon and its progeny. In: *Indoor Radon and Lung Cancer: Reality or Myth?* Part 2, Proceedings of the 29th Hanford Symposium on Health and the Environment, F.T. Cross, ed., pp. 555-568. Battelle Press, Columbus, Ohio.

Jostes, R.F., E.W. Fleck, K.P. Gaspar, T.L. Morgan, and F.T. Cross. Southern and PCR analysis of HPRT mutations induced by radon and its progeny. *Radiat. Res.* (in press).

Levin, A.J., J. Momand, and C.A. Finlay. 1991. The p53 suppressor gene. *Nature* 351:453-456.

TABLE 3. Inhalation Exposure Protocol for Radon Mutation Studies in Big Blue™ Transgenic Mice

Number of Animals	Exposure Regimen	Total Exposure, WLM[a]
3	1000 WL radon progeny 5 mg/m^3 uranium ore dust	960
3	1000 WL radon progeny 5 mg/m^3 uranium ore dust	640
3	1000 WL radon progeny 5 mg/m^3 uranium ore dust	320
3	Controls	

(a) Working level (WL) is defined as any combination of the short-lived radon progeny in 1 liter of air that will result in the ultimate emission of 1.3 x 10^5 MeV of potential alpha energy. Working-level month (WLM) is an exposure equivalent to 170 hours at a 1-WL concentration.

Raju, M.R., Y. Eisen, S. Carpenter, and W.C. Inkret. 1991. Radiobiology of α particles. III. Cell inactivation by α-particle traversals of the cell nucleus. *Radiat. Res.* 128:204-209.

Schneider, R.P., J.E. Hulla, and G.L. Stiegler. 1993. Mutation of DNA targets. In: *Pacific Northwest Laboratory Annual Report for 1992 to the DOE Office of Energy Research, Part 1, Biomedical Sciences*, pp. 69-73. PNL-8500, Pacific Northwest Laboratory, Richland, Washington. NTIS, Springfield, Virginia.

In Vivo/In Vitro Radon-Induced Cellular Damage

Principal Investigator: A. L. Brooks

Other Investigators: F. T. Cross, K. M. Groch, R. F. Jostes, and M. A. Khan

Major research efforts are being conducted, both *in vitro* with model cellular and molecular systems and *in vivo* in whole animals, to understand the health effects of inhaled radon and its progeny. This project provides important links relating the data from mechanistic model studies to those derived from animal studies, and renders both types of data more useful in predicting health hazards from radon-progeny exposure in homes. The current studies have been designed to define the relationships between inhalation exposure and radiation dose to the cells of the respiratory tract. This goal is accomplished by comparing cellular damage induced by alpha particles both *in vivo* and *in vitro*.

Animals and cells in culture were exposed to radon and radon progeny. Cellular damage was determined in deep-lung fibroblasts using the micronucleus assay. Research reported last year indicated that it was possible to use *in vivo/in vitro* dose–response data on micronuclei frequency to estimate the dose from inhalation exposure. It was determined that an exposure of 1 working-level month (WLM) *in vivo* caused the same amount of chromosome damage as would be induced by a 0.78-mGy *in vitro* dose. To further define these relationships and enable extrapolation to other species or exposure conditions, it is necessary to understand how physical and biological variables affect the response.

We have addressed several of these variables, including the influence of species, the repair of radon-induced damage, and the influence of aerosol characteristics on deposition, dose, and damage. *In vivo* exposure of rats and Chinese hamsters resulted in 0.58 and 1.80 micronuclei/1000 cell/WLM, respectively. The frequency of micronuclei decreased as a function of time after the end of the inhalation, with an estimated half-life of 30 days for both species. *In vitro* comparisons between rat and human cells indicated that the frequency of micronuclei in both cell lines increased linearly with dose, with slopes of 757 and 130 micronuclei/1000 cells/Gy. The relative biological effectiveness (RBE) of radon exposure with respect to ^{60}Co was determined using two different cell lines: Chinese hamster ovary cells (CHO) and primary cultures of rat lung fibroblasts. The RBE for radon-induced micronuclei was 12.0 and 9.6 for CHO and rat lung fibroblasts, respectively.

Finally, the influence of different carrier aerosols was evaluated to determine how their characteristics altered dose and damage in deep-lung fibroblasts per WLM for inhalation exposure to radon and its progeny. Rats were exposed to either a wax aerosol with 0.2 μ aerodynamic diameter (AMAD) or to uranium-ore dust, AMAD 0.5 $\mu \pm 2.0$. The standard deviation of the wax aerosol is being characterized. The rats exposed to this carrier had more than 2.5 times the amount of chromosome damage in the deep-lung cells per WLM than the animals exposed to uranium-ore-dust aerosols.

This research is addressing the following basic radiobiological questions associated with inhalation of radon (herein taken to mean "radon and its progeny") to help provide a mechanistic understanding of the action of radon on respiratory-tract cells, and to develop better

estimates of the risk from indoor radon exposure:

1. How do low-level exposures and exposure rates influence cancer risk?

2. What is the relationship between exposure and dose to respiratory cells?

3. How does the unattached fraction influence the distribution of dose and damage in the respiratory tract?

4. What is the relative biological effectiveness (RBE) for radon-induced damage with respect to low-LET radiation?

The current report provides information on the last three of these biological questions. Induced chromosome aberrations have been used to detect radiation dose from internally deposited radioactive materials following both experimental and environmental exposure. If chromosome damage is to be a useful indicator of dose, it is essential that damage be measured in the cells at risk or in surrogate cells that receive similar doses. Micronuclei provide a rapid measure of chromosome damage and also are used to evaluate damage in cells exposed either in the whole animal or under well-defined culture conditions.

Experimental Design and Methods

The frequency of micronuclei was measured in rat lung fibroblasts after the methods of Khan and Heddle (1992). Animals or cells were exposed either *in vitro* (Jostes *et al.* 1990) to radon in suspension cultures or after graded exposures to radon by *in vivo* (Cross *et al.* 1984) inhalation exposures. Additional studies were conducted and exposure–response relationships determined using fibroblasts isolated from Chinese hamsters after inhalation of radon. The change in aberration frequency was measured as a function of time after the exposure in both rats and Chinese hamsters. Animals were sacrificed at 0, 15, and 30 days after inhalation of radon and cells placed in culture for 72 hours. The cultures were treated with cytochalasin B to block cytokinesis, then micronuclei frequency determined.

Studies on the sensitivity of lung cells for the induction of micronuclei by radon were done by comparing micronuclei induced by *in vitro* radon exposure of primary cultures of rat deep-lung fibroblast cells to primary human tracheal-bronchial cells.

The RBE was evaluated by first determining that there was no difference in responses for cells exposed to ^{60}Co *in vitro* and *in vivo* using rat lung fibroblasts. Comparisons of the induced frequency of micronuclei then were made using both rat lung fibroblasts and CHO cells exposed *in vitro* to either radon or ^{60}Co.

The influence of aerosol carrier was determined by evaluation of micronuclei in rat lung fibroblasts following inhalation of radon using either wax or uranium-ore-dust carrier aerosols. All cells were scored on coded slides for the induction of micronuclei.

Results and Discussion

Influence of Species (*In Vivo*)

The results of the *in vivo* micronuclei studies that compare rats and Chinese hamsters are shown in Figure 1. The frequency of micronuclei per 1000 binucleated cells per WLM are plotted for the two species and illustrate that, per WLM, Chinese hamsters are three times more sensitive to the induction of micronuclei in the fibroblasts than are rats. This observation is interesting, because the rat is much more sensitive to the induction of lung tumors than the Syrian hamster (Cross *et al.* 1981). Information is needed to determine if the Syrian hamster is similar to the rat or the Chinese hamster for the induction of initial chromosome damage. It may be necessary to grow epithelial cells from the different species to resolve this difference. The current data show that, per WLM, more damage

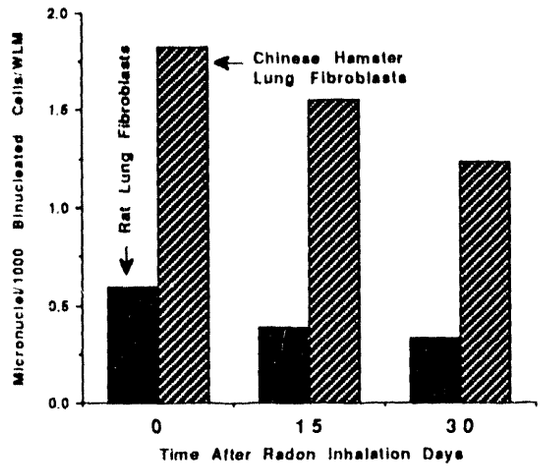

FIGURE 1. The Induction of Micronuclei per WLM Exposure in Primary Cultures of Lung Fibroblast from Rats and Chinese Hamsters Following Inhalation of Radon

is present in the hamster lung than in the rat, and that differences in sensitivity to the induction of cancer may not be related to the amount of initial chromosome damage induced.

Influence of Species (*In Vitro*)

The comparison of the response of human cells with rodent cells for the induction of micronuclei helps determine the influence of species and is essential for between-species extrapolation. Preliminary data have been derived by comparing dose–response relationships for primary human tracheal-bronchial epithelial cells with primary cultures of rat lung fibroblasts for the frequency of micronuclei induced by exposure to radon. Dose to the cell nuclei was calculated for each cell line using the methods of Jostes *et al.* (1991). At the time the *in vitro* radon exposure started, a fraction of the cell population was in the growth phase. The frequency of micronuclei increased linearly with dose (Figure 2), with a slope of 130 and 757 micronuclei/ 1000 binucleated cells/Gy for the human and rat cells, respectively. This shows that the human epithelial cells had less chromosome damage per unit of dose than rat fibroblasts. It is essential to expand this comparison to epithelial cells from additional experimental animal species.

Repair of Radon-Induced Damage

Repair of high-LET-induced cellular damage has been demonstrated using specialized systems such as premature chromosome condensation. We are reporting here on the loss of cells with chromosome damage from a cell population as a function of time after radon exposure. This loss is a form of tissue repair and may be critical to understanding how long damaged cells can remain in a cell population to interact with other insults during the multiple steps involved during cancer induction. Figure 3 illustrates the loss of micronuclei or chromosome aberrations from the rat or Chinese hamster deep-lung fibroblasts or from rat tracheal-epithelial cells as a function of time after *in vivo* inhalation exposure. The graph shows a solid line that represents a 30-day half-time for retention of cells with damage, and it seems that the data can be represented by this solid line. These results could be explained if cell turnover time in these two tissues was close to 30 days, and if cells with micronuclei or chromosome aberrations were eliminated as cells divide.

RBE for Radon-Induced Micronuclei

To estimate RBE, it is necessary to have a direct comparison of the dose–response relationships for radon relative to low-LET radiation; we have used ^{60}Co in this comparison. It is first essential to determine if there are influences of cell isolation on the response measured after either *in vitro* or *in vivo* exposure. Either rats were exposed to ^{60}Co and cells isolated for evaluation of chromosome damage, or the cells were isolated then exposed to ^{60}Co and the frequency of micronuclei determined. The results of this study are shown in Figure 4. No difference in the dose–response relationship was observed as a function of *in vivo* or *in vitro* exposure condi-

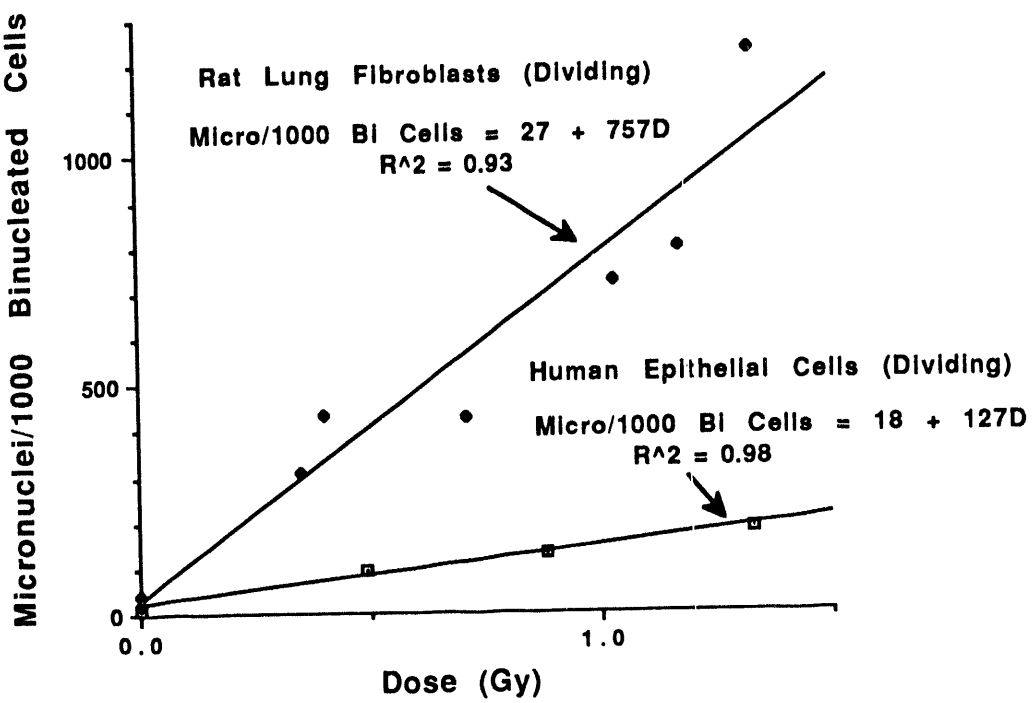

FIGURE 2. Radon-Induced Micronuclei in Proliferating Human Tracheal-Bronchial Epithelium and Rat Deep-Lung Fibroblasts

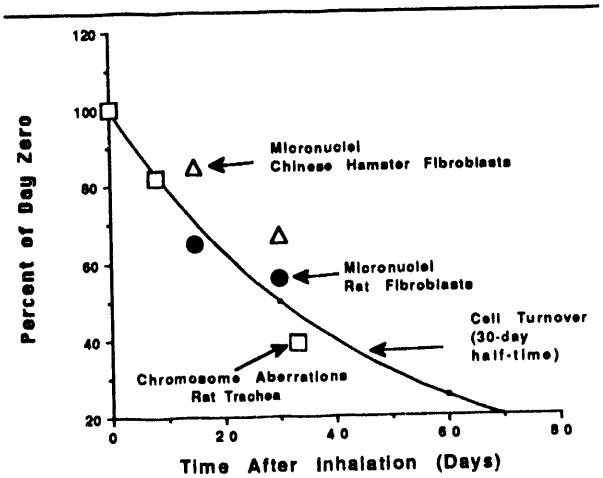

FIGURE 3. Repair of Radon-Induced Chromosome Damage in the Deep-Lung Fibroblasts of Rats or Chinese Hamsters or Tracheal Cells of Rats. The line on the figure represents predicted tissue repair if the cell turnover time is 30 days and if the aberrations are lost at each cell division.

tions. After this was established, it was possible to compare the slopes of the lines derived from exposure of cells *in vitro* to either radon or ^{60}Co, and to suggest that similar relationships would be observed in the animal. Figure 5 shows the results of these studies for both CHO cells and primary rat lung fibroblasts; the RBE for the two systems was 12.0 and 9.6, respectively. Such information suggests that there is little difference between the RBE derived using these two cell types. Understanding RBE relationships will make it possible to relate data from radon exposure to the large data base that exists for low-LET radiation.

Preliminary studies have been conducted to determine if changing the carrier aerosol will change the dose and damage in the deep lung per

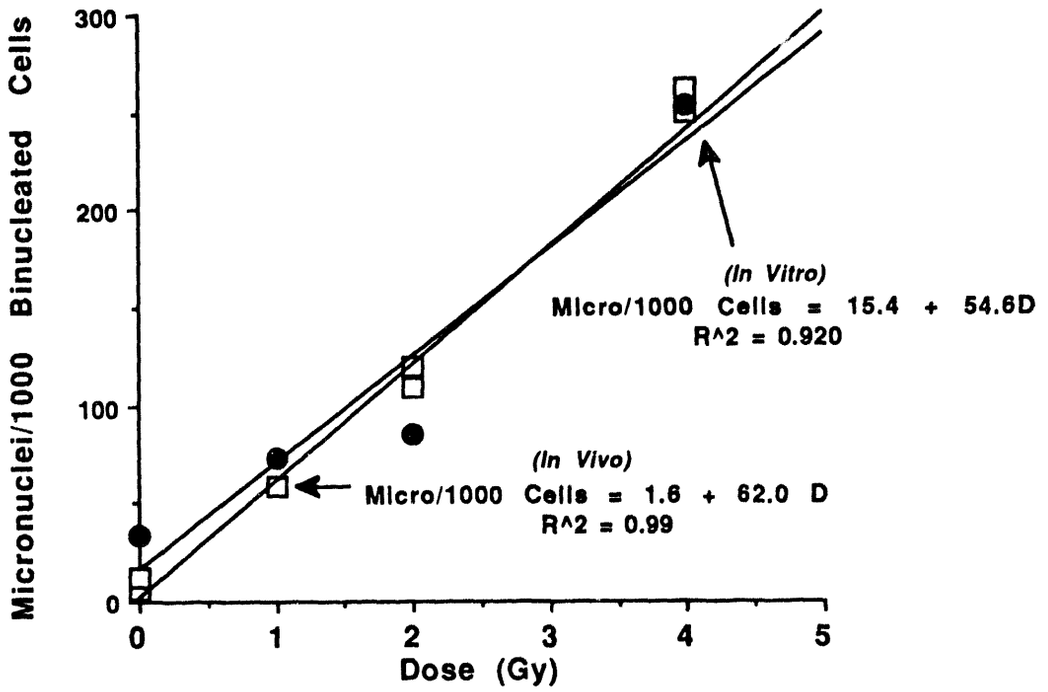

FIGURE 4. The Induction of Micronuclei in Primary Rat Lung Fibroblasts Following ^{60}Co Exposure Either *In Vitro* or *In Vivo*

WLM of exposure. A wax aerosol that is still being characterized was generated as a carrier aerosol. Following inhalation of radon with this erosol, the frequency of micronuclei/1000 cells/WLM was 2.5 times that seen when the rats were exposed using a uranium-ore-dust aerosol. The smaller and more uniform size of the wax aerosol seems to have a marked influence on the amount of dose delivered per WLM of exposure. The frequency of micronuclei induced for animals exposed to the different aerosol carriers per WLM is illustrated in Figure 6.

Summary

Studies have been conducted that demonstrate the usefulness of cellular damage as biomarkers of radiation dose to the lung. These studies demonstrate how exposure can be converted to dose, and include evaluation of the effect of species on primary damage induced in cells. The rate of loss of micronuclei from the lung-cell populations has been measured as an indication of tissue repair. The derivation of an RBE for the induction of micronuclei in two different cell types provides an estimate of the difference in initial damage from high- and low-LET radiation. Finally, the role of aerosol type on dose and cytogenetic damage in the deep lung has been determined. Approaches such as these help validate the usefulness of micronuclei and chromosome aberrations as markers of radiation dose, and will determine how cellular and molecular changes can be used to extrapolate data between species and improve our understanding of the risk associated with the inhalation of radon.

This report forms a basis for directions in the future. Studies are being conducted to compare the response of epithelial cells from different

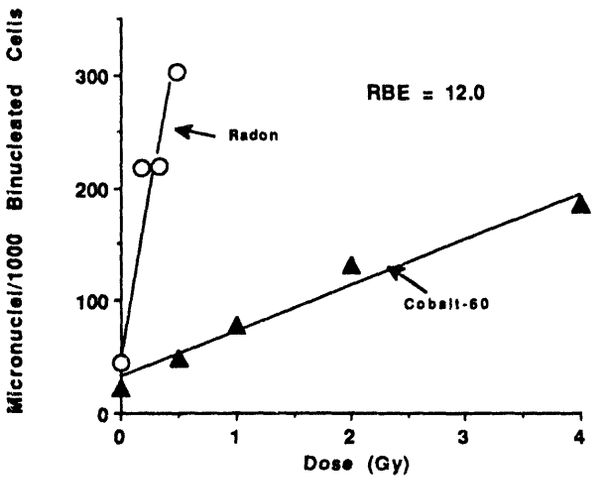

FIGURE 5A. The RBE of Radon Relative to ^{60}Co for the Induction of Micronuclei in CHO Cells

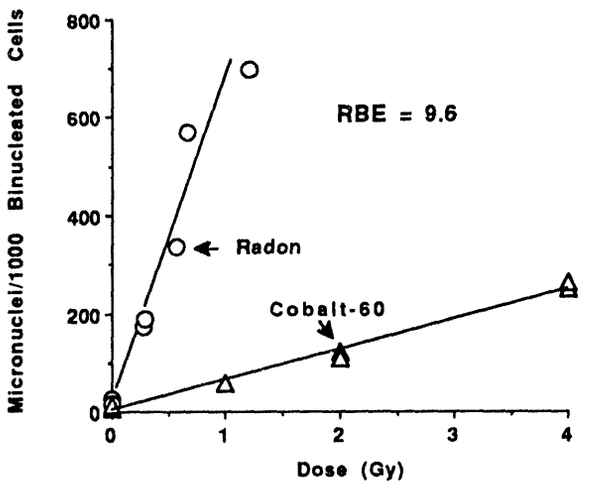

FIGURE 5B. The RBE of Radon Relative to ^{60}Co for the Induction of Micronuclei in Primary Deep-Lung Fibroblasts from Rats

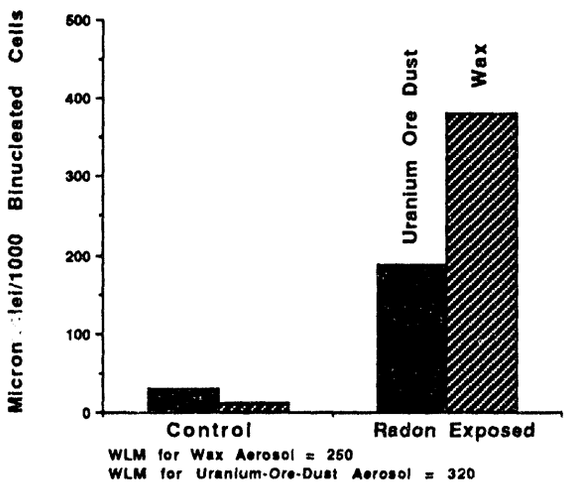

FIGURE 6. The Induction of Micronuclei in Primary Rat Lung Fibroblasts by Inhalation of Radon Using Either a Wax or Uranium-Ore-Dust Carrier Aerosol as a Carrier for the Radon Progeny

species with that in fibroblasts in the deep lung to provide a better link of the short-term data to that for the induction of cancer. Additional information is being derived on the influence of aerosol characteristics on the deposition and damage from inhaled radon. This work will provide links that will make it possible to extrapolate data from the mine to the home environment.

References

Cross, F.T., R.F. Palmer, R.H. Busch, R.E. Filipy, and B.O. Stuart. 1981. Development of lesions in Syrian Golden hamsters following exposure to radon daughters and uranium ore dust. *Health Phys.* 41:135-153.

Cross, F.T., R.F. Palmer, G.E. Dagle, R.H. Busch, and R.L.Buschbom. 1984. Influence of radon daughter exposure rate, unattachment fraction, and disequilibrium on occurrence of lung tumours. *Radiat. Prot. Dosim.* 7:381-384.

Jostes, R.F., T.E. Hui, A.C. James, F.T. Cross, J.L. Schwartz, J. Rotmensch, R. W. Atcher, H.H. Evans, J. Mencl, G. Bakale, and P.S. Rao. 1991. *In vitro* exposure of mammalian cells to radon: Dosimetric considerations. *Radiat. Res.* 127:211-219.

Jostes, R.F., E.W. Fleck, R.A. Gies, T.E. Hui, T.L. Morgan. J.L. Schwartz, J.K. Wiencke, and F.T. Cross. 1992. Cytotoxic, clastogenic, and mutagenic response of mammalian cells exposed *in vitro* to radon and its progeny. In: *Indoor Radon and Lung Cancer: Reality or Myth? Part 2,* F.T. Cross, ed., pp. 555-568. Proceedings of the 29th Hanford Symposium on Health and the Environment, October 1519, 1990, Richland, Washington. Battelle Press, Columbus, Ohio.

Khan, M.A., and J.A. Heddle. 1992. Optimization of the concurrent assay for gene mutation and chromosomal aberrations *in vivo:* Expression time in rats. *Environ. and Mol. Mutagen.* 20:165-171.

Dosimetry and Aerosol Technology of Radon Progeny

Principal Investigator: A. C. James

Other Investigators: A. Birchall[a], K. D. Thrall, T. E. Hui, J. K. Briant, P. K. Hopke[b], and P. T. Wasiolek[c]

These projects (Dosimetry of Radon Progeny and Aerosol Technology Development) develop and validate cellular dosimetry, microdosimetry of cellular components, and physiologically plausible biokinetic tissue models, and the application of these models to provide a coherent and comprehensive assessment of human cancer risks from exposures to radon and thoron progeny. This year we have focused on examining the practical implications of the dosimetry model recently adopted by the International Commission on Radiological Protection for comparing lung-cancer risks as a function of environmental conditions. We have collaborated with the Department of Chemistry, Clarkson University, in interpreting their measurements of the complete activity-size distribution of radon-progeny aerosols in normally occupied homes in terms of (1) the variability of equivalent dose rate to the lungs per unit radon gas concentration; (2) the significance of the so-called radon-progeny "cluster" aerosol, which is intermediate in size between the classical "unattached" and "attached" aerosol modes; and (3) the effects of air cleaning on lung dose. On a more fundamental level, we have analyzed the uncertainties involved in specifying the effective dose per unit exposure for uranium miners, and have compared the lung-cancer risk coefficient given by dosimetry with the best estimate from uranium-miner epidemiology. This comparison implies that use of the recommended ICRP risk-weighting factors results in an overestimate of lung-cancer risk for an adult male exposed at a moderately high dose rate by about a factor of three. Furthermore, if this implication is accepted for radon-progeny exposure, then it should also be considered for all alpha-emitting radionuclides. We propose that, in terms of alpha dose delivered at moderate dose rate to the sensitive lung tissues, the most likely estimate of the absolute lung-cancer risk coefficient is about 0.05 per Gy. In the area of physiologically based pharmacokinetic (PBPK) modeling, we have used experimental animal data to develop a model of dose to the human testes from periodic exposure to elevated concentrations of airborne radon and its progeny.

By improving and applying models relating lung and other tissue doses to conditions of exposure, these projects serve as a focus for integrating findings from the OHER Radon Research Program as a whole into a coherent and comprehensive assessment of the risks of radon-induced cancer in the human population, and for providing practical guidance on issues of environmental monitoring and radiological control. These projects serve as core components of the PNL Radon Research Program, which is directed toward an integrated understanding of radon-induced effects from the molecular/cellular level, through laboratory animals, to the human. Our

(a) Visiting Scientist from the National Radiological Protection Board (NRPB) in the United Kingdom.

(b) Department of Chemistry, Clarkson University, Potsdam, NY 13699.

(c) Current address: Department of Physics, New Mexico Tech., Socorro, NM 87801.

goal is to provide a coordinating dosimetric link between knowledge of the mechanisms of action of alpha particles at the cellular and tissue levels *in vitro* and in animals, the growing epidemiologic database on radon-associated cancer risks in the human, and mechanistic models for projecting cancer risks down to the low exposure rates generally encountered in homes. The development of mechanistic models of the rate processes determining the development and expression of lung and other cancers founded on animal experimentation and human epidemiologic experience with radon exposure will have broad application to radiological protection and risk assessment; the benefits will extend beyond the immediate need for a firm and defensible basis for optimizing control of radon risks in homes.

Finalization of the New ICRP Lung Dosimetry Model

During FY 1993, A. C. James, A. Birchall, T. E. Hui, and J. K. Briant participated in the work of finalizing the International Commission on Radiological Protection's (ICRP's) report on a "Human Respiratory Tract Model for Radiological Protection," and several of its annexes. This work included an assessment of the modeled effective dose to the lungs and upper respiratory tract for an underground uranium miner, and for various subjects exposed to radon and thoron progeny in the home or in an indoor workplace. Our assessment assisted the Commission in their deliberations on the most defensible method of apportioning the lung-cancer risk coefficient for radiological protection purposes between doses received by target cells in bronchial, bronchiolar, and alveolar tissue. Equal apportionment will be recommended in the final report on the new lung model. This report was adopted by the Commission at its meeting in April, 1993, and will be published as ICRP Publication 66 in 1994 (ICRP in press).

Comparison with Previous Models

Figure 1 compares the regionally apportioned lung dose conversion factor (DCF) for exposure to radon-progeny potential alpha energy, in mGy per working-level month (WLM), given as a function of particle size by the new ICRP model with values modeled previously for bronchial-target cells (NRC 1991; N. H. Harley, personal communication 1991). The regionally apportioned dose is significantly lower than that calculated by NRC (1991) for bronchial epithelium, most notably for "unattached" radon progeny (which are actually progeny atoms associated with a small cluster of other atoms or molecules to form a particle of about 0.001 μm in diameter), and for progeny "clusters" (of about 0.01 μm in diameter). For the unattached progeny, the regionally-apportioned dose is about twofold lower than that for bronchial epithelium obtained by Harley. For the progeny clusters, the regionally apportioned dose is similar to Harley's bronchial values, but this is up to about 30% higher for progeny attached to submicron-sized particles.

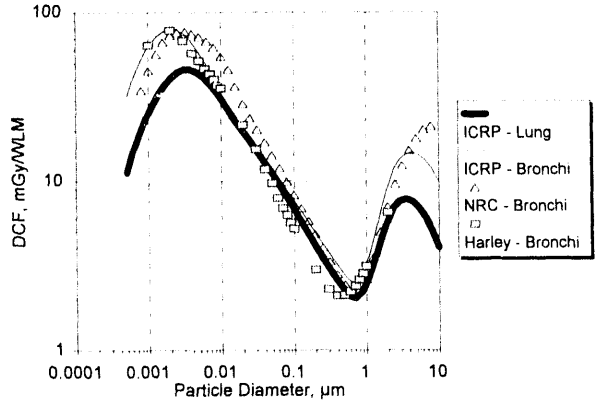

FIGURE 1. Dependence of Dose per Unit Exposure on Dosimetry Model and Extent of Target Tissue Considered, as a Function of Radon-Progeny Particle Diameter. Thick curve is the regionally apportioned dose to the lungs as a whole given by the new ICRP lung model. Thin curve is the dose to just bronchial epithelium, for comparison with that calculated by NRC (1991) and Harley (personal communication).

Analysis of Uncertainty in Effective Dose for Uranium Miners

We have carried out a detailed examination of the underlying assumptions made in evaluating the effective dose for uranium miners using the new ICRP respiratory tract model (Birchall and James in press). We estimated the magnitude of uncertainty or variability in key parameters of the model, and represented the probability of each parameter value by a rectangular, normal, or lognormal distribution, as appropriate. In this way, uncertainties were quantified both in environmental parameters (e.g., radon-progeny activity-size distribution and degree of hygroscopic particle growth) and in respiratory tract model parameters (e.g., breathing rate, regional particle deposition, mucous thickness, depth of target cells, and the apportionment of radiation detriment between secretory or basal cells in bronchial epithelium and between the bronchial, bronchiolar, and alveolar-interstitial regions of the lungs).

Figure 2 shows the results of performing Latin Hypercube analyses of the frequency distribution of calculated effective dose per unit exposure (E/P_p, expressed in mSv/WLM) for a uranium miner when the dosimetric modeling parameters were selected at random from their respective likelihood distributions. Two frequency distributions were studied: (a) that centered on ICRP's recommended regional apportionment of radiation detriment equally between bronchial, bronchiolar, and alveolar-interstitial target cells (ICRP in press), and (b) that centered on the estimated baseline regional distribution of spontaneous (non-radon induced) lung cancers in the general population. For comparison, Figure 2 also shows the current "best estimate" of 5 mSv/WLM, which will be recommended by ICRP as being equivalent to the projected lifetime lung-cancer risk from occupational exposure to radon progeny based on the uranium miner epidemiologic data (ICRP 1994). It is seen that the overall likelihood of a risk coefficient $\leq$ 5

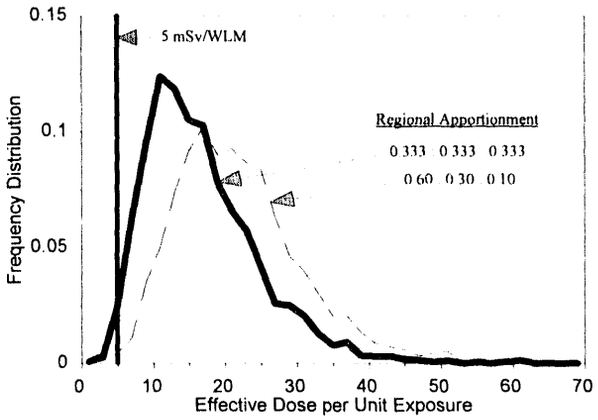

FIGURE 2. Frequency Distribution of Effective Dose per Unit Exposure (E/P_p) Generated by Varying All Parameters and Assumptions in the Dosimetry Calculation. Distributions are shown separately for regional apportionments centered on the ICRP recommendation of 0.333:0.333:0.333, and regional apportionment inferred from natural lung-cancer incidence.

mSv/WLM being obtained from the recommended methods of lung dosimetry is on the order of 1%. Calculated DCFs in this range are found to arise only from extreme values (or unlikely combinations) of input parameters.

Implications for Alpha-Emitter Risk-Weighting Factors

We have not attempted to analyze directly the uncertainties in each of ICRP's recommended dosimetric risk-weighting factors, which are also required to specify the effective dose. These additional parameters are: (1) the radiation weighting factor, w_R, of 20 for alpha particles; (2) the tissue weighting factor, w_T, of 0.12 for the lungs; (3) the total detriment coefficient at high dose rate, DE_H, of 0.112 per Sv (based on the Japanese atomic bomb-survivor studies); and (4) the dose and dose-rate effectiveness factor, DDREF, of 2 (assumed to apply for all exposures at moderate or low dose rates). The recommended values were used to calculate the distributions of E/P_p shown in Figure 2.

For ICRP's recommended equal apportionment of radiation detriment between bronchial,

bronchiolar, and alveolar-interstitial tissues, the arithmetic mean of calculated E/P_p is found to be 17.2 mSv/WLM. However, the direct combination of central estimates of each of the input dosimetric parameters gives a lower modal estimate for E/P_p of 13.4 mSv/WLM. It is reasonable to take an intermediate rounded value of approximately 15 mSv/WLM to be the "best estimate" of the DCF for uranium miners based on ICRP's forthcoming dosimetric recommendations. The corresponding lifetime risk coefficient for exposure of a uranium miner that is implied by ICRP's dosimetric methodology is $8.4\ 10^{-4}$ per WLM. However, the recommended value of the risk coefficient estimated directly from epidemiology of uranium miners is $2.8\ 10^{-4}$ per WLM (ICRP 1994). In other words, use of ICRP's dosimetric risk-weighting factors would seem to result in an overestimate of the observed risk of lung cancer from occupational radon-progeny exposure by a factor of three.

It is useful to consider the excess lifetime risk of lung cancer directly in terms of lung dose (strictly speaking, an absorbed dose that has been adjusted by the regional weighting factors) with a composite risk factor, Ω ($= w_T^{lung}\ w_R^{\alpha}\ DE_H$ / DDREF). If the ICRP recommended values for each of the primary risk-weighting factors are used, then the value of Ω is 0.1344 Gy^{-1}. However, if the epidemiologic risk estimate of $2.8\ 10^{-4}$ is taken, together with the best estimate of E/P_p of 15 mSv/WLM, *i.e.*, a regionally weighted lung dose of 6.25 mGy/WLM, then this implies a value of Ω of approximately 0.05 Gy^{-1}. Furthermore, if this implication is accepted for radon-progeny exposure, then it also must be considered for any alpha-emitting radionuclide in the lungs, since Ω is not specific to radon progeny.

Relating Lung Dose-Rate to Radon Gas Concentration in a Home

In practice, exposure to radon progeny in the home is controlled in relation to the measured indoor concentration of radon gas. To assess the attendant risks of indoor exposure, it is first necessary to translate exposure to radon gas into an equivalent dose to the lungs from the radon progeny. In a series of 208 measurements carried out by Clarkson University over three summer months in a single, normally occupied home in Arnprior, Ontario (Hopke *et al.* 1993), the mean equilibrium factor, F, between radon and its progeny was found to be 0.45, with a temporal standard deviation of $\pm$ 0.18. We have analyzed the resulting variability in lung dose-rate per unit radon concentration using the new ICRP lung model with Clarkson University's measurements of the complete activity-size distribution of radon progeny potential alpha energy.

In order to compare the calculated E/P_p indoors with the ICRP recommended value of 5 mSv/WLM for a uranium miner, we have normalized the indoor dose by the factor 5/17.2, *i.e.*, 0.29, which is the quotient of the epidemiologic-derived and mean dosimetric-derived coefficients. The average effective dose-rate per unit radon gas concentration obtained from the 208 indoor aerosol size measurements was 39 μSv/y per Bq(^{222}Rn)/m^3, with a temporal standard deviation of $\pm$ 16 μSv/y per Bq(^{222}Rn)/m^3 (assuming 80% occupancy). The lung dose rate was correlated with the measured fraction of potential alpha energy associated with particles smaller than 15 nm diameter, $f_p(15)$, which may consist of both unattached progeny (of about 1 nm diameter) and larger "clusters" of airborne molecules that are associated with a single progeny atom. The mean regression of the dose conversion factor (DCF) on the ultrafine fraction, $f_p(15)$, of the potential alpha-energy concentration (PAEC) was given by

$$DCF(Rn) = 24 + 62 f_p(15)$$

in μSv/y (effective dose rate) per Bq(^{222}Rn)/m^3, with a coefficient of determination, r^2, of 0.22. In this particular home, the variability of the

equilibrium factor was a greater contributor to the observed variation in the dose conversion factor with respect to radon gas concentration. In terms of exposure to potential alpha energy, the average dose conversion factor was 7.9 mSv/WLM, with a relatively small temporal standard deviation of ± 2.0 mSv/WLM.

Figure 3 compares the variability of the DCF relative to the radon gas concentration found in two additional, normally occupied homes in Princeton, New Jersey (Wasiolek *et al.* 1992), with the regression on the ultrafine fraction of potential alpha-energy concentration (PAEC), $f_p(15)$, found in the Arnprior home. On the average, the DCF with respect to radon gas concentration is lower in both of the Princeton homes. So is that with respect to potential alpha energy, which was found to be 5.5 ± 0.6 and 5.5 ± 0.8 in November, 1990, and February, 1991, respectively, in home #1, and 7.0 ± 2.0 in April, 1991 in home #2. One out of three occupants of both Princeton homes was a cigarette smoker, whereas there were no smokers in the Arnprior home.

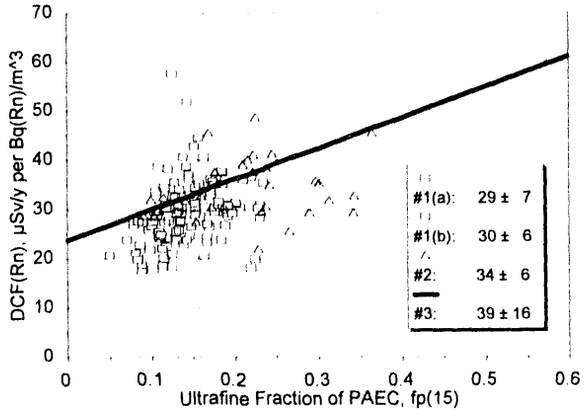

FIGURE 3. Variability of the Dose Conversion Factor (DCF) for Effective Dose-Rate per Unit Radon Gas Concentration in Normally Occupied Homes. Results labeled #1 (a) and (b) were obtained in two different periods of study in a Princeton, New Jersey, home. Results labeled #2 relate to a different home in Princeton, and the line shows the regression relationship found from 208 measurements in a Canadian home. Values shown are the means ± 1 standard deviation of individual measurements over time.

These data (together with that still being analyzed from another home in Parishville, New York) represent the only systematic studies of the variability of exposure-dose conversion factors in normally occupied homes that are available worldwide. Although substantial, the database does not yet include a representative cross-section of U.S. homes, nor a systematic study of seasonal factors in different climatic regions of the U.S. Furthermore, the ability to extrapolate lung cancer risks to homes from the uranium-miner epidemiologic studies is severely hampered by a lack of comparable information on the exposure environment in mines.

Dosimetric Significance of Radon Progeny Clusters

Figure 4 shows the contributions to the overall DCF made by various components of the radon-progeny particle-size spectrum, taken from measurements made over extended time periods. The first size-bin represents "unattached" progeny, with a median particle diameter of 0.9 nm. The second and third size-bins together represent progeny "clusters," with median diameters of 2.8 nm and 9 nm, respectively. The three remaining size-bins together represent the "attached" progeny aerosol, consisting of larger particles. In calculating DCFs for these attached progeny, we have assumed that the vector particles are hygroscopic to the extent that they grow by a factor of 1.5 within the respiratory tract (Li 1993).

On the average, and in all three homes studied, radon-progeny "cluster" particles were found to contribute significantly to the overall DCF. Their contribution was found to be at least as large as that from the classical "unattached" fraction. The mean fractional contribution of progeny clusters was 35% and 22% during the two separate periods of study in the first Princeton home, 35% in the second Princeton home, and 39% averaged over the three months of study in the Arnprior home.

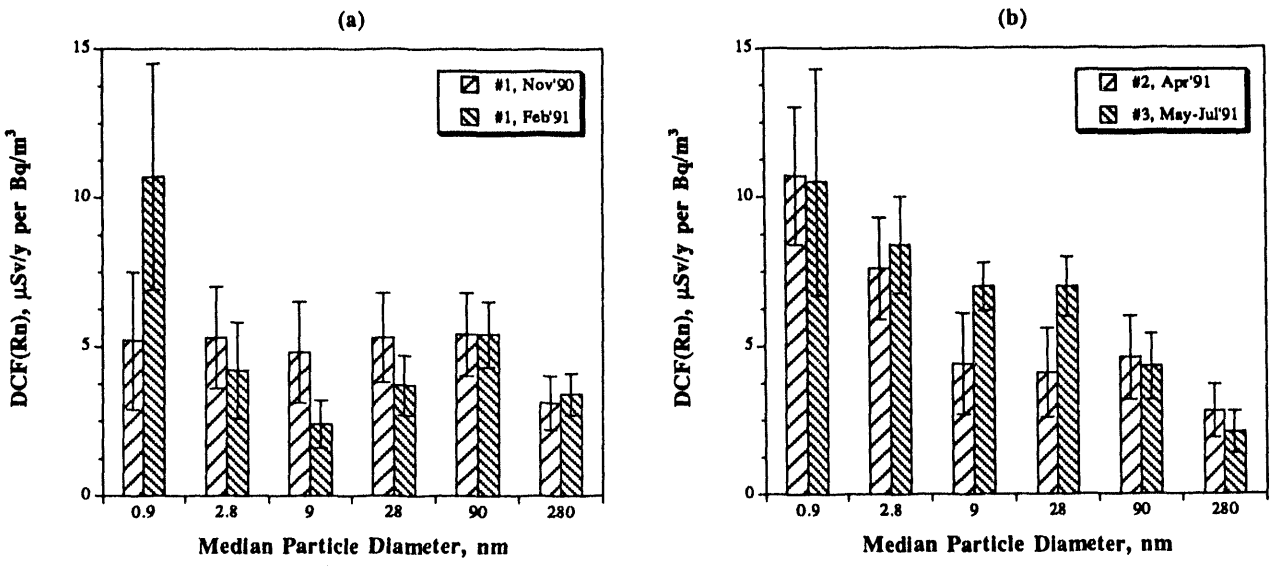

FIGURE 4. Contributions to Overall Dose Conversion Factor (DCF) According to Radon-Progeny Particle Size. The data are taken from (a) two studies in one home in Princeton, New Jersey, and (b) a study in a second Princeton home (#2) and a third home in Arnprior, Ontario (#3). Values shown are means ± 1 standard deviation of individual measurements over extended periods of time.

Effectiveness of Air Cleaning

Radon-Progeny Concentration

Figure 5 shows the effects of three different types of air-cleaning devices on the PAEC carried by (a) unattached progeny, (b) progeny clusters, and (c) attached progeny. The measurements were made in the Arnprior home by Hopke *et al.* (1993). In our analysis here, the PAEC has been normalized to the concentration of radon gas at the time of measurement. The devices tested were (1) the NO-RAD air ionizer system, with a 2.8 m^3 min^{-1} fan (Moeller *et al.* 1988); (2) an electronic (electrostatic) air cleaner, with a 3.9 m^3 min^{-1} fan; and (3) a high-efficiency room air filter, operated at a filtration rate of either 4.3 or 2.3 m^3 min^{-1}. Figure 5(a) shows that the ionizer/fan had the greatest effect in removing airborne unattached progeny, followed closely by the high-efficiency filter. As expected, the electronic air cleaner was only marginally effective in reducing the concentration of unattached progeny. In the case of progeny clusters (Figure 5[b]), the ionizer/fan device appeared to increase the airborne PAEC, whereas high-efficiency filtration gave a major reduction, and the electric cleaner a moderate reduction in airborne PAEC. Both high-efficiency filtration and electrostatic air cleaning produced a major reduction in the airborne PAEC of attached progeny, whereas the ionizer/fan device was less effective.

Effective Dose Rate

Figure 6 shows the measured effects of each of these air-cleaning devices on the DCF calculated with respect to the radon gas concentration. On the average, the DCF was reduced from the value of 39 μSv/y per Bq(^{222}Rn)/m^3 in the absence of air cleaning, to 33 μSv/y per Bq(^{222}Rn)/m^3 by the ionizer/fan device, 22 μSv/y per Bq(^{222}Rn)/m^3 by the electronic air cleaner, and 13 μSv/y per Bq(^{222}Rn)/m^3 by high-efficiency filtration. Clearly, the different filtration characteristics of these three air cleaners shown in Figure 5 implies that both their relative and absolute effectiveness for dose reduction in a

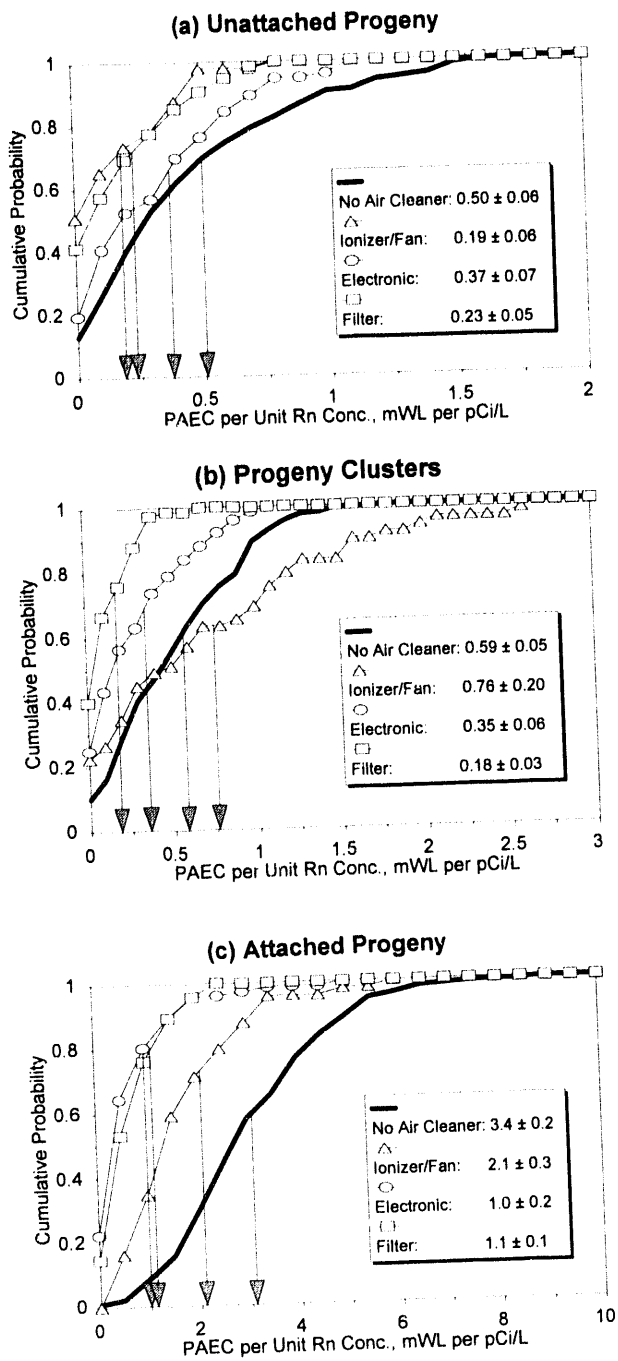

FIGURE 5. Cumulative Frequency Distribution of Airborne Potential Alpha-Energy Concentration (PAEC) (Normalized to Unit Radon Gas Concentration), Showing the Effects of Operating Three Different Types of Air Cleaner: (a) for unattached radon progeny, (b) for progeny clusters, and (c) for attached progeny. Values shown in the legend and marked by the arrows in the graph are means ± 95% confidence intervals.

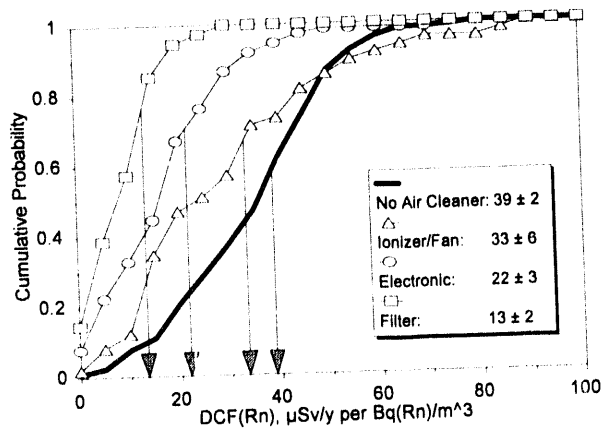

FIGURE 6. Cumulative Frequency Distribution of the Dose Conversion Factor (DCF) with Respect to Radon Gas, Showing the Effect of Operating Three Different Types of Air Cleaner. Values shown in legend are means ± 95% confidence intervals.

particular home environment will depend on the distribution of PAEC between unattached, clustered, and attached radon progeny. In the home studied here, the relatively high proportion of PAEC normally present in the form of progeny clusters (39%) was a factor in achieving a threefold dose reduction by high-efficiency filtration.

Modeling Dose to the Human Testes from Radon and Progeny

In the area of physiologically based pharmacokinetic (PBPK) modeling, we have used experimental animal data to develop a model of the uptake and retention of radon and its progeny in the human testes that results from periodic exposure to elevated concentrations of airborne radon and progeny (Figure 7). Based on this research, we prepared a report addressing testicular dose on behalf of British Nuclear Fuels PLC (BNFL), which was used by them in the early stages of a precedent-setting case in the English High Court. Our study countered a claim made by the plaintiffs that paternal preconception irradiation (PPI) of the testes in uranium miners by radon progeny had been linked with the occurrence of childhood leukemia in their offspring (McLaughlin *et al.*

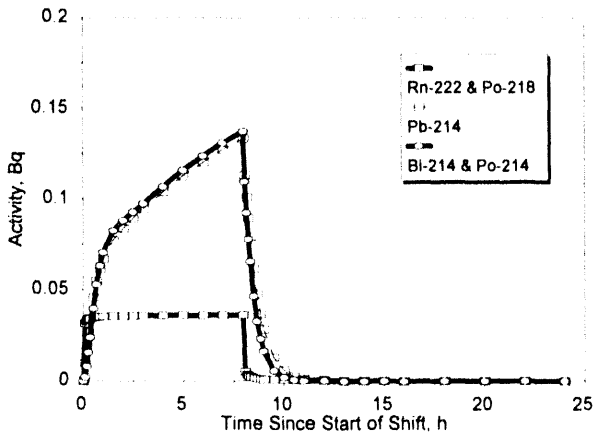

FIGURE 7. Modeled Build-Up of Alpha Activity in the Testes of an Underground Uranium Miner at Elliot Lake, Ontario, During a Working Shift, and Its Subsequent Decay

1992). This input on behalf of DOE/OHER enabled BNFL's legal counsel to firmly dismiss the claim, which could have confused the arguments later in the case concerning the plausibility of the PPI hypothesis founded only on a statistically weak study of childhood leukemia among children born near the Sellafield fuel reprocessing works.

References

Birchall, A., and A. C. James. Uncertainty analysis of the effective dose per unit exposure from radon progeny and implications for ICRP risk-weighting factors. *Radiat. Prot. Dosim.* (in press).

Hopke, P.K., N. Montassier, and P. Wasiolek. 1993. An evaluation of the effectiveness of several air cleaners for reducing the hazard from indoor radon progeny. *Aerosol Sci. & Technol.* 19:268-278.

International Commission on Radiological Protection (ICRP). 1994. *Protection Against Radon-222 at Home and at Work.* ICRP Publication 65. *Ann. ICRP* Vol. 23(2).

International Commission on Radiological Protection (ICRP). *Human Respiratory Tract Model for Radiological Protection.* ICRP Publication 66. *Ann. ICRP* (in press).

Li, W. 1993. *The Hygroscopicity of Indoor Aerosol Particles.* Ph.D. Thesis. Department of Chemistry, Clarkson University, Potsdam, New York.

McLaughlin, J.R., T.W. Anderson, E.A. Clarke, and W. King. 1992. *Occupational Exposure of Fathers to Ionizing Radiation and the Risk of Leukaemia in Offspring - A Case Control Study.* INFO-0424, Atomic Energy Control Board, Ottawa, Canada.

Moeller, D.W., S.N. Rudnick, and E.F. Mayer. 1988. Laboratory and field tests of a Hassock fan-ion generator radon decay product removal unit. *Radiat. Prot. Dosim.* 24:503-506.

National Research Council (NRC). 1991. *Comparative Dosimetry of Radon in Mines and Homes.* Report by a scientific panel. National Academy Press, Washington, D.C.

Wasiolek, P., P.K. Hopke, and A.C. James. 1992. Assessment of exposure to radon decay products in realistic living conditions. *J. Exposure Anal. & Environ. Epidem.* 2:309-322.

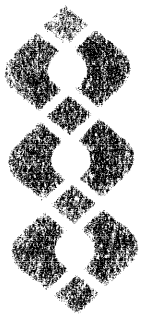

General Life Sciences Research

GnomeView: Beta Test Version

Principal Investigator: R. J. Douthart

Other Investigators: J. E. Pelkey and G. S. Thomas

GnomeView is a graphical user's interface to information generated by the Human Genome Project. GnomeView integrates information from different data sources into comprehensive graphical representations (maps) of the human genome. Currently, three different databases are integrated: the Human Genome Data Bank (GDB), the GenBank DNA Sequence Database, and On-Line Mammalian Inheritance in Man (OMIM). Two of the databases, GDB and GenBank, are abstracted into local versions residing on an internal database management system (DBMS), which is accessed in response to queries. The third database, OMIM, is accessed remotely during run time. GnomeView has been in beta testing at several universities and genome laboratories since April 1993.

The central data-organization theme of GnomeView (Douthart *et al.* 1993; Pelkey *et al.* 1993) is the genomic map. GnomeView utilizes the db_VISTA (Raima 1990) database management system (DBMS) to store, organize, and assemble information objects (map_objects) that constitute genomic maps. GnomeView is not a repository database per se, but uses information obtained from databases such as GenBank and the Human Genome Data Base (GDB) to obtain information about map_objects.

A dominant theme during the development of the GnomeView interface has been the preservation of the pictorial quality of the genomic map. The human genome effort will produce hundreds of thousands of map_objects, making pictorial map representation increasingly more difficult. Pictorial representations possibly may be abandoned as the increasing number of map_objects also increases the complexity of the representations; if this situation occurs, insights conveyed by such representations regarding genomic topology and the relationships between different maps and map_objects may be lost.

GnomeView employs object-density mapping, false color, zooming, progressive disclosure, label-overwrite avoidance, and other techniques to preserve pictorial map representations (Douthart *et al.* in press). These graphic representations can be interrogated to obtain detailed object lists and other information obtained from the databases as a result of user queries.

Beta Testing

GnomeView entered extended beta testing in 1993. The purpose of the beta test was to monitor usage and acceptance of the interfaces, and to elicit feedback on bugs found and on improvements desired. During this period of beta testing, the system and its user's manual have been available to scientists electronically free of charge. The beta testing terminated in September 1993. A number of electronic-mail addresses were established to facilitate the test, and although the trial has been officially terminated, these addresses are still being maintained:

gv-help@gnome.pnl.gov. Inquiries sent to this address receive a personal answer by a member of the GnomeView development team. General information questions and comments are handled at this address.

gv-bug@gnome.pnl.gov. Notification of bugs and suggestions for improvements are received from the user community at this address.

gv-request@gnome.pnl.gov. An automated response to messages sent to this address gives instructions on how to obtain GnomeView and its user's manual electronically. A log is kept of the addresses of the requesters. Specific information is asked about the potential user's site, but is not a mandatory prerequisite for receiving the interface.

gv-stat@gnome.pnl.gov. Every time a requester uses GnomeView, a signal is sent to this address. Vital information about actual usage is tallied by this mechanism. Table 1 summarizes usage during the period of extended beta testing. The requests are from leading genome and molecular biology laboratories around the world. Usage, however, was far from evenly distributed. More than 90% of the usage was from 19 sites that used GnomeView regularly during the beta test period. These data indicate that not only was beta testing successful, but that a small user's group is beginning to form.

Database Access

The unique aspects of GnomeView are its emphasis on graphical methods of scientific visualization and user interaction. To expedite development and entry into beta testing, local abstractions of both GDB and GenBank are made into GnomeView's local DBMS. Only OMIM is accessed when appropriate during run time. OMIM is accessed via the WAIS utility, which is in the public domain. Constant updating and redistribution has proven to be unnecessarily time-consuming. Distribution of a utility for updating on-site, while feasible, does not solve the problem of the ever-increasing demands on disk space for local storage of database abstractions that are approaching an exponential increase in size. Virtually all the GnomeView beta test sites expressed the desire for on-line access to all databases at run time.

Future Directions

Recent trends in the development of databases most pertinent to GnomeView include conversion to a standard relational DBMS and implementing a server-client methodology for user access. Server centers are being established with client access to numerous databases and analytical tools. An important center for client access to databases integrated in the GnomeView interface

TABLE 1. Beta Test Request and Logon Tallies, 1993

	April	May	June	July	Aug.	Sept.	Oct.[a]	Nov.	Totals
Requests	1	45	11	10	38	8	3	2	118
Stats (usage)	31	65	68	106	101	175	91	67	704

(a) Because electronic mail addresses have been maintained even after beta testing was terminated, requests have continued to be tracked.

is being established at Oak Ridge National Laboratory. These developments make on-line access from GnomeView much more desirable and easier to develop than in the past.

Since GnomeView's inception, the option of eventual on-line database access was always considered. The front and back ends are reasonably isolated such that decoupling from the internal DBMS and the substitution of on-line access can be done without undue difficulty. Feedback from the beta test sites indicates that on-line access of all databases is an absolute prerequisite for a product version of the interface.

The GnomeView internal DBMS was originally devised for the creation of hybrid maps between different mapping levels, for the storage of user input maps and map_objects, and for the creation of hybrid maps consisting of user-defined and database-defined map_objects. The internal DBMS, therefore, will be retained in the product version, even though it will no longer be used to house local abstractions of GDB and GenBank.

References

Douthart, R.J., J.E. Pelkey, and G.S. Thomas. 1993. Database integration and visualization of maps of the human genome using the GnomeView interface. *Proceedings of the 27th Hawaii Conference on System Science*, Maui, Hawaii.

Pelkey, J.E., G.S. Thomas, D.A. Thurman, V.B. Lortz, and R.J. Douthart. 1993. GnomeView: A tool for visual representation of Human Genome Data. *Proceedings of the 1993 ACM/SIGAPP Symposium on Applied Computing*, Indianapolis, Indiana, p. 21.

Raima Corporation. 1990. *db-VISTA User's Guide*, sixth edition, Raima Corporation, Bellevue, Washington.

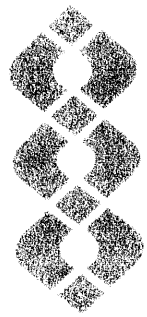

Publications and Presentations

Publications

1992

Alavanja, M.C.R., R. Brownson, M. Wood, Z. Hrubec, J.A. Mahaffey, and J.D. Boice, Jr. 1992. Radon dosimetry for a lung cancer study in Missouri. In: *Indoor Radon and Lung Cancer: Reality or Myth?* Part 2, F. T. Cross, ed., pp. 871–878, Proceedings of the 29th Hanford Symposium on Health and the Environment, Richland, Washington. Battelle Press, Columbus, Ohio.

Arnold, G.E., A.K. Dunker, S.J. Johns, and R.J. Douthart. 1992. Use of conditional probabilities for determining relationships between amino acid sequence and protein secondary structure. *Proteins Struct. Funct. Genet.* 12:382–399.

Bair, W.J. 1992. The revised International Commission on Radiological Protection (ICRP) dosimetric model for the human respiratory tract. In: *IRPA8, Vol. II*, Conference Proceedings of the Eighth International Congress of the International Radiation Protection Agency, May 17-22, 1992, Montreal, Canada, International Radiation Protection Association, Montreal, Canada.

Benson, J.M., A.L. Brooks, and R.F. Henderson. 1992. Comparative *in vitro* cytotoxicity of nickel compounds to pulmonary alveolar macrophages and to rat lung epithelial cells. In: *Nickel and Human Health: Current Perspectives*, E. Neiboer and J.O. Nriagu, eds., pp. 319–330. John Wiley and Sons, New York, New York.

Briant, J.K., D.D. Frank, A.C. James, and L.L. Eyler. 1992. Numerical simulation of aerosol particle transport by oscillating flow in respiratory airways. *Ann. Biomed. Eng.* 20: 573–581.

Briant, J.K., and M. Lippman. 1992. Particle transport through a hollow canine airway cast by high-frequency oscillatory ventilation. *Exp. Lung Res.* 18:385–407.

Brooks, A.L., R.A. Guilmette, P.J. Haley, F. F. Hahn, B.A. Muggenberg, J.A. Mewhinney, and R.O. McClellan. 1992. Distribution and biological effects of inhaled $^{239}Pu(NO_3)_4$ in cynomolgus monkeys. *Radiat. Res.* 130: 79–87.

Brooks, A.L., K. Rithidech, R.M. Kitchin, N.F. Johnson, D.G. Thomassen, and G.J. Newton. 1992. Evaluating chromosome damage to estimate dose to tracheal epithelial cells. In: *Indoor Radon and Lung Cancer: Reality or Myth?*, F. T. Cross, ed., Part 2, pp. 601–614, Proceedings of the 29th Hanford Symposium on Health and the Environment, Richland, Washington. Battelle Press, Columbus, Ohio.

Brooks, A.L., C.J. Mitchell, T. Loyd, K.E. McDonald, and N.F. Johnson. 1992. Genotoxic effects of silicon carbide fibers. *In Vitro Toxicol.* 5(1):51–60.

Brooks, A.L., K.E. McDonald, B.B. Kimsey, and R.M. Kitchin. 1992. Radioadaptive response *in vivo* in Chinese hamsters injected with alpha (^{239}Pu)- or beta/gamma (^{144}Ce)-emitting radionuclides. In: *Low Dose Irradiation and Biological Defense Mechanisms, Excerpts Med. Int. Congr. Ser.*, T. Sugahara, L.A. Sagan, and T. Aoyama, eds., pp. 319–322.

Elsevier Science Publishers, New York, New York.

Cross, F.T. 1992. A review of experimental animal radon health effects data. In: *Radiation Research: A Twentieth-Century Prospective*, Proceedings of the Ninth International Congress of Radiation Research, W.C. Dewey, M. Edington, R.J.M. Fry, E.J. Hall, and G.F. Whitmore, eds., Vol. 2, pp. 476–481. Academic Press, San Diego, California.

Cross, F.T., G.E. Dagle, R.A. Gies, L.G. Smith, and R.L. Buschbom. 1992. Experimental animal studies of radon and cigarette smoke. In: *Indoor Radon and Lung Cancer: Reality or Myth?* Part 2, F. T. Cross, ed., pp. 821–844, Proceedings of the 29th Hanford Symposium on Health and the Environment, Richland, Washington. Battelle Press, Columbus, Ohio.

Cross, F.T. 1992. Experimental, statistical, and biological models of radon carcinogenesis. *Radiat. Prot. Dosim.* 45:629–633.

Cross, F.T., ed. 1992. *Indoor Radon and Lung Cancer: Reality or Myth?* Proceedings of the 29th Hanford Symposium on Health and the Environment, Richland, Washington (in two volumes). Battelle Press, Columbus, Ohio.

Cross, F.T., G.E. Dagle, M.E. Foreman, R.A. Gies, E.S. Gilbert, A.C. James, R.F. Jostes, F.C. Leung, S.H. Moolgavkar, and L.G. Smith. 1992. Mechanisms of radon injury/ inhalation hazards to uranium miners. In: *DOE FY 1991 Radon Research Program Report*, pp. 213-218. DOE/ER-0536P, NTIS, Springfield, Virginia.

Dagle, G.E., E.P. Moen, R.A. Adee, T.E. Hui, A.C. James, R.E. Filipy, and R.L. Kathren. 1992. Microdistribution and microdosimetry of thorium deposited in the liver. *Health Phys.* 63(1):41–45.

Dagle, G.E., F.T. Cross, and R.A. Gies. 1992. Morphology of respiratory tract lesions in rats exposed to radon progeny. In: *Indoor Radon and Lung Cancer: Reality or Myth?* Part 2, F.T. Cross, ed., p. 659–676, Proceedings of the 29th Hanford Symposium on Health and the Environment, Richland, Washington. Battelle Press, Columbus, Ohio.

Egert, G.H., R.L. Kathren, F.T. Cross, and M.A. Robkin. 1992. The effect of home weatherization on indoor radon concentrations. In: *Indoor Radon and Lung Cancer: Reality or Myth?* Part 1, F.T. Cross, ed., pp. 51–54, Proceedings of the 29th Hanford Symposium on Health and the Environment, Richland, Washington. Battelle Press, Columbus, Ohio.

Fisher, D.R., T.E. Hui, V.P. Bond, and A.C. James. 1992. Microdosimetry of radon progeny: Application to risk assessment. In: *Indoor Radon and Lung Cancer: Reality or Myth?* Part 1, F.T. Cross, ed., 307–323, Proceedings of the 29th Hanford Symposium on Health and the Environment, Richland, Washington. Battelle Press, Columbus, Ohio.

Fix, J.J., E.S. Gilbert, R.H. Wilson, W.V. Baumgartner, and L.L. Nichols. 1992. Comments on evidence of biased recording of radiation does of Hanford workers. *Am. J. Ind. Med.* 22:281-283.

Foreman, M.E., L.S. McCoy, and M.E. Frazier. 1992. Involvement of oncogenes in radon-induced lung tumors in rats. In: *Indoor Radon and Lung Cancer: Reality or Myth?* Part 2, F.T. Cross, ed., pp. 649–658, Proceedings of the 29th Hanford Symposium on

Health and the Environment, Richland, Washington. Battelle Press, Columbus, Ohio.

Gies, R.A., F.T. Cross, G.E. Dagle, and R.L. Buschbom. 1992. The histomorphologic effects of inhaled radon, uranium ore dust, and cigarette smoke in the tracheal epithelium of the rat. In: *Abstracts, 37th Annual Meeting of the Health Physics Society*, June 21-22, Columbus, Ohio.

Gilbert, E.S. 1992. Leukemia among nuclear workers. *Epidemiology* 3(3)275-276 (letter).

Gilbert, E.S., F.T. Cross, C.L. Sanders, and G.E. Dagle. 1992. Models for comparing lung-cancer risks in radon- and plutonium-exposed experimental animals. In: *Indoor Radon and Lung Cancer: Reality or Myth?* Part 2, F.T. Cross, ed., pp. 783-802, Proceedings of the 29th Hanford Symposium on Health and the Environment, Richland, Washington. Battelle Press, Columbus, Ohio.

Hulla, J.E. 1992. The rat genome contains a p53 pseudogene: Detection of a processed pseudogene using PCR. *PCR Methods Applic.* 1:251-254.

James, A.C. 1992. Dosimetry of radon and thoron exposures: Implications for risks from indoor exposures. In: *Indoor Radon and Lung Cancer: Reality or Myth?* Part 1, F.T. Cross, ed., pp. 167-198. Proceedings of the 29th Hanford Symposium on Health and the Environment, Richland, Washington. Battelle Press, Columbus, Ohio.

Johnson, J.R., A.C. James, and R.L. Hill. 1992. Application of the proposed new ICRP lung model to bioassay. In: *IRPA8, Vol. II,* Conference Proceedings of the Eighth International Congress of the International Radiation Protection Association, May 17-22, 1992, Montreal, Canada, pp. 1093-1096. International Radiation Protection Association, Montreal, Quebec.

Johnson, N.F., M.D. Hoover, D.G. Thomassen, Y.S. Cheng, A. Dalley, and A.L. Brooks. 1992. *In vitro* activity of silicon carbide whiskers in comparison to other industrial fibers using four cell culture systems. *Am. J. Ind. Med.* 21:807-823.

Jostes, R.F., E.W. Fleck, R.A. Gies, T.E. Hui, T.L. Morgan, J.L. Schwartz, J.K. Wiencke, and F.T. Cross. 1992. Cytotoxic, clastogenic, and mutagenic response of mammalian cells exposed in vitro to radon and its progeny. In: *Indoor Radon and Lung Cancer: Reality or Myth?* Part 2, F.T. Cross, ed., pp. 555-568, Proceedings of the 29th Hanford Symposium on Health and the Environment, Richland, Washington. Battelle Press, Columbus, Ohio.

Kennedy, R.A., J.A. Mahaffey, S.K. Smith, and F. Carr, Jr. 1992. U.S. Department of Energy Chernobyl databases. In: *IRPA8, Vol. I,* Conference Proceedings of the Eighth International Congress of the International Radiation Protection Association, pp. 265-268. International Radiation Protection Association, Montreal, Quebec.

Khan, M.A., and J.A. Heddle. 1992. Optimization of the concurrent assay for gene mutations and chromosomal aberrations *in vivo*: Expression time in rats. *Environ. Mol. Mutagen.* 20:165-171.

Leung, F.C. 1992. Circadian rhythms of melatonin release from chicken pineal *in vitro*: Modified melatonin radioimmunoassay. *Soc. Exp. Biol. Med.* 198:826-832.

Leung, F.C., G.E. Dagle, and F.T. Cross. 1992. Involvement of growth factors and their receptors in radon-induced rat lung tumors. In: *Indoor Radon and Lung Cancer: Reality or Myth?* Part 2, F.T. Cross, ed., pp. 615-626, Proceedings of the 29th Hanford Symposium on Health and the Environment, Richland, Washington. Battelle Press, Columbus, Ohio.

Loo, J.A., R.R. Ogorzalek-Loo, D.R. Goodlett, R.D. Smith, A.F. Fuciarelli, D.L. Springer, B.D. Thrall, and C.G. Edmonds. 1992. Elucidation of covalent modifications and noncovalent awsociations in proteins by electrospray ionization mass spectrometry. In: *Techniques in Protein Chemistry, Vol. IV.*, RH Angelette, ed., pp. 23-31. Academic Press, New York, New York.

Lutze, L.H., R.A. Winegar, R. Jostes, F.T. Cross, and J.E. Cleaver. 1992. Radon-induced deletions in human cells: Role of nonhomologous strand rejoining. *Cancer Res.* 52:5126-5129.

Lyon, M., and J.B. Martin. 1992. Computerized occupational protection records systems. *Nuclear Plant J.* May/June:92-96.

Miller, R.T., R.J. Douthart, and A.K. Dunker. 1992. An alphabet of amino acid conformation in protein. In: *Proceedings of the 26th Annual Hawaii International Conference on Systems Science: Architecture and Biotechnology Computing.* IEEE Computer Society Press, Washington, D.C.

Miller, R.T., R.J. Douthart, and A.K Dunker. 1992. Learning an objective alphabet of amino acid conformation in protein. In: *Techniques in Protein Chemistry, Vol. IV.* Plenum Publishing Corp., New York, New York.

Minnick, M.F., L.C. Stillwell, J.M. Heineman, and G.L. Stiegler. 1992. A highly repetitive DNA sequence possibly unique to canids. *Gene* 110:235-238.

Perry, R.E., R.E. Weller, R.L. Buschbom, G.E. Dagle, and J.F. Park. 1992. Radiographically determined growth dynamics of primary lung tumors in dogs by inhalation of plutonium. *Am. J. Vet. Res.* 53(10): 1740-1743.

Sanders, C.L., G.E. Dagle and J.A. Mahaffey. 1992. Incidence of brain tumors in rats exposed to an aerosol of $^{239}PuO_2$. *Int. J. Radiat. Biol.* 62:97-102.

Sanders, C.L. 1992. Life-span studies in rats exposed to $^{239}PuO_2$ aerosol. II. Nonpulmonary tumor formation in control and exposed groups. *J. Environ. Pathol. Toxicol. Oncol.* 11(5,6):265-277.

Sanders, C.L., and K.E. McDonald. 1992. Malignancy of proliferative pulmonary lesions in the Syrian hamster following inhalation of $^{239}PuO_2$. *J. Environ. Pathol. Toxicol. Oncol.* 11(3):151-156.

Sanders, C.L. 1992. Microdosimetric and cellular basis for a lung tumor threshold following inhalation of $^{239}PuO_2$. In: *Acute and Late Effects on the Lungs from Inhaled Radioactive Materials and External Irradiation,* Proceedings of the EULEP Symposium, Erfurt, Germany.

Sanders, C.L. 1992. Pleural mesothelioma in the rat following exposure to $^{239}PuO_2$. *Health Phys.* 63:695-697.

Schwartz, J.L., J. Rotmensch, R.W. Atcher, R.F. Jostes, F.T. Cross, T.E. Hui,

D. Chen, S. Carpenter, H.H. Evans, J. Mencl, G. Bakale, and P.S. Rao. 1992. Interlaboratory comparison of different alpha particle and radon sources: Cell survival and relative biological effectiveness. *Health Phys.* 62(5): 458–461.

Sikov, M.R., R.J. Traub, and H.K. Meznarich. 1992. Comparative placental transfer, localization, and effects of radionuclides in experimental animal and human pregnancies. In: *Proceedings of the AECL Fetal Dosimetry Workshop Conference*, E.S. Lamothe, ed., pp. 1–6, Chalk River, Ontario, Canada. AECL-10578, Health Physics Branch, Chalk River, Ontario.

Sikov, M.R., R.J. Traub, T.E. Hui, H.K. Meznarich, and K.D. Thrall. 1992. *Contribution of Maternal Radionuclide Burdens to Prenatal Radiation Doses.* NUREG/CR-5631, PNL-7445, Rev. 1. Prepared for the U.S. Nuclear Regulatory Commission, Washington, D.C., by Pacific Northwest Laboratory, Richland, Washington.

Sikov, M.R., F.T. Cross, T.J. Mast, H.E. Palmer, A.C. James, and B.D. Thrall. 1992. Developmental toxicology of radon exposures. In: *Indoor Radon and Lung Cancer: Reality or Myth?* Part 2, F. T. Cross, ed., pp. 677–692, Proceedings of the 29th Hanford Symposium on Health and the Environment, Richland, Washington. Battelle Press, Columbus, Ohio.

Sikov, M.R. 1992. *Effects of Low-Level Fetal Irradiation on the Central Nervous System* (proceedings of a workshop). PNL-8009, Pacific Northwest Laboratory, Richland, Washington.

Sikov, M.R. 1992. Hazards and risks associated from prenatal irradiation: Emphasis on internal radionuclide exposures. *Radiat. Prot. Dosim.* 41(4):265–272.

Smith, S.K., J.C. Prather, E.K. Ligotke, and C.R. Watson. 1992. *National Radiobiology Archives Distributed Access User's Manual Version 1.1, Rev. 1.* PNL-7877, Pacific Northwest Laboratory, Richland, Washington.

Stark, P., B.D. Thrall, G.G. Meadows, and M.M. Abdel-Monem. 1992. Synthesis and evaluation of novel spermidine derivatives as targeted chemotherapeutic agents. *J. Med. Chem.* 35:4264–4269.

Stevens, R.G., and B.S. Blumberg. 1992. Serum albumin and the risk of cancer. In: *Macronutrients: Invesigating Their Role in Cancer,* M.S. Micozzi and T.E. Moon, eds., pp. 283–292. Marcel Dekker Inc., New York, New York.

Stevens, R.G., and K. Neriishi. 1992. Iron and oxidative damage in human cancer. In: *Biological Consequences of Oxidative Stress: Implications for Cardiovascular Disease and Carcinogenesis*, L. Spatz and A.D. Bloom, eds. Oxford University Press, New York, New York.

Thrall, B.D., and D.L. Springer. 1992. Sequence-specific blocks in DNA/RNA polymerases induced by benzo[a]pyrene diol epoxide. *Toxicologist* 12:251 (abstract).

Thrall, B.D., D.B. Mann, M.J. Smerdon, and D.L. Springer. 1992. DNA polymerase, RNA polymerase, and exonuclease activities on a DNA sequence modified by benzo[a]pyrene diol epoxide. *Carcinogenesis* 13:1529–1534.

Trumble, W.R., B.A. Shurf, J.L. Reasoner, P.A. Seward, B.A. Denovan, J.W. West, and

R.J. Douthart. 1992. Protein expression for an *Escherichia coli/Bacillus subtilis* multifunctional shuttle plasmid with synthetic promoter sequences. Protein Expression and Purification, Vol. 3.

Wasiolek, P.T., P.K. Hopke, and A.C. James. 1992. Assessment of exposure to radon decay products in realistic living conditions. *J. Exposure Anal. Environ. Epidemiol.* 2:309–322.

Weller, R.E. 1992. Intrathoracic neoplasia: Epidemiology and etiology. In: *Proceedings of the 10th American College of Veterinary Internal Medicine Forum*, pp. 652-654. Omnipress, Madison, Wisconsin.

Weller, R.E. 1992. Paraneoplastic syndromes. In: *Handbook of Small Animal Practice, 2nd edition*, R.V. Morgan, ed., pp. 813-822. Churchill Livingstone, New York, New York.

Weller, R.E., G.E. Dagle, R.E. Perry, and J.F. Park. 1992. Primary pulmonary chondrosarcoma in a dog. *Cornell Vet.* 82(4):447–452.

Weller, R.E., and W.E. Hoffman. 1992. Renal function in dogs with lymphosarcoma and associated hypercalcemia. *J. Small Anim. Pract.* 33:61-66.

Zangar, R.C., D.L. Springer, J.A. McCrary, R.F. Novak, T. Primiano, and D.R. Buhler. 1992. Changes in adult metabolism of aflatoxin B_1 in rats neonatally exposed to diethystilbestrol. Alterations in α-class glutathione S-transferases. *Carcinogenesis* 13:2375-2379.

1993

Briant, J.K., and M. Lippmann. 1993. Aerosol bolus transport through a hollow airway cast by steady flow in different gases. *Aerosol Science and Technology* 19:27-39.

Brooks, A.L., R.M. Kitchin, N.F. Johnson, and E.S. Gilbert. 1993. The role of cellular and molecular studies in evaluation of health effects from combined radiation and chemical exposure. Proceedings of the American Statistical Association Conference on Radiation and Health: Radiation Risk and Interactions. *Radiat. Res.* 133:121-122 (abstract).

Brooks, A.L., M.A. Khan, R.F. Jostes, and F.T. Cross. Metaphase chromosome aberrations as markers of radiation exposure and dose. In: *The Laboratory and Epidemiology: The Development and Application of Biomarkers to the Study of Human Health Effects*, L.E. Sever, ed., Proceedings of the 31st Hanford Symposium on Health and the Environment, October 19-23, 1992, Richland, Washington. *J. Toxicol. Environ. Health* 40:277-288.

Cross, F.T. 1993. A review of experimental animal radon health effects data. In: *Radon Monitoring in Radiation Protection Environmental and/or Earth Sciences.* G. Furlan and L. Tommasino, eds., pp. 34-43. World Scientific, Singapore.

Dagle, G.E., P. Fritsch, F.F. Hahn, J.R. Maisin, R. Masse, M. Morin, G. Patrick, C.L. Sanders. 1993. Report of joint U.S. Department of Energy Biological Effects Task Group and European Late Effects Project Group (BETG/EULEP) Workshop on Lung Pathology, October 12-13, 1992. In: European Late Effects Project Group Newsletter 73, pp. 24-30.

Douthart, R.J., J.E. Pelkey, and G.S. Thomas. Database integration and visualization of maps of the human genome using the GnomeView interface. Proceedings of the 27th Hawaii Conference on System Science, Maui, Hawaii.

Evans, H.H., J. Mencl, G. Bakale, P.S. Rao, R.F. Jostes, T.E. Hui, F.T. Cross, and J.L. Schwartz. 1993. Interlaboratory comparison of the effects of radon on L5178Y cells: Dose contribution of radon daughter association with cells. *Radiat. Res.* 136:48-56.

Gies, R.A., F.T. Cross, and G.E. Dagle. A histopathological comparison of mixed exposures to radon progeny and uranium ore dust in rats. Abstracts of the 38th Annual Meeting of the Health Physics Society, July 11-15, 1993. *Health Phys.* 64(6):S53 (abstract).

Hui, T.E., F.T. Cross, A.C. James, R.F. Jostes, J.L. Schwartz, and K.L. Swinth. 1993. Evaluation of an alpha probe detector for *in vitro* cellular dosimetry. *Health Phys.* 64(6): 647-652.

Hulla, J.E., Z.Y. Chen, and D.L. Eaton. 1993. Aflatoxin B_1-induced rat hepatic hyperplastic nodules do not exhibit a site-specific mutation within the *p53* gene. *Cancer Res.* 53:9-11.

Hulla, J.E., and R.P. Schneider. 1993. Structure of the rat p53 tumor suppressor gene. *Nucleic Acids Res.* 21(3):723-717.

Jostes, R.F. T.E. Hui, and F.T. Cross. 1993. Single-cell gel technique supports hit probability calculations. *Health Phys.* 64(6):675-679.

Light-Wahl, K.J., D.L. Springer, B.E. Winger, C.G. Edmonds, D.G. Camp, II, B.D. Thrall, and R.D. Smith. 1993. Observation of a small oligonucleotide duplex by electrospray ionization mass spectrometry. *J. Am. Chem. Soc.* 115:803-804.

Light-Wahl, K.J., B.E. Winger, and R.D. Smith. 1993. Observation of a the multimeric forms of Concanavalin A by electrospray ionization mass spectrometry. *J. Am. Chem. Soc.* 115:5869-5870.

Mahaffey, J.A., M.A. Parkhurst, A.C. James, F.T. Cross, M.C.R. Alavanja, J.D. Boice, S. Ezrine, P. Henderson, and R.C. Brownson. 1993. Estimating past exposure to indoor radon from household glass. *Health Phys.* 64(4):381-391.

Meznarich, H.K., L.S. McCoy, T.L. Bale, G.L. Stiegler, and M.R. Sikov. 1993. Brain fibronectin expression in prenatally irradiated mice. *J. Toxicol. Environ. Health* 40:263-275.

Miller, D.L., and R.M. Thomas. 1993. A comparison of hemolytic and sonochemical activity of ultrasonic cavitation in a rotating tube. *Ultrasound in Med. & Biol.* 19(1): 83-90.

Miller, D.L., and R.M. Thomas. 1993. Frequency dependence of cavitation activity in a rotating tube exposure system compared to the mechanical index. *J. Acoust. Soc. Am.* 93(6): 3475-3480.

Miller, D.L., and R.M. Thomas. 1993. Ultrasonic gas body activation in *elodea* leaves and the mechanical index. *Ultrasound in Med. & Biol.* 19(4):343-351.

Pelkey, J.E., G.S. Thomas, D.A. Thurman, V.B. Lortz, and R.J. Douthart. 1993. GnomeView: A tool for visual representation of human genome data. Proceedings of the 1993 ACM/SIGAPP Symposium on Applied Computing, Indianapolis, Indiana, p. 21.

Sanders, C.L., K.E. Lauhala, K.E. McDonald, and G.A. Sanders. 1993. Lifespan studies in rats exposed to $^{239}PuO_2$ aerosol. I. Dosimetry. *Health Phys.* 64:509-521.

Sever, L.E. 1993. Neuroepidemiology of intrauterine radiation exposure. In: *Neuroepidemiology: Theory and Methods. Epidemiology of Neurological Disorders*, C.A. Molgaard, ed., pp. 241-256. Academic Press, Orlando, Florida.

Sikov, M.R., R.J. Traub, T.E. Hui, H.K. Meznarich, and K.D. Thrall. 1993. *Contribution of Maternal Radionuclide Burdens to Prenatal Radiation Doses.* NUREG/CR-5631, PNL-7445, Rev. 1, Addendum 1. Prepared for the U.S. Nuclear Regulatory Commission, Washington, D.C., by Pacific Northwest Laboratory, Richland, Washington.

Sikov, M.R., and T.E. Hui. 1993. Relationships between annual limits on intake and prenatal doses. In: *Contribution of Maternal Radionuclide Burdens to Prenatal Radiation Doses.* NUREG/CR-5631, PNL-7445, Rev. 1, Addendum 1. Prepared for the U.S. Nuclear Regulatory Commission, Washington, D.C., by Pacific Northwest Laboratory, Richland, Washington.

Springer, D.L., R.J. Bull, S.C. Goheen, D.M. Sylvester, and C.G. Edmonds. 1993. Electrospray ionization mass spectrometric characterization of acrylamide adducts to hemoglobin. *J. Toxicol. Environ. Health* 40:161-176.

Watson, C.R. 1993. SNODOG Glossary: Part 1, Introduction. PNL-8650, Part 1, Pacific Northwest Laboratory, Richland, Washington.

Watson, C.R. 1993. SNODOG Glossary: Part 2, Usage of Terms. PNL-8650, Part 2, Pacific Northwest Laboratory, Richland, Washington.

Wier, M.S., D.L. Springer, A.F. Fuciarelli, B.D. Thrall, and C.G. Edmonds. 1993. Characterization of natural and radiation-induced modifications of histones. In: *Techniques in Protein Chemistry Vol. V.* Academic Press, New York, New York.

Zangar, R.C., D.L. Springer, and D.R. Buhler. 1993. Alterations in cytochrome P-450 levels in adult rats following neonatal exposure to xenobiotics. *J. Toxicol. Environ. Health* 38:43-55.

In Press

Bair, W.J., M.R. Bailey, F.T. Cross, R.G. Cuddihy, P. Gehr, A.C. James, J.R. Johnson, R. Masse, M. Roy, and W. Stahlhofen. *Human Respiratory Tract Model for Radiological Protection. A Report of Committee 2 of the International Commission on Radiological Protection (ICRP).* (in press)

Beach, C., A.F. Fuciarelli, and J.D. Zimbrick. Electron migration along 5-bromouracil-substituted DNA irradiated in solution and in cells. *Radiat. Res.* (in press).

Birchall, A., and A.C. James. A general method for dealing with radioactive progeny and its application to modeling thorium in the lungs. *Health Phys.* (in press)

Birchall, A., and A.C. James. Uncertainty analysis of the effective dose per unit exposure from radon progeny using the new ICRP lung model. *Radiat. Prot. Dosim.* (in press).

Brooks, A.L., K.E. McDonald, C. Mitchell, D. S. Culp, A. Lloyd, N.F. Johnson, and R.M. Kitchin. The combined genotoxic effects of radiation and occupational pollutants. In: *Current Topics in Occupational Health*, T.S. Tenforde, ed., Proceedings of the 30th Hanford Symposium on Health and the Environment, Richland, Washington (in press).

Cross, F.T. Evidence of cancer risk from radon experimental animal studies. In: *National Council of Radiation Protection and Measurements (NCRP) Scientific Committee 85 Report: Risk of Lung Cancer from Radon* (in press).

Cross, F.T. Evidence of cancer risk from experimental animal radon studies. In: *Pedagogical Symposium: Radiation and Society*, Proceedings of the 203rd National Meeting of the American Chemical Society, April 5-10, 1992, San Francisco, California (in press).

Cross, F.T., J. Lubin, R. Masse, J. Samet, and G. A. Swedjemark. Inputs to the quantification of risk. In: *CEC/DOE Radon-Related Risk Recommendations Report*, Chapter 4 (in press).

Edmonds, C.G., M.S. Weir, A.F. Fuciarelli, B.D. Thrall, and D.L. Springer. Electrospray ionization mass spectrometry and tandem mass spectrometry of chick erythrocyte histones. *Mass Spectrom. Rev.* (rapid communication) (in press).

Fuciarelli, A.F., E.C. Sisk, and J.D. Zimbrick. Electron migration in gamma-irradiated solutions of DNA. *Int. J. Radiat. Biol.* (in press).

Hui, T.E., A.L. Brooks, and A.C. James. Microdosimetry of micronuclei induction and cell killing in mammalian cells irradiated in vitro by alpha particles. *Int. J. Radiat. Biol.* (in press).

James, A.C., W. Stahlhofen, G. Rudolf, J.K. Briant, M.J. Egan, W. Nixon, and A. Birchall. Annexe D: Deposition of inhaled particles. In: *A Report of Committee 2 of the International Commission on Radiological Protection (ICRP) on a Human Respiratory Tract Model for Radiological Protection* (in press).

James, A.C., M. Roy, and A. Birchall. Annexe F: Reference values for regional deposition. In: *A Report of Committee 2 of the International Commission on Radiological Protection (ICRP) on a Human Respiratory Tract Model for Radiological Protection* (in press).

James, A.C., J.K. Briant, J.S. Durham, and A. Birchall. Annexe H: Absorbed fractions for alpha, beta, positron, and electron emissions In: *A Report of Committee 2 of the International Commission on Radiological Protection (ICRP) on a Human Respiratory Tract Model for Radiological Protection* (in press).

James, A.C. Annexe J: Example hand calculation of respiratory tract doses. In: *A Report of Committee 2 of the International Commission on Radiological Protection (ICRP) on a Human Respiratory Tract Model for Radiological Protection* (in press).

Jostes, R.F., E.W. Fleck, K.P. Gaspar, T.L. Morgan, and F.T. Cross. Southern and PCR analysis of HPRT mutations induced by radon and its progeny. *Radiat. Res.* (in press).

Khan, M.A., F.T. Cross, R.F Jostes, and A.L. Brooks. Differences in radon-induced micronuclei between human bronchial epithelial cells and rat lung cells. In: *Environmental Mutagens and Human Health,* Proceedings of the 18th Annual Conference of the Environmental Mutagen Society of India, February 10-12, 1993, Madras, India (in press).

Khan, M.A., R.F. Jostes, F.T. Cross, R.A. Gies, and A.L. Brooks. *In vivo* induction of micronuclei in rat and Chinese hamster lung fibroblasts from radon inhalation. In: *Proceedings of the Annual Meeting of the Society of Toxicology*, March 14-18, 1993, New Orleans, Louisiana, (in press).

Khan, M.A., F.T. Cross, R.F. Jostes, T.E. Hui, J.E. Morris, and A.L. Brooks. Radon progeny-induced micronuclei in deep-lung fibroblasts of rats *in vivo* and *in vitro*. *Radiat. Res.* (in press).

Manley-Beach, C., A.F. Fuciarelli, and J.D. Zimbrick. Radiation-induced electron migration along 5-bromouracil-substituted DNA in cells. *Radiat. Res.* (in press).

Masse, R., and F.T. Cross. Annexe C: Effects of radiation in the respiratory tract. In: *A Report of Committee 2 of the International Commission on Radiological Protection (ICRP) on a Human Respiratory Tract Model for Radiological Protection* (in press).

Miller, R.T., R.J. Douthart, and A.K. Dunker. Identifying repeated structural elements in proteins. Proceedings of the 27th Hawaii Conference on System Science, Maui, Hawaii (in press).

Sanders, C.L., and G.E. Dagle. A threshold model of pulmonary carcinogenesis: Carcinoma in the rat after deposition of plutonium or quartz. In: *Current Topics in Occupational Health*, T.S. Tenforde, ed., Proceedings of the 30th Hanford Symposium on Health and the Environment, Richland, Washington. *Appl. Occup. Environ. Hyg. J.* (in press).

Sanders, C.L., K.E. Lauhala, K.E. McDonald, and B.G. Moore. Carcinoma of the upper respiratory tract in rats following nose-only inhalation of $^{239}PuO_2$. *J. Aerosol Medicine* (in press).

Solomon, S.B., R. O'Brien, M. Wilks, and A.C. James. Application of the ICRP's new lung model to an underground uranium mine. *Radiat. Prot. Dosim.* (in press).

Thrall, B.D., D.B. Mann, M.J, Smerdon, and D.L. Springer. Nucleosome structure modulates benzo[a]pyrene diol epoxide adduct formation. *Biochemistry* (in press).

Wolff, S., V. Afzal, R. Jostes, and J.K. Wiencke. Indications of repair of radon-induced chromosome damage in human lymphocytes: An adaptive response induced by low doses of x rays. *Environ. Health Perspect.* (in press).

Presentations

1992

Brooks, A.L., M.R. Raju, M.K. Murphy, W.F. Harvey, G.J. Newton, and R. Guilmette. 1992. Comparison of the effectiveness of collimated and noncollimated random ^{238}Pu sources on the induction of micronuclei and cell killing in lung epithelial cells. Presented at the 40th Annual Meeting of the Radiation Research Society, March 15-18, Salt Lake City, Utah.

Brooks, A.L., J. Adelstein, B. Boecker, K. Kase, A. Kronenburg, B. McNeil, R. Shore, and W. Templeton. 1992. Identification of research needs in radiation protection. Presented at the 40th Annual Meeting of the Radiation Research Society, March 15-18, Salt Lake City.

Brooks, A.L. 1992. Radioadaptive response *in vivo* in Chinese hamsters injected with alpha-(^{239}Pu) or beta-gamma-(^{144}Ce) emitting radionuclides. Presented at the International Conference on Low Dose Irradiation and Biological Defense Mechanisms, July 11-19, Kyoto, Japan.

Brooks, A.L., R.M. Kitchin, N.F. Johnson, and E.S. Gilbert. 1992. The role of cellular and molecular studies in evaluation of health effects from combined radiation and chemical exposures. Presented at the American Statistical Association Conference on Radiation and Health, June 28-July 2, Hilton Head Island, South Carolina.

Brooks, A.L. 1992. Use of cell and molecular techniques in risk assessment. Presented at the Hanford Technical Exchange Program on Human Health and Ecological Risk: Science and Policy Issues Important to the DOE Approach to Environmental Cleanup, October 14, Richland, Washington.

Brooks, A.L., M.A. Khan, R.F. Jostes, and F.T. Cross. 1992. Metaphase chromosome aberrations as markers of radiation exposure and dose. Presented at the 31st Hanford Symposium on Health and the Environment, The Laboratory and Epidemiology: The Development and Application of Biomarkers to the Study of Human Health Effects, October 19-23, Richland, Washington.

Cross, F.T. 1992. Evidence of cancer risk from experimental animal radon studies. Presented at the Pedagogical Symposium: "Radiation and Society," of the 203rd National Meeting of the American Chemical Society, April 5-10, San Francisco, California (invited presentation).

Cross, F.T. 1992. DOE and PNL programs on risk of environmental radon exposures. Presented at the Florida Institute of Phosphate Research, October 16, Bartow, Florida.

Dagle, G.E., F.T. Cross, R.A. Gies, and R. Buschbom. 1992. Lung tumors in rats exposed to inhaled uranium ore dust and radon progeny. Presented at the 24th Annual Meeting of the European Society for Radiation Biology, October 4-8, Erfurt, Germany.

Douthart, R.J. 1992. A computer graphics window to the human genome. Presented at Baylor College of Medicine, Houston, Texas.

Douthart, R.J. 1992. GnomeView: Human genome data base integration with color graphics. Presented at Washington State University, Pullman, Washington.

Douthart, R.J. 1992. Invited lecture and GnomeView demonstration given at the Human Genome Informatics Workshop, Lawrence Berkeley Laboratory, Berkeley, California.

Douthart, R.J. 1992. Invited lecture and GnomeView demonstration given at the Johns Hopkins University Medical School, Baltimore, Maryland.

Douthart, R.J. 1992. The insulin gene that wasn't. Presented at the Biotechnology Training Program Workshop, Washington State University, Pullman, Washington.

Edmonds, C.G., D.L. Springer, D.M. Sylvester, S.C. Goheen, and R.J. Bull. 1992. Characterization of acrylamide adducted hemoglobin and proteolytically derived peptides based on electrospray ionization mass spectrometry. Presented at the 40th ASMS Conference on MS and Allied Topics, May 31–June 5, Washington, D.C.

Edmonds, C.G., A.L. Fuciarelli, and D.L. Springer. 1992. Electrospray ionization mass spectrometry for natural and radiation-induced modifications in histone proteins. Presented at the 40th ASMS Conference on MS and Allied Topics, May 31–June 5, Washington, D.C.

Edmonds, C.G., J.A. Loo, R.D. Smith, A.F. Fuciarelli, B.D. Thrall, J.E. Morris, and D.L. Springer. 1992. Evaluation of histone sequence and modifications by electrospray ionization mass spectrometry and tandem mass spectrometry. Presented at the 31st Hanford Symposium on Health and the Environment, "The Laboratory and Epidemiology: The Development and Application of Biomarkers to the Study of Human Health Effects," October 19–23, Richland, Washington.

Edmonds, C.G., J.A. Loo, R.D. Smith, A.F. Fuciarelli, B.D. Thrall, J.E. Morris, and D.L. Springer. 1992. Evaluation of histone sequence and modifications by electrospray ionization mass spectrometry and tandem mass spectrometry. Presented at the Pacific Conference on Chemistry and Spectroscopy, October 21, Foster City, California.

Fuciarelli, A.F., E.C. Sisk, and J.D. Zimbrick. 1992. Measurement of free radical-induced base damage in DNA. Presented at the 31st Annual Meeting of the Society of Toxicology, February 23–27, Seattle, Washington.

Fuciarelli, A.F., E.C. Sisk, and J.D. Zimbrick. 1992. 5-bromouracil radiolysis as a molecular indicator of electron migration in aqueous solutions of DNA. Presented at the 40th Annual Meeting of the Radiation Research Society, March 14–18, Salt Lake City, Utah.

Fuciarelli, A.F., M. Kennedy, J.D. Zimbrick, and J.A. Raleigh. 1992. Radiation-induced intramolecular cyclization reactions in DNA: Molecular modeling and experimental analysis. Presented at the conference "Pathways to Radiation Damage in DNA," June 14–18, Oakland University, Rochester, Michigan.

Fuciarelli, A.F., E.C. Sisk, and J.D. Zimbrick. 1992. Electron transfer in irradiated solutions of DNA. Presented at the Ninth Annual Meeting of the Pacific Northwest Association of Toxicologists (PANWAT), September 24–25, Richland, Washington.

Gies, R.A., F.T. Cross, G.E. Dagle, R.L. Buschbom, and J.C. Aryan. 1992. The histomorphologic effects of inhaled radon, uranium ore dust, and cigarette smoke in the tracheal epithelium of the rat. Presented at the 37th Annual Meeting of the Health Physics Society, June 21–25, Columbus, Ohio.

James, A.C. 1992. Implications of a new ICRP lung model for the uranium and sand mining industries. Overview presented at the International Workshop on the Health Effects of Inhaled Radionuclides: Implications for Radiation Protection in Mining, September, Jabiru, Northern Territory, Australia (keynote address).

James, A.C. 1992. The ICRP Task Group's new lung model for dosimetry and bioassay. Overview presented at the 17th Annual Meeting of the Australian Radiation Protection Society, September 21–23, Darwin, Northern Territory, Australia (invited presentation).

Jarvis, M.G., K.D. Thrall, T.E. Hui, J.R. Johnson, J.A. Leonowich, T.T. Jarvis, and J.V. Mohatt. 1992. The integrated use of instrumentation and PBPK models to establish occupational exposure. Presented at the 31st Hanford Symposium on Health and the Environment, The Laboratory and Epidemiology: The Development and Application of Biomarkers to the Study of Human Health Effects, October 19–23, Richland, Washington.

Jostes, R.F., T.E. Hui, R.A. Gies, and F.T. Cross. 1992. Use of the single-cell gel technique to support hit-probability calculations in mammalian cells exposed to radon and radon progeny. Presented at the 40th Annual Meeting of the Radiation Research Society, March 14–18, Salt Lake City, Utah.

Khan, M.A., R.F. Jostes, J.E. Morris, R.A. Gies, and A.L. Brooks. 1992. The induction and repair of micronuclei in deep lung fibroblasts of rats from *in vitro* and *in vivo* radon-progeny exposure. Presented at the Ninth Annual Meeting of the Pacific Northwest Association of Toxicologists, September 24-25, Richland, Washington.

Khan, M.A., R.F. Jostes, F.T. Cross, K. Rithidech, and A.L. Brooks. 1992. Micronucleus: A biomarker of genotoxic damage induced *in vivo* and *in vitro* from radiation and chemical exposure. Presented at the 31st Hanford Symposium on Health and the Environment, The Laboratory and Epidemiology: The Development and Application of Biomarkers to the Study of Human Health Effects, October 19–23, Richland, Washington.

Loo, J.A., R.R. Ogorzalek-Loo, R.D. Smith, A.F. Fuciarelli, D.L. Springer, and C.G. Edmonds. 1992. Evaluation of covalent modifications and noncovalent associations in proteins by electrospray ionization–mass spectrometry. Presented at the Sixth Symposium of the Protein Society, July 25–29, San Diego, California.

Loo, J.A., A.F. Fuciarelli, D.L. Springer, C.G. Edmonds, R.R. Ogorzalek-Loo, and R.D. Smith. 1992. Elucidation of covalent modifications and noncovalent associations in proteins by electrospray ionization–mass spectrometry. Presented at the Sixth Annual Symposium of the Protein Society, July 25–29, San Diego, California.

Meznarich, H.K., L.S. McCoy, and M.R. Sikov. 1992. Brain fibronectin expression in prenatally irradiated mice. Presented at the 31st Hanford Symposium on Health and the Environment, "The Laboratory and Epidemiology: The Development and Application of Biomarkers to the Study of Human Health Effects," October 19–23, Richland, Washington.

Miller, R.T., A.K. Dunker, and R.J. Douthart. 1992. Amino acid conformations as an alphabet. Presented at the West Coast Theoretical Chemistry Conference, Richland, Washington.

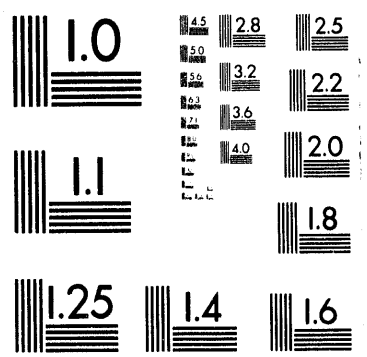
1.0
1.1
1.25
1.4
1.6
1.8
2.0
2.2
2.5
2.8
3.2
3.6
4.0
4.5
5.0
5.6
6.3
7.1

2 of 2

Miller, R.T., R.J. Douthart, and A.K. Dunker. 1992. An informatics approach to protein folding. Presented at the Sixth Annual Meeting of the Protein Society, San Diego, California.

Miller, R.T., R.J. Douthart, and A.K. Dunker. 1992. Learning an objective alphabet of amino acid conformations. Presented at the Sixth Annual Symposium of the Protein Society, July 25-29, San Diego, California.

Sanders, C.L. 1992. Inhaled plutonium and lung cancer in an animal model. Seminar presented to Physics Applications, Westinghouse Hanford, Richland, Washington.

Sanders, C.L. 1992. Is inhaled plutonium really all that toxic? Seminar presented to the Department of Environmental Science, Washington State University–Tri Cities, Richland, Washington.

Sanders, C.L. 1992. Microdosimetric and cellular basis for a lung tumor threshold following inhalation of ^{239} PuO^2. Presented at the 24th Annual Meeting of the European Society for Radiation Biology, October 4-8, Erfurt, Germany.

Sanders, C.L. 1992. Pulmonary carcinogenesis of inhaled plutonium. Seminar given at the Department of Pharmacology/Toxicology, Washington State University, Pullman, Washington.

Sanders, C.L., D.M. Sylvester, and D.L. Springer. 1992. Recognition of acrylamide adducts in peptides from hemoglobin. Presented at the 31st Annual Meeting of the Society of Toxicology, February 23-27, Seattle, Washington.

Sanders, C.L. 1992. Spatial distribution of inhaled $^{239}PuO_2$ and pulmonary carcinogenesis in three strains of the rat. Presented at the 40th Annual Meeting of the Radiation Research Society, March 14–18, Salt Lake City, Utah.

Springer, D.L., C.G. Edmonds, D.M. Sylvester, C.L. Sanders, and R.J. Bull. 1992. Partial characterization of proteolytically derived peptides from acrylamide-adducted hemoglobin. Presented at the 31st Annual Meeting of the Society of Toxicology, February 23–27, Seattle, Washington.

Springer, D.L., C.G. Edmonds, C. Goheen, D.M. Sylvester, and R.J. Bull. 1992. Electrospray ionization mass spectrometric characterization of adducts to hemoglobin. Presented at the 31st Hanford Symposium on Health and the Environment, "The Laboratory and Epidemiology: The Development and Application of Biomarkers to the Study of Human Health Effects," October 19–23, Richland, Washington.

Thrall, B.D., and D.L. Springer. 1992. Sequence-specific blocks in DNA/RNA polymerases induced by benzo[a]pyrene diol epoxide. Presented at the 31st Annual Meeting of the Society of Toxicology, February 23–27, Seattle, Washington.

Thrall, B.D., C.G. Edmonds, and D.L. Springer. 1992. Translesional synthesis by model DNA polymerases on an oligonucleotide modified by benzo[a]pyrene diol epoxide. Presented at the Eighth Annual Meeting of the Pacific Northwest Association of Toxicologists (PANWAT), September 24–25, Richland, Washington.

Thrall, K.D., T.E. Hui, J. R. Johnson, M.F. Jarvis, and T.T. Jarvis. 1992. Use of models to establish occupational exposure to chemicals and/or radioactivity. Presented at the Joint Meeting of the International Society of Exposure

Analysis and the International Society of Environmental Epidemiology, August 26–29, Cuernavaca, Morelos, Mexico.

Weller, R.E. 1992. Intrathoracic neoplasia: Epidemiology and etiology. Presented at the 10th American College of Veterinarians Internal Medicine Forum, May 30, San Diego, California.

Weller, R.E. 1992. Cancer diagnosis in the dog and cat. Presented at the XIIIth Pan American Congress of Veterinary Sciences, October 8, Santiago, Chile.

Weller, R.E. 1992. Epidemiology and etiology of neoplasia in the dog and cat. Presented at the XIIIth Pan American Congress of Veterinary Sciences, October 8, Santiago, Chile.

Zimbrick, J.D., C.M. Beach, E.C. Sisk, and A.F. Fuciarelli. 1992. Electron migration in 5-bromouracil-substituted DNA and oligonucleotides in irradiated aqueous solutions. Presented at the conference "Pathways to Radiation Damage in DNA," June 14–18, Oakland University, Rochester, Michigan (invited paper).

Zimbrick, J. 1992. Implications of radiation repair genes for radiation protection. Presented at the 37th Annual Meeting of the Health Physics Society, June 21–25, Columbus, Ohio (invited paper).

1993

Birchall, A., and A.C. James. 1993. Sensitivity analysis of the effective dose per unit exposure from radon progeny using the new ICRP lung model. Presented at the workshop, "Intakes of Radionuclides: Detection, Assessment, and Limitation of Occupational Exposure," September 13-17, Bath, England.

Brooks, A.L., and K.E. McDonald. 1993. Use of fluorescent *in situ* hybridization techniques in A_L cells to define the kinetics and survival of radiation-induced chromosome aberrations. Presented at the Sixth International Conference on Environmental Mutagens, February 21–26, Melbourne, Australia.

Brooks, A.L. 1993. Overview of the cell and molecular research in the DOE/OHER Radon Program, Presented at the Principal Scientists' Meeting, February 28-March 1, Washington, D.C.

Brooks, A.L., R.F. Jostes, M.A. Khan, and F.T. Cross. 1993. Radon-induced cytogenetic instability. Presented at the 41st Annual Meeting of the Radiation Research Society, March 20–25, Dallas, Texas.

Brooks, A.L., M.A. Khan, R.F. Jostes, K.E. McDonald, and F.T. Cross. 1993. *In vitro/in vivo* radon-induced chromosome damage. Presented at the Environmental Mutagen Society Annual Meeting, April 17-22, Norfolk, Virginia.

Brooks, A.L. 1993. Radon awareness and disclosure. Presented as testimony for the joint hearing before the Subcommittee on Health and the Environment and the Subcommittee on Transportation and Hazardous Materials of the Committee on Energy and Commerce, House of Representatives, Serial No. 103-139, July, Washington, D.C.

Brooks, A.L. 1993. The use of cellular and molecular changes to help understand exposure-dose-response relationships for radon-induced damage. Presented at the National Academy of Sciences Meeting on Radon Risks, August 24, Washington, D.C.

Brooks, A.L. 1993. Realistic risk estimates: How they can be achieved. Presented at the

DOE Contractor's Meeting, October 18-20, New York, New York.

Brooks, A.L. 1993. Cellular and molecular studies: How do they help define radon risk? Presented at the joint meeting of NIH/DOE/ EPA, October 29, Washington, D.C.

Cross, F.T. 1993. Radon interactions and the evidence on exposure rate effect from experimental animal studies. Presented at the National Research Council Radon: Molecular and Cellular Radiobiology Workshop, August 26-27, Washington, D.C.

Cross, F.T. 1993. Radon hazards in homes project. Presented at the U.S. DOE/OHER Radon Research Program Contractor's Meeting, October 17-19, New York, New York.

Douthart, R.J., J.E. Pelkey, and G.S. Thomas. 1993. A demonstration of the GnomeView interface. Presented at the DOE Human Genome Workshop, Sante Fe, New Mexico.

Douthart, R.J. 1993. GnomeView: A graphical inter face to the human genome. Presented at the DOE Human Genome Workshop, Sante Fe, New Mexico.

Durham, J.S., and A.C. James. 1993. Electron and beta dosimetry for the new ICRP respiratory tract model. Presented at the 38th Annual Meeting of the Health Physics Society, July 11-15, Atlanta, Georgia.

Edmonds, C.G., M.S. Weir, B.D. Thrall, J.E. Morris, and D.L. Springer. 1993. Evaluation of variable post-translational modification of human histones by electrospray ionization mass spectrometry and tandem mass spectrometry. Presented at the 41st ASMS Conference on Mass Spectrometry and Allied Topics, May 31-June 5, San Francisco, California.

Fuciarelli, A.F., E.C. Sisk, J.H. Miller, and J.D. Zimbrick. 1993. Electron migration in gamma-irradiated solutions of DNA. Presented at the Biophysical Society Meeting, February 14-18, Washington, D.C.

Fuciarelli, A.F., E.C. Sisk, J.H. Miller, and J.D. Zimbrick. 1993. Electron migration in gamma-irradiated solutions of DNA. Presented at the 41st Annual Meeting of the Radiation Research Society, March 20-25, Dallas, Texas (invited plenary session).

Fuciarelli, A.F., E.C. Sisk, L.E. Matson, K. Miaskiewicz, J.H. Miller, and J.D. Zimbrick. 1993. Electron migration in gamma-irradiated solutions of DNA. Presented at the conference on DNA Damage: Effects on DNA Structure and Protein Recognition (New York Academy of Sciences), July 31-August 4, Burlington, Vermont.

Gies, R.A., F.T. Cross, and G.E. Dagle. 1993. A histopathological comparison of mixed exposures to radon progeny and uranium ore dust in rats. Presented at the 38th Annual Meeting of the Health Physics Society, July 11-15, Atlanta, Georgia.

James, A.C. 1993. Application of the dog data to improve the human respiratory tract model for radiological protection. Presented at the DOE/ OHER Dog Workshop, February 16-18, Albuquerque, New Mexico.

James, A.C. 1993. An overview of the ICRP Task Group on the Human Respiratory Tract Model. Presented at the 33rd Annual Congress of the South African Association of Physicists in Medicine and Biology, University of the Orange Free State, March 8-10, Bloemfontein, South Africa.

James, A.C. 1993. The new ICRP lung model. Presented at the South African Association of Physicists in Medicine and Biology Joint Medical Physics and Radiation Protection Summer School, March 11-12, Allemanskraal Dam, South Africa.

James, A.C. 1993. Teach-in on the new ICRP lung model. Presented at the Atomic Energy Corporation of South Africa Ltd. Research Establishment, March 16, Pelindaba, Transvaal, South Africa.

James, A.C. 1993. Teach-in on the new ICRP lung model. Presented at the Koeberg Nuclear Power Station Establishment, March 18, Capetown, Cape Province, South Africa.

James, A.C. 1993. Dosimetric factors in evaluating radon risks. Presented at the National Research Council's Committee on Health Risks of Exposure to Radon (BEIR VI) Workshop, April 19, Albuquerque, New Mexico.

James, A.C. 1993. Physical factors affecting health risks from indoor radon. Presented at the CEC/USDOE/USEPA International Workshop on Indoor Radon Remedial Action, June 27- July 2, Rimini, Italy.

James, A.C. 1993. Radon health effects data in animals and their relationship to human cancer. Presented to the Subcommittee on Environmental Carcinogenesis, National Cancer Advisory Board, National Institutes of Health, September 20, Bethesda, Maryland.

James, A.C. 1993. The ICRP's new lung model for radiological protection. Presented at the American Nuclear Society's Topical Workshop on the Technical Basis for Measuring, Modeling, and Mitigating Toxic Aerosols, September 27-30, Albuquerque, New Mexico.

James, A.C. 1993. The Dosimetry of Radon Progeny project. Presented at the DOE Contractor's Meeting, October 18-20, New York, New York.

James, A.C. 1993. New ICRP lung dosimetry and its risk implications for alpha emitters. Presented at the special symposium in honor of Dr. William J. Bair, "Radiobiology of Inhaled Nuclides," November 9-10, Richland, Washington.

Jostes, R.F., T.E. Hui, A.L. Brooks, and F.T. Cross. 1993. Southern blot and PCR analysis of HPRT mutations induced by radon and its progeny. Presented at the Sixth International Conference on Environmental Mutagens, February 21-26, Melbourne, Australia.

Jostes, R.F., T.E. Hui, A.L. Brooks, and F.T. Cross. 1993. Use of the single-cell gel technique to support hit probability calculations in mammalian cells exposed to radon and radon progeny. Presented at the Sixth International Conference on Environmental Mutagens, February 21-26, Melbourne, Australia (invited speaker).

Jostes, R.F. 1993. Overview of the PNL Mechanisms of Radon Damage program. Presented at the Department of Radiobiology and Radiation Biology, Colorado State University, March 20, Fort Collins, Colorado.

Jostes, R.F., E.W. Fleck, T.L. Morgan, G. L. Stiegler, and F.T. Cross. 1993. Southern and PCR analysis of HPRT mutations induced by radon and its progeny. Presented at the 41st Annual Meeting of the Radiation Research Society, March 20-25, Dallas, Texas.

Jostes, R.F., E. W. Fleck, T. L. Morgan, G. L. Stiegler, and F.T. Cross. 1993. Southern and PCR analysis of HPRT mutations induced by

radon and its progeny. Presented at the 17th Annual Meeting of the Cell Kinetics Society, April 15–18, Richland, Washington.

Jostes, R.F., F.T. Cross, R.A. Gies, T.E. Hui, A.D. Layton, L. Stillwell, and G.L. Stiegler. Update on the Mechanisms of Radon Damage project. Presented at the 1993 Annual Radon Contractor's meeting, October 17-19, New York, New York.

Khan, M.A., F.T. Cross, R.F. Jostes, and A.L. Brooks. 1993. Differences in radon-induced micronuclei between human bronchial epithelial cells and rat lung cells. Presented at the International Symposium on Environmental Mutagens and Human Health, February 10–12, Madras, India.

Khan, M.A., R.F. Jostes, J.A. Morris, and A.L. Brooks. 1993. The *in vivo/in vitro* induction of micronuclei in rat lung fibroblasts from radon exposure. Presented at the Sixth International Conference on Environmental Mutagens, February 21–26, Melbourne, Australia.

Khan, M.A., R.F. Jostes, F.T. Cross, R.A. Gies, and A.L. Brooks. 1993. *In vivo* induction of micronuclei in rat and Chinese hamster lung fibroblasts from radon inhalation. Presented at the Society of Toxicology Annual Meeting, March 14–18, New Orleans, Louisiana.

Miaskiewicz, K., J.H. Miller, R.L. Ornstein, A.F. Fuciarelli, J.D. Zimbrick, and J.A. Raleigh. 1993. DNA intramolecular crosslinks: Theory and experiment. Presented at the 41st Annual Meeting of the Radiation Research Society, March 20-25, Dallas, Texas.

Miller, R.T., R.J. Douthart, and A.K. Dunker. 1993. An alphabet of amino acid conformation in protein. Presented at the 26th Annual Hawaii International Conference on System Science, Maui, Hawaii.

Miller, R.T., R.J. Douthart, and A.K. Dunker. 1993. A set of distinguishable amino acid conformations. Presented at the Biophysical Society Meeting, San Francisco, California.

Miller, R.T., R.J. Douthart, and A.K. Dunker. 1993. Identifying repeated structures in proteins. Presented at the Seventh Annual Meeting of the Protein Society, San Diego, California.

Murad, A.O., B.D. Thrall, and D.L. Springer. 1993. Measuring benzo[a]pyrene diol epoxide adducts in specific sequences with defined chromatin structure and inducible transcription. Presented at the American Society for Cell Biology Annual Meeting, December 15, New Orleans, Louisiana.

O'Brien, R.S., S.B. Solomon, and A.C. James. 1993. Application of the ICRP Task Group's new lung model to an underground uranium mine. Presented at the workshop, "Intakes of Radionuclides: Detection, Assessment, and Limitation of Occupational Exposure," September 13-17, Bath, England.

Pelkey, J.E., G.S. Thomas, and R.J. Douthart. 1993. GnomeView: A graphical interface to the human genome. Presented at the DOE Human Genome Workshop, Santa Fe, New Mexico.

Pelkey, J.E., G.S. Thomas, D.A. Thurman, V.B. Lortz, and R.J. Douthart. 1993. GnomeView: A tool for visual representation of human genome data. Presented at the 1993 ACM/SIGAPP Symposium on Applied Computing, Indianapolis, Indiana.

Sanders, C.L. 1993. Rat strain and respiratory tract carcinogenesis from inhaled transuranics

and radon. Presented at the Inhalation Toxicology Research Institute, Albuquerque, New Mexico.

Sikov, M.R., H.K. Meznarich, K.D. Thrall, and T.E. Hui. 1993. Use of data from experimental animals for dosimetry of radionuclides in the human embryo/fetus. Presented at the Teratology Society 1993 Annual Meeting, June 26-July 1, Tucson, Arizona.

Springer, D.L., B.D. Thrall, D.B. Mann, and M.J. Smerdon. 1993. Nucleosome modulation of benzo[a]pyrene diol epoxide adduct formation. Presented at the 15th Annual West Coast Chromatin and Chromosomes Meeting, December 9-12, Pacific Grove, California.

Thrall, K.D., T.E. Hui, and A.C. James. 1993. Physiologically based pharmacokinetic modeling of radon, thoron, and their short-lived progeny. Presented at the Society of Toxicology Annual Meeting, March 14-18, New Orleans, Louisiana.

Thrall, B.D., and D.L. Springer. 1993. Reassembly of nucleosomes on a plasmid DNA model alters restriction enzyme accessibility. Presented at Society of Toxicology Annual Meeting, March 14-18, New Orleans, Louisiana.

Thrall, B.D., and D.L. Springer. 1993. Benzo-[a]pyrene diol epoxide adduct formation on a reconstituted plasmid DNA system. Presented at the 1993 Environmental Mutagen Society Meeting, April 17-22, Norfolk, Virginia.

Thrall, B.D., D.B. Mann, and D.L. Springer. 1993. Nucleosome structure modulates benzo-[a]pyrene diol epoxide adduct formation. Presented at the 10th Annual Meeting of the Pacific Northwest Association of Toxicologists, October 22-24, Eatonville, Washington.

Weir, M.S., D.L. Springer, A.F. Fuciarelli, B.D. Thrall, and S.G. Edmonds. 1993. Characterization of natural and radiation induced modifications of histones. Presented at the Seventh Symposium of the Protein Society, July 24-28, San Diego, Caifornia.

Author Index

Author Index

Appendix

Appendix

Dose-Effect Studies with Inhaled Plutonium in Beagles

On the following pages (A.3-A.11), data are presented for all dogs assigned to current life-span dose-effect studies with inhaled $^{239}Pu(NO_3)_4$. Data from dogs exposed to inhaled $^{239}PuO_2$ or $^{238}PuO_2$ did not change from the previous year and were omitted from this appendix. Information is presented on the estimated initial lung deposition, based on external thorax counts and on estimated lung weights (0.011 x body weight) at time of exposure. Information is also provided on the current interpretation of the most prominent clinicopathological features associated with the death of animals. These data represent information currently available, and are presented as reference material for scientists who desire to follow in detail the progress of these experiments.

INHALED PLUTONIUM NITRATE IN DOGS

DOSE GROUP	DOG IDENT	BIRTH DATE	INITIAL ALVEOLAR DEPOSITION BQ	BQ/G LUNG	BQ/ KG	INHALATION EXPOSURE WGT (KG)	AGE (MO)	EXPO DATE	DEATH INFORMATION DEATH DATE	MONTHS POST INH	AGE (MO)	COMMENTS ON DEAD DOGS
CONTROL	1356 M	5/11/74	0	0.00	0.00	13.0	20.3	1/20/76	4/07/87	134.5	154.9	Hypothyroidism
CONTROL	1365 M	5/14/74	0	0.00	0.00	10.2	20.2	1/20/76	7/16/88	149.8	170.1	Pneumonia
CONTROL	1376 F	6/17/74	0	0.00	0.00	9.5	19.1	1/20/76	5/11/80	51.7	70.8	Pneumonia
CONTROL	1393 M	6/22/74	0	0.00	0.00	9.6	21.9	4/20/76	6/19/87	133.9	155.9	Pneumonia
CONTROL	1409 M	7/07/74	0	0.00	0.00	12.3	21.5	4/20/76	7/17/89	158.9	180.3	Herniated Vertebral Disc
CONTROL	1418 M	7/16/74	0	0.00	0.00	10.6	23.3	6/23/76	8/26/89	158.1	181.4	Adenoma, Pituitary
CONTROL	1425 M	7/17/74	0	0.00	0.00	15.6	23.2	6/23/76	8/02/82	73.3	96.5	Epileptic Seizures
CONTROL	1455 F	8/05/74	0	0.00	0.00	6.1	20.5	4/20/76	8/20/87	136.0	156.5	Pyometra
CONTROL	1483 F	9/03/74	0	0.00	0.00	9.8	21.7	6/23/76	12/20/91	185.9	207.5	Heart Failure
CONTROL	1516 F	10/05/74	0	0.00	0.00	9.4	20.6	6/23/76	2/24/92	188.1	208.7	Carcinoma, Thyroid
CONTROL	1525 M	10/12/74	0	0.00	0.00	12.5	21.3	7/22/76	11/14/87	135.8	157.1	Transitional Carcinoma, Urethra
CONTROL	1526 M	10/12/74	0	0.00	0.00	10.8	21.3	7/22/76	8/28/90	169.2	190.5	Seborrheic Dermatitis
CONTROL	1528 F	10/29/74	0	0.00	0.00	10.6	20.8	7/22/76	4/06/87	128.5	149.2	Cerebral Hemorrhage
CONTROL	1543 M	11/03/74	0	0.00	0.00	16.0	20.6	7/22/76	8/12/86	120.7	141.3	Herniated Vertebral Disc
CONTROL	1563 F	9/06/75	0	0.00	0.00	12.0	18.3	3/15/77	2/10/92	178.9	197.2	Adenocarcinoma, Ovary
CONTROL	1572 F	9/09/75	0	0.00	0.00	10.2	19.3	4/19/77	2/01/90	153.5	172.8	Heart Failure
CONTROL	1577 M	9/08/75	0	0.00	0.00	12.2	18.2	3/15/77	4/04/90	156.6	174.9	Hemangioma, Spleen (Ruptured)
CONTROL	1584 F	9/12/75	0	0.00	0.00	12.5	19.2	4/19/77	11/29/88	139.4	158.6	Carcinoma, Thyroid
CONTROL	1594 F	9/13/75	0	0.00	0.00	13.9	19.2	4/19/77	11/02/90	162.5	181.7	Pneumonia; Hepatocellur Carcinoma
CONTROL	1633 F	4/12/76	0	0.00	0.00	11.6	18.9	11/07/77	11/10/86	108.1	126.9	Carcinoma, Thyroid

INHALED PLUTONIUM NITRATE IN DOGS

DOSE GROUP	DOG IDENT	BIRTH DATE	INITIAL ALVEOLAR DEPOSITION BQ	BQ/G LUNG	BQ/ KG	INHALATION EXPOSURE WGT (KG)	AGE (MO)	EXPO DATE	DEATH INFORMATION DEATH DATE	MONTHS POST INH	AGE (MO)	COMMENTS ON DEAD DOGS
CONTROL-SAC	1388 M	6/22/74	0	0.00	0.00	12.0	21.9	4/20/76	9/11/81	64.7	86.7	Sacrificed
CONTROL-SAC	1405 M	7/05/74	0	0.00	0.00	10.3	21.5	4/20/76	8/13/84	99.8	121.3	Heart Base Tumor
CONTROL-SAC	1450 F	7/23/74	0	0.00	0.00	13.7	20.9	4/20/76	11/04/81	66.5	87.4	Sacrificed
CONTROL-SAC	1509 M	9/26/74	0	0.00	0.00	11.7	20.9	6/22/76	10/30/86	124.3	145.1	Sacrificed
CONTROL-SAC	1608 M	9/20/75	0	0.00	0.00	12.0	17.8	3/15/77	2/14/91	167.0	184.8	Rhabdomyosarcoma, Oral Cavity
CONTROL-SAC	1638 F	4/22/76	0	0.00	0.00	9.1	18.5	11/07/77	9/08/87	118.0	136.5	Sacrificed
VEHICLE	1361 M	5/14/74	0	0.00	0.00	14.0	21.0	2/12/76	4/04/89	157.7	178.7	Heart Failure
VEHICLE	1381 F	6/21/74	0	0.00	0.00	8.7	19.7	2/12/76	12/05/89	165.7	185.5	Mammary Tumor
VEHICLE	1392 M	6/22/74	0	0.00	0.00	12.8	22.0	4/22/76	1/16/90	164.8	186.8	Sebaceous Carcinoma, Skin (Lung Metastasis)
VEHICLE	1406 M	7/05/74	0	0.00	0.00	15.5	21.6	4/22/76	1/21/88	141.0	162.6	Malignant Melanoma, Oral Cavity
VEHICLE	1412 F	7/15/74	0	0.00	0.00	8.9	19.0	2/12/76	7/06/89	160.8	179.7	Mammary Tumor
VEHICLE	1421 M	7/16/74	0	0.00	0.00	13.0	23.5	6/29/76	2/26/88	139.9	163.4	Mastocytoma
VEHICLE	1457 F	8/05/74	0	0.00	0.00	11.5	20.6	4/22/76	11/07/89	162.5	183.1	Hypothyroidism
VEHICLE	1491 F	9/05/74	0	0.00	0.00	8.6	21.8	6/29/76	5/10/89	154.3	176.1	Mammary Tumor
VEHICLE	1504 F	9/26/74	0	0.00	0.00	10.2	21.1	6/29/76	2/22/89	151.8	172.9	Malignant Lymphoma
VEHICLE	1514 M	9/26/74	0	0.00	0.00	13.4	21.1	6/29/76	8/06/82	73.2	94.3	Malignant Lymphoma
VEHICLE	1524 M	10/12/74	0	0.00	0.00	12.1	21.5	7/27/76	3/27/88	140.0	161.5	Uremic Syndrome
VEHICLE	1531 F	10/29/74	0	0.00	0.00	8.8	20.9	7/27/76	9/15/91	181.6	202.5	Malignant Melanoma, Oral Cavity
VEHICLE	1542 M	11/03/74	0	0.00	0.00	12.5	20.8	7/27/76	5/01/89	153.1	173.9	Malignant Lymphoma
VEHICLE	1566 M	9/06/75	0	0.00	0.00	14.5	19.9	5/05/77	1/18/90	152.5	172.4	Malignant Lymphoma

INHALED PLUTONIUM NITRATE IN DOGS

DOSE GROUP	DOG IDENT	BIRTH DATE	INITIAL ALVEOLAR DEPOSITION BQ	BQ/G LUNG	BQ/ KG	INHALATION EXPOSURE WGT (KG)	AGE (MO)	EXPO DATE	DEATH INFORMATION DEATH DATE	MONTHS POST INH	AGE (MO)	COMMENTS ON DEAD DOGS
VEHICLE	1578 M	9/08/75	0	0.00	0.00	10.2	19.9	5/05/77	2/13/90	153.3	173.2	Uremic Syndrome
VEHICLE	1593 F	9/13/75	0	0.00	0.00	11.0	19.7	5/05/77	12/31/90	163.9	183.6	Uremic Syndrome
VEHICLE	1601 F	9/15/75	0	0.00	0.00	7.8	19.6	5/05/77	4/08/90	155.1	174.8	Uremic Syndrome
VEHICLE	1620 M	2/29/76	0	0.00	0.00	13.7	21.1	12/01/77	1/06/87	109.2	130.2	Herniated Vertebral Disc
VEHICLE	1634 F	4/12/76	0	0.00	0.00	10.8	19.6	12/01/77	11/05/92	179.2	198.8	Adenoma, Pituitary
VEHICLE	1651 F	4/26/76	0	0.00	0.00	9.9	19.2	12/01/77	11/11/92	179.4	198.5	Granulosa, Cell Tumor, Ovary
LOWEST	1416 M	7/16/74	0	0.00	0.00	10.2	22.1	5/20/76	2/15/90	164.9	187.0	Heart Failure
LOWEST	1458 F	8/05/74	0	0.00	0.00	8.5	21.5	5/20/76	9/21/89	160.1	181.6	Malignant Pheochromocytoma, Adrenal
LOWEST	1465 F	8/19/74	154	1.24	13.65	11.3	21.0	5/20/76	5/16/89	155.9	176.9	Uremic Syndrome
LOWEST	1466 F	8/19/74	191	1.38	15.18	12.6	21.0	5/20/76	1/04/90	163.5	184.5	Uremic Syndrome
LOWEST	1470 F	8/21/74	114	1.06	11.71	9.7	21.0	5/20/76	4/09/84	94.7	115.6	Meningioma
LOWEST	1489 F	9/05/74	0	0.00	0.00	9.5	20.5	5/20/76	8/04/84	98.5	119.0	Carcinoma, Esophagus
LOWEST	1501 M	9/08/74	0	0.00	0.00	12.5	20.4	5/20/76	1/03/84	91.5	111.8	Carcinoma, Thyroid
LOWEST	1513 M	9/26/74	0	0.00	0.00	11.6	19.8	5/20/76	10/08/90	172.6	192.4	Hepatitis; Lung Tumor
LOWEST	1515 M	9/26/74	0	0.00	0.00	11.7	19.8	5/20/76	12/06/90	174.6	194.3	Carcinoma, Urethra; Hepatocellular Carcinoma
LOWEST	1519 M	10/05/74	84	0.64	7.09	11.8	19.5	5/20/76	7/13/90	169.8	189.2	Uremic Syndrome
LOWEST	1520 M	10/05/74	47	0.37	4.09	11.4	19.5	5/20/76	5/21/90	168.0	187.5	Carcinoma, Bile Duct
LOWEST	1570 F	9/08/75	67	0.60	6.57	10.2	19.4	4/19/77	6/19/87	122.0	141.3	Fibrosarcoma, Stomach
LOWEST	1573 M	9/08/75	0	0.00	0.00	11.7	19.4	4/19/77	9/06/90	160.6	179.9	Gastric Dilatation
LOWEST	1581 M	9/10/75	0	0.00	0.00	16.3	19.3	4/19/77	7/31/86	111.4	130.7	Hemangiosarcoma, Spleen

INHALED PLUTONIUM NITRATE IN DOGS

DOSE GROUP	DOG IDENT	BIRTH DATE	INITIAL ALVEOLAR DEPOSITION BQ	BQ/G LUNG	BQ/ KG	INHALATION EXPOSURE WGT (KG)	AGE (MO)	EXPO DATE	DEATH INFORMATION DEATH DATE	MONTHS POST INH	AGE (MO)	COMMENTS ON DEAD DOGS
LOWEST	1583 F	9/12/75	139	1.42	15.67	8.9	19.2	4/19/77	10/13/89	149.8	169.0	Carcinoma, Thyroid
LOWEST	1592 F	9/13/75	142	0.93	10.25	13.9	19.2	4/19/77	10/17/89	149.9	169.1	Pneumonia
LOWEST	1596 M	9/13/75	0	0.00	0.00	13.9	19.2	4/19/77	7/02/91	170.4	189.6	Senility; Carcinoma, Bile Duct
LOWEST	1600 F	9/14/75	44	0.35	3.83	11.4	19.2	4/19/77	6/27/90	158.3	177.4	Uremic Syndrome
LOWEST	1603 M	9/14/75	61	0.39	4.24	14.4	19.2	4/19/77	12/26/90	164.2	183.4	Uremic Syndrome
LOWEST	1606 F	9/20/75	194	1.31	14.36	13.5	19.0	4/19/77	6/22/90	158.1	177.1	Hemangiosarcoma, Spleen
LOWEST-SAC	1335 M	4/16/74	178	1.41	15.48	11.5	18.0	10/16/75	11/13/75	0.9	18.9	Sacrificed
LOWEST-SAC	1339 F	5/01/74	74	0.70	7.67	9.7	17.5	10/16/75	11/13/75	0.9	18.4	Sacrificed
LOWEST-SAC	1351 M	5/10/74	248	2.21	24.30	10.2	17.2	10/16/75	11/13/75	0.9	18.1	Sacrificed
LOW	1415 M	7/15/74	86	0.71	7.80	11.0	22.2	5/20/76	12/27/89	163.3	185.4	Transitional Carcinoma, Urinary Bladder
LOW	1417 M	7/16/74	395	3.33	36.59	10.8	22.1	5/20/76	10/05/89	160.5	182.7	Malignant Lymphoma
LOW	1423 M	7/17/74	356	3.08	33.90	10.5	22.1	5/20/76	6/27/89	157.2	179.4	Panophthalmitis
LOW	1472 F	8/21/74	374	4.04	44.49	8.4	21.0	5/20/76	11/22/89	162.1	183.1	Uremic Syndrome; Carcinoma, Bile Duct
LOW	1484 F	9/03/74	401	4.14	45.54	8.8	20.5	5/20/76	10/26/90	173.2	193.7	Malignant Lymphoma
LOW	1487 F	9/03/74	222	1.77	19.47	11.4	20.5	5/20/76	7/05/90	169.5	190.0	Gastric Dilatation
LOW	1490 F	9/05/74	581	5.45	59.92	9.7	20.5	5/20/76	10/19/88	149.0	169.5	Mammary Tumor
LOW	1503 F	9/26/74	324	2.94	32.38	10.0	19.8	5/20/76	12/13/84	102.8	122.6	Carcinoma, Thyroid
LOW	1507 M	9/26/74	165	1.21	13.31	12.4	19.8	5/20/76	6/07/88	144.6	164.4	Malignant Melanoma, Oral Cavity
LOW	1565 F	9/06/75	283	2.30	25.31	11.2	19.4	4/19/77	9/28/85	101.3	120.7	Hemangiosarcoma, Spleen
LOW	1567 M	9/06/75	370	2.81	30.86	12.0	19.4	4/19/77	6/15/90	157.9	177.3	Nephritis

INHALED PLUTONIUM NITRATE IN DOGS

DOSE GROUP	DOG IDENT	BIRTH DATE	INITIAL ALVEOLAR DEPOSITION BQ	BQ/G LUNG	BQ/KG	INHALATION EXPOSURE WGT (KG)	AGE (MO)	EXPO DATE	DEATH INFORMATION DEATH DATE	MONTHS POST INH	AGE (MO)	COMMENTS ON DEAD DOGS
LOW	1575 M	9/08/75	100	0.63	6.94	14.4	19.4	4/19/77	12/28/87	128.3	147.6	Transitional Carcinoma, Urethra
LOW	1579 M	9/09/75	308	1.98	21.83	14.1	19.3	4/19/77	6/05/90	157.5	176.9	Hepatocellular Carcinoma
LOW	1580 F	9/10/75	335	2.62	28.87	11.6	19.3	4/19/77	1/06/92	176.6	195.9	Transitional Carcinoma, Urinary Bladder
LOW	1585 F	9/12/75	301	2.14	23.50	12.8	19.2	4/19/77	8/31/89	148.4	167.6	Carcinoma, Thyroid
LOW	1590 F	9/13/75	228	1.62	17.81	12.8	19.2	4/19/77	3/18/87	118.9	138.1	Mammary Tumor
LOW	1591 M	9/13/75	423	2.48	27.31	15.5	19.2	4/19/77	8/15/89	147.9	167.1	Malignant Lymphoma
LOW	1599 F	9/14/75	381	3.43	37.73	10.1	19.2	4/19/77	3/12/86	106.7	125.9	Carcinoma, Adrenal
LOW	1602 M	9/14/75	553	3.31	36.37	15.2	19.2	4/19/77	8/10/86	111.7	130.9	Epileptic Seizures
LOW	1607 M	9/20/75	167	1.27	13.94	12.0	19.0	4/19/77	7/26/88	135.2	154.2	Hepatocellular Carcinoma
MED-LOW	1363 M	5/14/74	3144	28.30	311.28	10.1	20.2	1/20/76	5/12/87	135.7	155.9	Pneumonia; Carcinoma, Adrenal; Adenoma, Bile Duct
MED-LOW	1380 M	6/17/74	2339	15.75	173.24	13.5	19.1	1/20/76	5/24/87	136.1	155.2	Pneumonia
MED-LOW	1386 M	6/21/74	1266	7.73	84.98	14.9	22.0	4/20/76	1/04/86	116.5	138.5	Hemangiosarcoma, Spleen
MED-LOW	1391 M	6/22/74	1991	10.77	118.49	16.8	21.9	4/20/76	7/22/85	111.0	133.0	Carcinoma, Thyroid; Lung Tumor
MED-LOW	1413 F	7/15/74	1090	8.85	97.36	11.2	18.2	1/20/76	3/01/85	109.3	127.5	Malignant Lymphoma
MED-LOW	1422 F	7/17/74	3656	44.32	487.51	7.5	18.1	1/20/76	7/11/90	173.7	191.8	Lung Tumor; Adenoma, Bile Duct
MED-LOW	1427 F	7/17/74	2518	23.36	256.96	9.8	21.1	4/20/76	8/23/89	160.1	181.2	Malignant Melanoma, Oral Cavity
MED-LOW	1439 F	7/20/74	1962	15.12	166.31	11.8	21.0	4/20/76	3/30/88	143.3	164.3	Malignant Lymphoma
MED-LOW	1444 F	7/22/74	1831	15.55	171.10	10.7	21.0	4/20/76	5/17/90	168.9	189.8	Transitional Carcinoma, Urinary Bladder
MED-LOW	1456 F	8/05/74	2248	27.25	299.75	7.5	20.5	4/20/76	4/21/87	132.0	152.5	Pneumonia
MED-LOW	1523 F	10/12/74	2041	17.50	192.50	10.6	21.3	7/22/76	12/21/90	173.0	194.3	Malignant Melanoma, Oral Cavity

INHALED PLUTONIUM NITRATE IN DOGS

DOSE GROUP	DOG IDENT	BIRTH DATE	INITIAL ALVEOLAR DEPOSITION BQ	BQ/G LUNG	BQ/ KG	INHALATION EXPOSURE WGT (KG)	AGE (MO)	EXPO DATE	DEATH INFORMATION DEATH DATE	MONTHS POST INH	AGE (MO)	COMMENTS ON DEAD DOGS
MED-LOW	1530 F	10/29/74	2646	30.84	339.21	7.8	20.8	7/22/76	9/17/86	121.9	142.6	Bone Tumor; Lung Tumor
MED-LOW	1540 M	10/30/74	2015	12.05	132.57	15.2	20.7	7/22/76	11/25/86	124.1	144.9	Lung Tumor
MED-LOW	1568 M	9/06/75	1702	11.63	127.94	13.3	18.3	3/15/77	12/02/86	116.6	134.9	Pneumonia
MED-LOW	1569 F	9/08/75	2152	20.81	228.93	9.4	18.2	3/15/77	9/27/87	126.4	144.6	Lung Tumor
MED-LOW	1574 M	9/08/75	1715	14.43	158.76	10.8	18.2	3/15/77	7/14/90	160.0	178.2	Lung Tumor
MED-LOW	1582 F	9/12/75	2095	20.93	230.25	9.1	18.1	3/15/77	8/12/88	136.9	155.0	Mammary Tumor; Carcinoma, Bile Duct
MED-LOW	1587 M	9/12/75	1947	12.64	139.09	14.0	18.1	3/15/77	1/14/86	106.0	124.1	Hemangiosarcoma, Subcutis; Lung Tumor
MED-LOW	1595 M	9/13/75	1850	12.37	136.03	13.6	18.0	3/15/77	1/09/90	153.9	171.9	Uremic Syndrome
MED-LOW	1604 M	9/14/75	3145	32.86	361.49	8.7	18.0	3/15/77	4/03/90	156.6	174.6	Encephalopathy
MED-LOW-SAC	1336 M	4/16/74	759	5.35	58.83	12.9	18.0	10/16/75	11/13/75	0.9	18.9	Sacrificed
MED-LOW-SAC	1341 F	5/10/74	692	6.29	69.19	10.0	17.2	10/16/75	11/13/75	0.9	18.1	Sacrificed
MED-LOW-SAC	1344 F	5/10/74	1531	13.64	150.07	10.2	17.2	10/16/75	11/14/75	1.0	18.2	Sacrificed
MED-LOW-SAC	1359 M	5/14/74	1850	11.68	128.47	14.4	20.2	1/20/76	1/23/76	0.1	20.3	Sacrificed
MED-LOW-SAC	1375 F	6/17/74	1850	15.29	168.18	11.0	19.1	1/20/76	1/23/76	0.1	19.2	Sacrificed
MED-LOW-SAC	1389 M	6/22/74	989	9.08	99.86	9.9	21.9	4/20/76	5/04/76	0.5	22.4	Sacrificed
MED-LOW-SAC	1390 M	6/22/74	1582	12.29	135.19	11.7	21.9	4/20/76	5/04/76	0.5	22.4	Sacrificed
MED-LOW-SAC	1407 F	7/07/74	1850	21.29	234.18	7.9	18.5	1/20/76	1/23/76	0.1	18.6	Sacrificed
MED-LOW-SAC	1445 F	7/22/74	1252	8.89	97.82	12.8	21.0	4/20/76	5/05/76	0.5	21.5	Sacrificed
MED-LOW-SAC	1522 F	10/12/74	2880	27.56	303.17	9.5	21.3	7/22/76	10/18/76	2.9	24.2	Sacrificed
MED-LOW-SAC	1529 F	10/29/74	1586	13.86	152.48	10.4	20.8	7/22/76	10/19/76	2.9	23.7	Sacrificed

INHALED PLUTONIUM NITRATE IN DOGS

DOSE GROUP	DOG IDENT	BIRTH DATE	INITIAL ALVEOLAR DEPOSITION BQ	BQ/G LUNG	BQ/ KG	INHALATION EXPOSURE WGT (KG)	AGE (MO)	EXPO DATE	DEATH INFORMATION DEATH DATE	MONTHS POST INH	AGE (MO)	COMMENTS ON DEAD DOGS
MED-LOW-SAC	1539 M	10/30/74	2398	17.58	193.41	12.4	20.7	7/22/76	10/20/76	3.0	23.7	Sacrificed
MED-LOW-SAC	1564 F	9/06/75	1479	15.64	172.01	8.6	18.3	3/15/77	3/20/78	12.2	30.4	Sacrificed
MED-LOW-SAC	1571 F	9/08/75	2533	23.26	255.82	9.9	18.2	3/15/77	3/21/78	12.2	30.4	Sacrificed
MED-LOW-SAC	1576 M	9/08/75	2601	19.71	216.79	12.0	18.2	3/15/77	3/17/82	60.1	78.3	Sacrificed
MED-LOW-SAC	1588 M	9/12/75	1839	12.86	141.48	13.0	18.1	3/15/77	3/22/78	12.2	30.3	Sacrificed
MED-LOW-SAC	1589 F	9/13/75	1526	13.09	143.95	10.6	18.0	3/15/77	6/08/82	62.8	80.8	Sacrificed; Lung Tumor
MED-LOW-SAC	1598 F	9/14/75	3448	42.94	472.38	7.3	18.0	3/15/77	3/10/82	59.8	77.8	Sacrificed
MED-LOW-SAC	1605 F	9/20/75	932	7.71	84.76	11.0	17.8	3/15/77	3/24/82	60.3	78.1	Sacrificed
MEDIUM	1362 M	5/14/74	9879	63.25	695.70	14.2	20.2	1/20/76	12/20/88	155.0	175.2	Bone Tumor; Hepatocellular Carcinoma; Carcinoma, Bile Duct; Lung Tumors
MEDIUM	1364 M	5/14/74	17146	135.54	1490.94	11.5	20.2	1/20/76	8/02/84	102.4	122.6	Lung Tumor
MEDIUM	1379 M	6/17/74	10280	61.89	680.82	15.1	19.1	1/20/76	1/20/88	144.0	163.1	Carcinoma, Bile Duct; Lung Tumor; Bone Tumor
MEDIUM	1385 M	6/21/74	13794	79.36	873.01	15.8	19.0	1/20/76	7/12/84	101.7	120.7	Bone Tumor; Lung Tumor
MEDIUM	1387 F	6/22/74	12769	181.37	1995.11	6.4	19.0	1/20/76	8/13/80	54.8	73.7	Bone Tumor
MEDIUM	1404 M	7/05/74	9620	51.44	565.88	17.0	21.5	4/20/76	2/03/84	93.5	115.0	Pleuritis
MEDIUM	1408 F	7/07/74	12240	115.30	1268.35	9.7	18.5	1/20/76	10/12/83	92.7	111.2	Bone Tumor
MEDIUM	1414 F	7/15/74	8610	92.08	1012.93	8.5	18.2	1/20/76	8/14/86	126.8	145.0	Bone Tumor; Lung Tumor; Carcinoma, Bile Duct
MEDIUM	1428 F	7/17/74	13986	116.65	1283.12	10.9	21.1	4/20/76	10/28/85	114.3	135.4	Bone Tumor; Lung Tumor
MEDIUM	1446 F	7/22/74	13099	112.34	1235.73	10.6	21.0	4/20/76	8/10/86	123.7	144.6	Pyometra; Adenoma, Bile Duct
MEDIUM	1521 F	10/12/74	7570	61.45	675.91	11.2	21.3	7/22/76	6/07/85	106.5	127.8	Bone Tumor; Lung Tumor
MEDIUM	1534 M	10/28/74	10900	76.23	838.48	13.0	20.8	7/22/76	5/26/85	106.1	126.9	Heart Failure

INHALED PLUTONIUM NITRATE IN DOGS

DOSE GROUP	DOG IDENT	BIRTH DATE	INITIAL ALVEOLAR DEPOSITION BQ	BQ/G LUNG	BQ/ KG	INHALATION EXPOSURE WGT (KG)	AGE (MO)	EXPO DATE	DEATH INFORMATION DEATH DATE	MONTHS POST INH	AGE (MO)	COMMENTS ON DEAD DOGS
MEDIUM	1535 F	10/30/74	12758	115.98	1275.76	10.0	20.7	7/22/76	10/06/86	122.5	143.2	Bone Tumor; Lung Tumor
MEDIUM	1618 F	2/29/76	10239	88.65	975.14	10.5	20.3	11/07/77	7/12/89	140.1	160.4	Bone Tumor
MEDIUM	1637 M	4/12/76	7100	56.62	622.80	11.4	18.9	11/07/77	11/28/88	132.7	151.6	Lung Tumor
MEDIUM	1639 F	4/22/76	9188	78.80	866.78	10.6	18.5	11/07/77	12/24/89	145.5	164.1	Radiation Pneumonitis; Lung Tumor
MEDIUM	1640 M	4/22/76	11344	85.94	945.35	12.0	18.5	11/07/77	3/20/84	76.4	94.9	Lung Tumor
MEDIUM	1645 F	4/23/76	9520	77.28	850.04	11.2	18.5	11/07/77	8/07/86	105.0	123.5	Lung Tumor
MEDIUM	1647 M	4/23/76	10863	98.75	1086.28	10.0	18.5	11/07/77	1/13/90	146.2	164.7	Lung Tumor; Carcinoma, Bile Duct
MEDIUM	1656 M	4/26/76	7816	62.88	691.67	11.3	18.4	11/07/77	1/02/91	157.8	176.2	Pneumonia; Lung Tumor
MED-HIGH	1419 M	7/16/74	57683	524.39	5768.30	10.0	23.3	6/23/76	10/22/82	76.0	99.2	Bone Tumor; Lung Tumor
MED-HIGH	1429 M	7/17/74	50912	370.27	4072.96	12.5	23.2	6/23/76	5/29/81	59.2	82.4	Bone Tumor; Lung Tumor
MED-HIGH	1459 F	8/05/74	97865	926.75	10194.27	9.6	22.6	6/23/76	9/25/80	51.1	73.7	Radiation Pneumonitis; Lung Tumor
MED-HIGH	1471 F	8/21/74	92781	795.72	8752.94	10.6	22.1	6/23/76	5/01/79	34.2	56.3	Radiation Pneumonitis
MED-HIGH	1485 F	9/03/74	86210	955.76	10513.41	8.2	21.7	6/23/76	12/30/80	54.2	75.9	Bone Tumor
MED-HIGH	1492 F	9/05/74	91516	875.75	9633.24	9.5	21.6	6/23/76	10/16/80	51.8	73.4	Bone Tumor
MED-HIGH	1498 F	9/08/74	74666	678.78	7466.60	10.0	21.5	6/23/76	4/09/82	69.5	91.0	Bone Tumor; Lung Tumor
MED-HIGH	1502 F	9/26/74	111289	717.53	7892.81	14.1	20.9	6/23/76	1/21/81	55.0	75.9	Bone Tumor; Lung Tumor
MED-HIGH	1508 M	9/26/74	63503	395.41	4349.53	14.6	20.9	6/23/76	1/24/80	43.0	63.9	Bone Tumor
MED-HIGH	1512 M	9/26/74	89192	526.52	5791.70	15.4	20.9	6/23/76	12/23/79	42.0	62.9	Bone Tumor
MED-HIGH	1619 F	2/29/76	55148	477.47	5252.20	10.5	20.3	11/07/77	1/21/83	62.5	82.7	Bone Tumor
MED-HIGH	1621 M	2/29/76	49343	358.86	3947.46	12.5	20.3	11/07/77	11/19/84	84.4	104.7	Bone Tumor; Lung Tumor

INHALED PLUTONIUM NITRATE IN DOGS

DOSE GROUP	DOG IDENT	BIRTH DATE	INITIAL ALVEOLAR DEPOSITION BQ	BQ/G LUNG	BQ/ KG	INHALATION EXPOSURE WGT (KG)	AGE (MO)	EXPO DATE	DEATH INFORMATION DEATH DATE	MONTHS POST INH	AGE (MO)	COMMENTS ON DEAD DOGS
MED-HIGH	1636 M	4/12/76	44851	302.03	3322.33	13.5	18.9	11/07/77	5/03/83	65.8	84.7	Bone Tumor
MED-HIGH	1641 M	4/22/76	47171	366.52	4031.74	11.7	18.5	11/07/77	6/28/85	91.7	110.2	Lung Tumor
MED-HIGH	1646 F	4/23/76	39255	346.47	3811.14	10.3	18.5	11/07/77	11/11/82	60.1	78.6	Bone Tumor
MED-HIGH	1648 M	4/23/76	30014	216.55	2382.10	12.6	18.5	11/07/77	7/11/85	92.1	110.6	Bone Tumor; Lung Tumor
MED-HIGH	1652 F	4/26/76	48822	452.89	4981.79	9.8	18.4	11/07/77	7/20/83	68.4	86.8	Bone Tumor; Lung Tumor
MED-HIGH	1655 M	4/26/76	40481	432.95	4762.42	8.5	18.4	11/07/77	3/18/85	88.3	106.7	Lung Tumor; Bone Tumor
MED-HIGH	1659 F	4/29/76	36641	254.28	2797.06	13.1	18.3	11/07/77	8/19/83	69.4	87.7	Bone Tumor
MED-HIGH	1660 M	4/29/76	56149	392.65	4319.15	13.0	18.3	11/07/77	9/05/84	81.9	100.2	Bone Tumor; Lung Tumor
MED-HIGH-SAC	1329 F	4/16/74	13420	123.23	1355.55	9.9	18.0	10/16/75	11/14/75	1.0	19.0	Sacrificed
MED-HIGH-SAC	1346 M	5/10/74	24272	158.74	1746.19	13.9	17.2	10/16/75	11/14/75	1.0	18.2	Sacrificed
MED-HIGH-SAC	1347 F	5/10/74	25463	257.21	2829.27	9.0	17.2	10/16/75	11/14/75	1.0	18.2	Sacrificed
HIGH	1420 M	7/16/74	142080	1254.02	13794.17	10.3	23.3	6/23/76	7/12/78	24.6	47.9	Radiation Pneumonitis
HIGH	1424 M	7/17/74	284204	2609.77	28707.52	9.9	23.2	6/23/76	8/31/77	14.3	37.5	Radiation Pneumonitis
HIGH	1510 F	9/26/74	257860	2056.30	22619.33	11.4	20.9	6/23/76	11/09/77	16.6	37.5	Radiation Pneumonitis
HIGH	1517 F	10/05/74	191845	1797.99	19777.84	9.7	20.6	6/23/76	11/02/77	16.3	36.9	Radiation Pneumonitis
HIGH	1518 M	10/05/74	131905	1142.03	12562.38	10.5	20.6	6/23/76	12/18/79	41.8	62.4	Radiation Pneumonitis; Lung Tumor

Distribution

Distribution

DOMESTIC

S. Addison
Radiological Safety Division
University of Washington
GS-05
Seattle, WA 98105

R. E. Albert
Department of Environmental Health
University of Cincinnati Medical Center
3223 Eden Avenue
Cincinnati, OH 45267-0056

E. L. Alpen
University of California
230 Donner Laboratory
Berkeley, CA 94720

A. Andersen
Center for Devices & Radiological Health
Food & Drug Administration
5600 Fishers Lane, HFZ-100
Rockville, MD 20857

D. Anderson
ENVIROTEST
1108 NE 200th Street
Seattle, WA 98155-1136

G. Anderson
Department of Oceanography
University of Washington
Seattle, WA 98115

V. E. Archer
Rocky Mountain Center for Occupational & Environmental Health - Building 512
University of Utah
50 North Medical Drive
Salt Lake City, UT 84112

Assistant Secretary
Environment, Safety & Health
EH-1, FORS
U.S. Department of Energy
Washington, DC 20585

O. Auerbach
VA Hospital
East Orange, NJ 97919

Auxier & Associates
412 Executive Tower Dr.
Suite 402
Knoxville, TN 37921

F. I. Badgley
13749 NE 41st Street
Seattle, WA 98125

R. E. Baker
8904 Roundleaf Way
Gaithersburg, MD 20879-1630

R. W. Barber
EH-33, GTN
U.S. Department of Energy
Washington, DC 20585

W. W. Barker, Chairman
Department of Biology
Central Washington University
Ellensburg, WA 98926

B. J. Barnhart
ER-72, GTN
U.S. Department of Energy
Washington, DC 20585

N. F. Barr
ER-72, GTN
U.S. Department of Energy
Washington, DC 20585

M. M. Bashor, Ph.D.
ATSDR, Mail Stop E-28
1600 Clifton Road NE
Atlanta, GA 30333

J. W. Baum
Brookhaven National Laboratory
Building 703-M
Upton, NY 11973

J. R. Beall
ER-72, GTN
U.S. Department of Energy
Washington, DC 20585

P. M. Beam
EM-431/TREV
U.S. Department of Energy
Washington, DC 20585-0002

S. Benjamin
Director, CRHL
Foothills Campus
Colorado State University
Fort Collins, CO 80523

G. L. Bennett
NASA Headquarters
Code CT
Washington, DC 20546-0001

R. P. Berube
EH-20, FORS
U.S. Department of Energy
Washington, DC 20585

M. H. Bhattacharyya
BIM Div., Bldg. 202
Argonne National Laboratory
9700 South Cass Avenue
Argonne, IL 60439

R. W. Bistline
Rockwell International
Rocky Flats Plant
P. O. Box 464
Golden, CO 80401

B. B. Boecker
Lovelace Inhalation Toxicology
Research Institute
P. O. Box 5890
Albuquerque, NM 87185

V. P. Bond
Life Sciences,
Chemistry and Safety
Brookhaven National Laboratory
Building 460
Upton, NY 11973

R. Borders
Health Protection Division
U.S. Department of Energy
P.O. Box 5400
Albuquerque, NM 87115

Dr. H. Box, Director
Biophysics
Roswell Park Cancer Institute
Elm & Carlton Streets
Buffalo, NY 14263-0001

J. D. Brain
Harvard University School of
Public Health
665 Huntington Avenue
Boston, MA 02115

B. D. Breitenstein
Brookhaven National Laboratory
P.O. Box 83
Upton, NY 11973

J. K. Briant
P. O. Box 3029
Richland, WA 99352

F. W. Bruenger
Division of Radiobiology
Building 586
University of Utah
Salt Lake City, UT 84112

D. R. Buhler
Toxicology Program
Oregon State University
Corvallis, OR 97331

R. J. Bull
Washington State University
College of Pharmacy
Pullman, WA 99164-6510

G. Burley
Office of Radiation Programs,
U.S. Environmental
Protection Agency
ANR-458
Washington, DC 20460

L. K. Bustad
College of Veterinary Medicine
Washington State University
Pullman, WA 99163

C. E. Carter
National Institute of
Environmental Health
Sciences
P.O. Box 12233
Research Triangle Park,
NC 27709

H. W. Casey
School of Veterinary Medicine
Louisiana State University
Baton Rouge, LA 70803

R. J. Catlin
Health Science Center
University of Texas
13307 Queensbury Lane
Houston, TX 77079

N. Cohen
New York University
Medical Center
P.O. Box 817
Tuxedo, NY 10987

D. A. Cool
Office of Nuclear
Regulatory Research
Nuclear Regulatory Commission
Washington, DC 20585

D. K. Craig
Savannah River Laboratories
P.O. Box 616
Aiken, SC 29802

E. P. Cronkite
Medical Department
Brookhaven National
Laboratory
Upton, NY 11973

J. Crowell
The Maxima Corporation
107 Union Valley Road
Oak Ridge, TN 37830

G. Davis
Medical Sciences Division
Oak Ridge Associated
Universities
P.O. Box 117
Oak Ridge, TN 37830-0117

G. DePlanque, Director
U.S. Nuclear Regulatory
Commission
Washington, DC 20555

G. P. Dix
3028 St. Tropex Street
Las Vegas, NV 89128

T. J. Dobry, Jr.
DP-6.2, GTN
U.S. Department of Energy
Washington, DC 20585

DOE/Office of Scientific &
Technical Information (12)

Savannah River Operations
Office
Environmental Division
U.S. Department of Energy
P.O. Box A
Aiken, SC 29801

D. Doyle
Argonne National Laboratory
9700 South Cass Avenue
Argonne, IL 60439

H. Drucker
Argonne National Laboratory
9700 South Cass Avenue
Argonne, IL 60439

J. A. Louis Dubeau
Comprehensive Cancer Center
University of Southern
California
Los Angeles, CA 90033-0800

A. P. Duhamel
ER-74, GTN
U.S. Department of Energy
Washington, DC 20585

D. Dungworth
Department of Veterinary
Pathology
School of Veterinary Medicine
University of California
Davis, CA 95616

Dr. Patricia W. Durbin
Division of Biology and
Medicine
Lawrence Berkeley Laboratory
University of California
Berkeley, CA 94704

K. F. Eckerman
Health and Safety Research
Division
Oak Ridge National Laboratory
P.O. Box 2008
Oak Ridge, TN 37831-6383

C. W. Edington, Director
National Academy of Sciences
JH 554
2101 Constitution Avenue, NW
Washington, DC 20418

G. R. Eisele
Medical Division
Oak Ridge Associated
Universities
P.O. Box 117
Oak Ridge, TN 37830

M. Eisenbud
711 Bayberry Drive
Chapel Hill, NC 27514

N. B. Everett
Department of Biological Structure
University of Washington
School of Medicine
Seattle, WA 98105

H. Falk, M.D.
CDC, CEHIC/EHHE
1600 Clifton Road NE
Atlanta, GA 30333

K. P. Ferlic
DP-65, GTN
U.S. Department of Energy
Washington, DC 20585

B. H. Fimiani
Battelle Washington Operations
370 L'Enfant Promenade, Suite 900
901 D Street, SW
Washington, DC 20024

Dr. W. Michael Foster
Environmental Physiology, EHS
615 N. Wolfe St., No. 7006
Baltimore, MD 21205

M. E. Frazier
U.S. Department of Energy
ER-72, GTN
Germantown, MD 20875

H. L. Friedell
Biochemical Oncology
Case-Western Reserve University, Wearn B21
2058 Abington Road
Cleveland, OH 44106

T. Fritz
Argonne National Laboratory
9700 South Cass Avenue
Argonne, IL 60439

D. J. Galas
Darwin Molecular Corp.
2405 Carillon Point
Kirkland, WA 98033

D. E. Gardner
Northrop Services, Inc.
P.O. Box 12313
Research Triangle Park, NC 27709

T. F. Gesell
Idaho State University
Campus Box 8106
Pocatello, ID 83209

R. D. Gilmore, President
Environmental Health Sciences, Inc.
Nine Lake Bellevue Building
Suite 220
Bellevue, WA 98005

M. Goldman
Department of Radiological Sciences (VM)
University of California
Davis, CA 95616

R. Goldsmith
EH-42, GTN
U.S. Department of Energy
Washington, DC 20585

G. Goldstein
EH-42, GTN
U.S. Department of Energy
Washington, DC 20585

J. A. Graham
ECAO, Mail Drop 52
U.S. Environmental Protection Agency
Research Triangle Park, NC 27711

R. A. Griesemer, Director
National Toxicology Program
National Institutes of Health
P.O. Box 12233
Research Triangle Park, NC 27709

G. H. Groenewold
Energy and Mineral Research Center
University of North Dakota
Box 8123, University Station
Grand Forks, ND 58202

F. F. Hahn
Lovelace Inhalation Toxicology Research Institute
P.O. Box 5890
Albuquerque, NM 87115

E. J. Hall
Radiological Research Laboratory
Columbia University
630 West 168th Street
New York, NY 10032

R. Hamlin
Department of Veterinary Physiology
The Ohio State University
1900 Coffey Road
Columbus, OH 43201

J. W. Healy
51 Grand Canyon Drive
White Rock, NM 87544

C. H. Hobbs
Lovelace Inhalation Toxicology Research Institute
P.O. Box 5890
Albuquerque, NM 87185

L. M. Holland
Los Alamos National Laboratory
P.O. Box 1663
Los Alamos, NM 87545

R. Hornung
DSHEFS, NIOSH
Robert A. Taft Laboratories
4676 Columbia Parkway
Cincinnati, OH 45220

F. Hutchinson
Department of Therapeutic Radiology, HRT 315
Yale University School of Medicine
333 Cedar Street
New Haven, CT 06510-8040

H. Ishikawa, General Manager
Nuclear Safety Research Association
P.O. Box 1307
Falls Church, VA 22041

E. D. Jacobson
Center for Devices & Radiological Health
U.S. Food & Drug Administration
5600 Fishers Lane, HFZ-100
Rockville, MD 20857

A. W. Johnson
San Diego State University
6310 Alvardo Court, Suite 110
San Diego, CA 92120

R. K. Jones
The Lovelace Foundation for Medical Education & Research
Building 9200, Area Y
Sandia Base
Albuquerque, NM 87108

G. Y. Jordy
ER-41, GTN
U.S. Department of Energy
Washington, DC 20585

C. M. Kelly
Air Products and Chemicals, Inc.
P.O. Box 538
Allentown, PA 18105

M. Krebs
Office of Energy Research
ER-1, FORS
U.S. Department of Energy
Washington, DC 20585

W. Lowder
U.S. Department of Energy-EMEL
375 Hudson Street
New York, NY 10014-3621

W. M. Leach
U.S. Food & Drug Administration
5600 Fishers Lane, HFZ-100
Rockville, MD 20857

Librarian
Documents Department — The Libraries
Colorado State University
Ft. Collins, CO 80523

Librarian
Electric Power Research Institute
3412 Hillview Avenue
P.O. Box 10412
Palo Alto, CA 94303

Librarian
Health Sciences Library, SB-55
University of Washington
Seattle, WA 98195

PNL-9000, Pt. 1
UC-408

Librarian
Los Alamos National Laboratory
Report Library, MS P364
P.O. Box 1663
Los Alamos, NM 87545

Librarian
Oregon Regional Primate Research Center
505 NW 185th Avenue
Beaverton, OR 97006

Library
Serials Department (#80-170187)
University of Chicago
1100 East 57th Street
Chicago, IL 60637

Librarian
Washington State University
Pullman, WA 99164-6510

J. B. Little
Department of Physiology
Harvard School of Public Health
665 Huntington Avenue
Boston, MA 02115

R. Loesch
EH-411, GTN
U.S. Department of Energy
Washington, DC 20585

A. B. Lovins
Rocky Mountain Institute
1739 Snowmass Creek Road
Snowmass, CO 81654-9199

D. L. Lundgren
Lovelace Inhalation Toxicology Research Institute
P.O. Box 5890
Albuquerque, NM 87185

O. R. Lunt
Laboratory of Biomedical & Environmental Sciences
University of California
900 Veteran Avenue
Los Angeles, CA 90024-1786

J. R. Maher
ER-65, GTN
U.S. Department of Energy
Washington, DC 20585

T. D. Mahony
750 Swift Boulevard
Richland, WA 99352

S. Marks
8024 47th Place West
Mukilteo, WA 98275

D. R. Mason
Nuclear Safety Branch
U.S. Department of Energy
P.O. Box A
Aiken, SC 29801

W. H. Matchett
Graduate School
New Mexico State University
Box 3G
Las Cruces, NM 88003-0001

R. O. McClellan, President
Chemical Industry Institute of Toxicology
P.O. Box 12137
Research Triangle Park, NC 27709

J. F. McInroy
Los Alamos National Laboratory
P.O. Box 1663, MS K4-84
Los Alamos, NM 87545

Medical Officer
Monsanto Research Corp.
Mound Laboratory
P.O. B[illegible]2
Miamisburg, OH 45342

T. Meinhardt
DSHEFS, NIOSH
Robert A. Taft Laboratories
4676 Columbia Parkway
Cincinnati, OH 45220

C. B. Meinhold
National Council on Radiation Protection
7910 Woodmont Avenue
Suite 800
Bethesda, MD 20814

H. Menkes
Assistant Professor of Medicine & Environmental Medicine
The John Hopkins University
Baltimore, MD 21205

D. B. Menzel
Southern Occupational Health Center
University of California, Irvine
Irvine, CA 92717

C. Miller
P.O. Box 180
Watermill, NY 11976

S. Miller
Department of Radiobiology
University of Utah
Salt Lake City, UT 84112

K. Z. Morgan
113 Danbury Drive
Oakridge, TN 37830

P. E. Morrow
Department of Biophysics
Medical Center
University of Rochester
Rochester, NY 14642

O. R. Moss
Chemical Industry Institute of Toxicology
P.O. Box 12137
Research Triangle Park, NC 27709

W. F. Mueller
New Mexico State University
Box 4500
Las Cruces, NM 88003-4500

D. S. Nachtwey
NASA-Johnson Space Center
Mail Code SD-5
Houston, TX 77058

R. Nathan
Battelle Columbus Laboratory
505 King Avenue
Columbus, Ohio 43201

National Library of Medicine
TSD-Serials
8600 Rockville Pike
Bethesda, MD 20014

N. S. Nelson
Office of Radiation Programs, ANR-461
U.S. Environmental Protection Agency
401 M Street SW
Washington, DC 20460

P. Nettesheim
National Institutes of Environmental Health Sciences
Research Triangle Park, NC 27711

W. R. Ney, Executive Director
National Council on Radiation Protection and Measurements
7910 Woodmont Avenue
Suite 800
Bethesda, MD 20814

S. W. Nielsen
Department of Pathology
New York State Veterinary College
Cornell University
Ithaca, NY 14850

R. A. Nilan
Division of Sciences
Washington State University
Pullman, WA 99164

M. Nolan
10958 Rum Cay Court
Columbia, MD 21044

Nuclear Regulatory Commission
Advisory Committee on Reactor Safeguards
Washington, DC 20555

A. Patrinos, Director
Office of Health and Environmental Research
ER-70, GTN
U.S. Department of Energy
Washington, DC 20585

J.E. Pelkey
c/o Cray Computer Corp.
1110 Bayfield Drive
Colorado Springs, CO 80906

A. F. Perge
RW-43, FORS
U.S. Department of Energy
Washington, DC 20585

D. F. Petersen
Los Alamos National Laboratory
P.O. Box 1663
Los Alamos, NM 87545

G. R. Petersen
EH-421, GTN
U.S. Department of Energy
Washington, DC 20585

H. J. Pettengill
EH-40, GTN
U.S. Department of Energy
Washington, DC 20585

H. Pfuderer
Oak Ridge National Laboratory
P.O. Box X
Oak Ridge, TN 37830

O. G. Raabe
Laboratory for Energy-Related Health Research
University of California
Davis, CA 95616

R. Rabson
ER-17, GTN
U.S. Department of Energy
Washington, DC 20585

D. P. Rall, Director
National Institutes of Environmental Health Sciences
P.O. Box 12233
Research Triangle Park, NC 27709

R. D. Reed, Chief
Rocky Flats Area Office
Albuquerque Operations Office
U.S. Department of Energy
P.O. Box 928
Golden, CO 80402-0928

C. R. Richmond
Oak Ridge National Laboratory
4500N, MS-62523
P.O. Box 2008
Oak Ridge, TN 37831-6253

B. Robinson
Monsanto Research Corp.
Mound Laboratory
P.O. Box 32
Miamisburg, OH 45342

S. L. Rose
ER-72, GTN
U.S. Department of Energy
Washington, DC 20585

G. Runkle, Chief
U.S. Department of Energy, AL
HPB/EHD
P.O. Box 5400
Albuquerque, NM 87115

G. Saccomanno
Pathologist and Director of Laboratories
St. Marys and V. A. Hospitals
Grand Junction, CO 81501

U. Saffiotti
Laboratory of Experimental Pathology
National Cancer Institute
Building 41, Room C-105
Bethesda, MD 20892

C. L. Sanders
Inhalation Toxicology Research Institute
P. O. Box 5890
Albuquerque, NM 87185

L. Sagan
Electric Power Research Institute
3412 Hillview Avenue
P.O. Box 10412
Palo Alto, CA 94304

M. Sage
CDC (F-28)
CEHIC
1600 Clifton Road NE
Atlanta, GA 30333

J. M. Samet
New Mexico Tumor Registry
University of New Mexico
Cancer Research and Treatment Center
Albuquerque, NM 87131

R. A. Scarano
Mill Licensing Section
Nuclear Regulatory Commission
Washington, DC 20585

R. A. Schlenker
Environmental Health and Safety Department
Building 201
Argonne National Laboratory
9700 South Cass Avenue
Argonne, IL 60439

C. R. Schuller
Battelle - Seattle
4000 NE 41st Street
Seattle, WA 98105

M. Schulman
ER-70, GTN
U.S. Department of Energy
Washington, DC 20585

T. M. Seed
BIM 202
Argonne National Laboratory
9700 South Cass Avenue
Argonne, IL 60439

R. B. Setlow
Brookhaven National Laboratory
Upton, NY 11973

R. Shikiar
Battelle - Seattle
4000 NE 41st Street
Seattle, WA 98105

H. P. Silverman
Beckman Instruments
2500 Harbor Blvd.
Fullerton, CA 92634

W. K. Sinclair
National Council on Radiation Protection
7910 Woodmont Avenue
Suite 800
Bethesda, MD 20814

D. H. Slade
ER-74, GTN
U.S. Department of Energy
Washington, DC 20585

D. A. Smith
ER-72, GTN
U.S. Department of Energy
Washington, DC 20585

G. S. Smith
New Mexico State University
Box 3-I
Las Cruces, NM 88003-0001

J. M. Smith
CDC
CEHIC
1600 Clifton Road NE
Atlanta, GA 30333

M. Smith
Department of Ecology
NUC Waste Library
PV-11 Building 99
South Sound
Olympia, WA 98504

Dr. H. Spitz
Department of Mechanical, Industrial, & Nuclear Engineering
University of Cincinnati
MS 072
Cincinnati, OH 45267

J. N. Stannard
17441 Plaza Animado #132
San Diego, CA 92128

R. J. Stern
EH-10, FORS
U.S. Department of Energy
Washington, DC 20585

E. T. Still
Kerr-McGee Corporation
P.O. Box 25861
Oklahoma City, OK 73125

B. Stuart
Brookhaven National Laboratory
Upton, NY 11973

D. Swanger
Biology Department
Eastern Oregon State College
La Grande, OR 97850

J. Swinebroad
PE-43, GTN
U.S. Department of Energy
Washington, DC 20585

M. Tanaka
Physics Library, 510A
Brookhaven National Laboratory
Upton, NY 11973

G. N. Taylor
Division of Radiobiology
Building 351
University of Utah
Salt Lake City, UT 84112

Technical Information Service
E. I. duPont de Nemours & Co.
Savannah River Laboratory
Room 773A
Aiken, SC 29801

J. W. Thiessen
P.O. Box 399
Somers, MT 59932

R. G. Thomas
Argonne National Laboratory
Environmental Res. Bldg. 203
9700 South Cass Avenue
Argonne, IL 60439

T. Thomas
EH-41, GTN
U.S. Department of Energy
Washington, DC 20585

D. Thomassen
Health Effects Research Division
U.S. Department of Energy
ER-72, GTN
Germantown, MD 20874

L. H. Toburen
National Academy of Sciences
Board of Radiation Research
NAS/Room 342
2101 Constitution NW
Washington, DC 20318

P. W. Todd
University of Colorado
Chemical Engineering Dept.
Campus Box 424
Boulder, CO 80309

Trend Publishing, Inc.
National Press Building
Washington, D.C. 20045

G. E. Tripard
Acting Director, NRC
Washington State University
Pullman, WA 99164-1300

P. T'so
School of Hygiene & Public Health, Room 3120
The Johns Hopkins University
615 North Wolfe Street
Baltimore, MD 21205

A. C. Upton
New York University Medical Center
Institute of Environmental Medicine
P. O. Box 817
Tuxedo, NY 10987

E. J. Vallario
15228 Red Clover Drive
Rockville, MD 20853

R. L. Van Citters, Dean
Research and Graduate Programs
University of Washington
Seattle, WA 98105

Dr. C. R. Vest
Marymount University
2807 North Glebe Road
Arlington, VA 22207

G. J. Vodapivc
DOE - Schenectady Naval Reactors Office
P.O. Box 1069
Schenectady, NY 12301

G. L. Voelz
Los Alamos National Laboratory
P.O. Box 1663, MS K4-04
Los Alamos, NM 87545

B. W. Wachholz
Radiation Effects Branch
National Cancer Institute
Executive Plaza North
6130 Executive Blvd.
Rockville, MD 20842

N. Wald
School of Public Health
University of Pittsburgh
Pittsburgh, PA 15213

A. Waldo
U.S. Department of Energy (EH-231)
1000 Independence Avenue SW
Washington, DC 20585

P. Watson
Associate Professor
Department of Chemistry
Oregon State University
Corvallis, OR 97331

M. E. Weaver
University of Oregon Health Science Center
School of Dentistry
Portland, OR 97201

M. H. Weeks
U.S. AEHA, Bldg. 2100
Edgewood Arsenal
Aberdeen Proving Ground, MD 21014

I. Wender
Department of Chemical Engineering
1249 Benedum Hall
University of Pittsburgh
Pittsburgh, PA 15261

K. Wilzbach
Argonne National Laboratory
9700 South Cass Avenue
Argonne, IL 60439

F. J. Wobber
ER-75, GTN
U.S. Department of Energy
Washington DC 20585

R. W. Wood
ER-73, GTN
U.S. Department of Energy
Washington, DC 20585

M. E. Wrenn
Environmental Radiation & Toxicology Laboratory
University of Utah
1771 South 900 W. #10
Salt Lake City, UT 84104

Dr. Chui-hsu Yang
NASA Johnson Space Center
NASA Road 1
Mail Code: SD4
Houston, TX 77058

Dr. S. Yaniv
18 Cedarwood Court
Rockville, MD 20852

P. L. Ziemer
EH-1, Forrestal
U.S. Department of Energy
Washington, DC 20585

J. D. Zimbrick
National Academy of Sciences/NRC
Board of Radiation Effects/342
2101 Constitution Ave., NW
Washington, DC 20418

FOREIGN

A. Aarkrog
Riso National Laboratory
ECO/MIL
DK-4000 Roskilde
DENMARK

G. E. Adams, Director
Medical Research Council
Radiobiology Unit
Harwell, Didcot
Oxon OX11 ORD
ENGLAND

A. L. Alejandrino, Head
Biomedical Research, ARD
Republic of the Philippines
Philippine Nuclear Research Institute
P.O. Box 932, Manila
THE PHILIPPINES

M. Anderson
Library
Department of National Health & Welfare
Ottawa, Ontario
CANADA

Atomic Energy of Canada, Ltd.
Scientific Document Distribution Office
Station 14, Chalk River Nuclear Laboratories
Chalk River, Ontario KOJ 1JO
CANADA

D. C. Aumann
Institut für Physikalische Chemie
Universität Bonn
Abt. Nuklearchemie
Wegelerstraße 12, 5300 Bonn 1
GERMANY

M. R. Balakrishnan, Head
Library & Information Services
Bhabha Atomic Research Centre
Bombay-400 085
INDIA

G. W. Barendsen
Laboratory for Radiobiology
AMC, FO 212
Meibergdreef 9
1105 AZ Amsterdam
THE NETHERLANDS

A. M. Beau, Librarian
Département de Protection Sanitaire
Commissariat à l'Énergie Atomique
BP 6
F-92265 Fontenay-aux-Roses
FRANCE

G. Bengtsson
Director-General
Statens Stralskyddsinstitut
Box 60204
S-104 01 Stockholm
SWEDEN

D. J. Beninson
Director, Licenciamento de Instalaciones Nulceares
Comisión Nacional de Energía Atómica
Avenida del Libertador 8250
2° Piso Of. 2330
1429 Buenos Aires
ARGENTINA

A. Bianco
Viale Seneca, 65
10131 Torino
ITALY

J. Booz
KFA Jülich Institut für Medezin
Kernsforschungsanlage Jülich
Postfach 1913, D-5170 Jülich
GERMANY

M. J. Bulman, Librarian
Medical Research Council
Radiobiology Unit
Harwell, Didcot
Oxon OX11 ORD
ENGLAND

M. Calamosia
ENEA-LAB Fisica E Tossicologia Aerosol
Via Mazzini 2
I-40138 Bologna
ITALY

Cao Shu-Yuan, Deputy Head
Laboratory of Radiation Medicine
North China Institute of Radiation Protection
P.O. Box 120
Tai-yuan, Shan-Xi
PEOPLE'S REPUBLIC OF CHINA

M. Carpentier
Commission of the European Communities
200 Rue de la Loi
J-70 6/16, B-1049 Brussels
BELGIUM

M. W. Charles, Group Head
Nuclear Electric PLC
Radiation Biophysics,
Berkeley Technology Centre, Berkeley
Gloucestershire GL 13 9PB
ENGLAND

Chen Xing-An
Laboratory of Industrial Hygiene
Ministry of Public Health
2 Xinkang Street
Deshengmenwai, Beijing
PEOPLE'S REPUBLIC OF CHINA

R. Clarke
National Radiological Protection Board
Harwell, Didcot
Oxon OX11 ORQ
ENGLAND

G. F. Clemente, Director
Radiation Toxicology Laboratory
Casaccia Centre for Nuclear Studies (CSN)
Casella Postale 2400
I-00100 Roma
ITALY

H. Coffigny
Institut de Protection et de Sûreté Nucléaire
Département de Protection Sanitaire
Service de Pathologie Expérimentale
BP 6
F-92265 Fontenay-aux-Roses
FRANCE

Commission of the European Communities
DG XII - Library SDM8 R1
200 Rue de la Loi
B-1049 Brussels
BELGIUM

M. S. Davies
Medical Research Council
20 Park Crescent
London W1N 4AL
ENGLAND

Deng Zhicheng
North China Institute of Radiation Protection
Tai-yuan, Shan-Xi
PEOPLE'S REPUBLIC OF CHINA

M. Di Paola
ENEA, PAS/VALEPID
C.R.E. Casaccia
Casella Postale 2400
I-00100 Roma
ITALY

Director
Commissariat à l'Énergie Atomique
Centre d'Etudes Nucléaires
Fontenay-aux-Roses (Seine)
FRANCE

Director
Laboratorio di Radiobiologia Animale
Centro di Studi Nucleari Della Casaccia
Comitate Nazionale per l'Energia Nucleare
Casella Postale 2400
I-00100 Roma
ITALY

M. Dousset
Health Ministry
Frue de la Gruerie
F-91190 Gifsur Yvette
FRANCE

J. Eapen
Biochemistry Division
Bhabha Atomic Research Centre
Bombay-400 085
INDIA

Estacao Agronómica Nacional
Biblioteca
2780 Oeiras
PORTUGAL

L. Feinendegen, Director
Institut für Medezin
Kernsforschungsanlage Jülich
Postfach 1913, D-5170 Jülich
GERMANY

T. M. Fliedner
Institut für Arbeits- u. Sozialmedizin
Universität Ulm
Oberer Eselsberg M 24, 309
D-7900 Ulm
GERMANY

L. Friberg
The Karolinska Institute
Stockholm
SWEDEN

A. Geertsema
Sasol Technology (Pty), Ltd.
P.O. Box 1
Sasolburg 9570
REPUBLIC OF SOUTH AFRICA

T. Giuseppe
ENEA-PAS-FIBI-AEROSOL
Via Mazzini 2
I-40138 Bologna
ITALY

H. L. Gjørup, Head
Health Physics Department
Atomic Energy Commission
Research Establishment
Risø, Roskilde
DENMARK

A. R. Gopal-Ayengar
73-Mysore Colony
Mahul Road, Chembur
Bombay-400 074
INDIA

C. L. Greenstock
Radiation Biology
AECL Research
Chalk River, Ontario
KOJ 1JO
CANADA

R. V. Griffith
International Atomic Energy Agency
Wagramerstraße 5
P.O. Box 200
A-1400 Vienna
AUSTRIA

Y. Hamnerius
Applied Electron Physics
Chalmers University of Technology
S-412 96 Göteborg
SWEDEN

G. P. Hanson, Chief
Radiation Medicine Unit
World Health Organization
CH-1211 Geneva 27
SWITZERLAND

J. L. Head
Department of Nuclear Science & Technology
Royal Naval College, Greenwich
London SE10 9NN
ENGLAND

W. Hofmann
Division of Biophysics
University of Salzburg
Hellbrunner Str 34
A-5020 Salzburg
AUSTRIA

J. Inaba, Director
Division of Comparative Radiotoxicology
National Institute of Radiological Sciences
9-1, Anagawa-4-chome
Chiba-shi 260
JAPAN

International Atomic Energy Agency
Documents Library
Attn: Mrs. Javor
Kaerntnerring 11
A-1010 Vienna 1
AUSTRIA

E. Iranzo
Jefe, División Protección Radiológica
Junta de Energia Nuclear
Ciudad Universitari
Madrid 3
SPAIN

W. Jacobi
Institut für Strahlenschutz
Post Schleissheim
Ingolstadter Landstrasse 1
D-8042 Neuherberg
GERMANY

K. E. Lennart Johansson
Radiofysiska Inst.
Regionsjukhuset
S-901-82 Umeå
SWEDEN

A. M. Kellerer
Institut für Strahlen biologie, GSF
Ingolstadter Landstrasse 1
D-8042 Neuherberg b. München
GERMANY

T. Kivikas
Studsvik Nuclear
S-611 82 Nyköping
SWEDEN

H.-J. Klimisch
BASF Aktiengesellschaft
Abteilung Toxikologie, Z470
D-6700 Ludwigshafen
GERMANY

H. E. Knoell
Battelle-Institut e.V.
Am Römerhof 35
Postfach 900160
D-6000 Frankfurt am Main 90
GERMANY

Dr. L. Lafuma
Department de Protection Sanitair
Commissariate a l'Energie Atomique
92260 Fontenay-Aux-Roses
FRANCE

J. R. A. Lakey
Department of Nuclear Science & Technology
Royal Naval College
Greenwich Naval College
SW10 9NN
ENGLAND

Li De-Ping, Professor & Director
North China Institute of Radiation Protection, NMI
P.O. Box 120
Tai-yuan, Shan-Xi
PEOPLE'S REPUBLIC OF CHINA

Librarian
Alberta Environmental Centre
Bag 4000
Vegreville, Alberta T9C 1T4
CANADA

Librarian
Centre d'Etudes Nucléaires de Saclay
P.O. Box 2, Saclay
Fig-sur-Yvette (S&O)
FRANCE

Librarian
CSIRO
Division of Wildlife and Ecology
P.O. Box 84
Lyneham, ACT 2602
AUSTRALIA

Librarian
HCS/EHE
World Health Organization
CH-1211 Geneva 27
SWITZERLAND

Librarian
Kernforschungzentrum Karlsruhe
Institut für Strahlenbiologie
Postfach 3640
D-75 Karlsruhe 1
GERMANY

Librarian
Max-Planck Institut für Biophysics
Forstkasstraße
D-6000 Frankfurt/Main
GERMANY

Librarian
Medical Research Council
Radiobiology Unit
Chilton
Oxon OX11 ORD
ENGLAND

Librarian
Ministry of Agriculture, Fisheries & Food
Fisheries Laboratory
Lowestoft, Suffolk NR33 OHT
ENGLAND

Librarian
National Institute of Radiological Sciences
9-1, Anagawa-4-chome
Chiba-shi 260
JAPAN

Library
Atomic Energy Commission of Canada, Ltd.
Whiteshell Nuclear Research Establishment
Pinawa, Manitoba ROE 1L0
CANADA

B. Lindell
National Institute of Radiation Protection
Fack S-104 01
Stockholm 60
SWEDEN

J. R. Maisin
Radiobiology Department
C.E.N. - S.C.K.
Mol
BELGIUM

A. M. Marko
9 Huron Street
Deep River, Ontario KOJ 1PO
CANADA

R. Masse
Institut de Protection et de Sûreté Nucléaire
Département de Protection Sanitaire
Service d'Etudes Appliquées de Protection Sanitaire
BP No. 6
F-92260 Fontenay-aux-Roses
FRANCE

H. Matsudaira,
Director General
National Institute of Radiological Sciences
9-1, Anagawa-4-chome
Chiba-shi 260
JAPAN

O. Matsuoka
Research Consultant
Abiko Research Laboratory
Central Research Institute of Electric Power Industry
1646, Abiko, Abiko City
Chiba-ken 270-11
JAPAN

N. Matsusaka
Department of Veterinary Medicine
Faculty of Agriculture
Iwate University
Ueda, Morioka
Iwate 020
JAPAN

S. Mattsson
Department of Radiation Physics
Malmö General Hopsital
S-214 01 Malmö
SWEDEN

R. G. C. McElroy
Atomic Energy Commission of Canada, Ltd.
Dosimetric Research Branch
Chalk River, Ontario KOJ 1JO
CANADA

F.-I. S. Medina
Cytogenetics Laboratory
Biomedical Research Division
A.R.C.
Philippine Atomic Energy Commission
P.O. Box 932, Manila
THE PHILIPPINES

M. L. Mendelsohn
Radiation Effects Research Foundation
1-8-6 Nakagawa
Nagasaki 850
JAPAN

Meng Zi-Qiang
Department of Environmental Science
Shanxi University
Tai-Yuan, Shan-xi
PEOPLE'S REPUBLIC OF CHINA

P. Metalli
ENEA-PAS
CRE Casaccia
Casella Postale 2400
I-00100 Roma
ITALY

H. J. Metivier
Institut de Protection et de Sûreté Nucléaire
Centre d'Études de Service de Fontenay-aux-Roses
BP 6
F-92265 Fontenay-aux-Roses
FRANCE

A. R. Morgan
Biotechnology
Building 353
AEA Technology
Harwell, Didcot
Oxfordshire OX11 ORA
ENGLAND

Y. I. Moskalev
Institute of Biophysics
Ministry of Public Health
Givopisnaya 46, Moscow
RUSSIA

J. Muller
7 Millgate Crescent
Willowdale, Ontario M2K 1L5
CANADA

J. C. Nénot, Deputy Director
Département de Protection
Centre d' Etudes Nucléaires
BP 6
F-92260 Fontenay-aux-Roses
FRANCE

R. Osborne
Atomic Energy Commission of Canada, Ltd.
Biology and Health Physics Division
Chalk River Nuclear Laboratories
P.O. Box 62
Chalk River, Ontario KOJ 1JO
CANADA

J. Pacha
Silesian Medical School
Fac. of Pharmacy
Ul. Jagiellonska 4
41-200 Sosnowiec
POLAND

H. G. Paretzke
GSF Institut für Strahlenschutz
Ingolstadter Landstraße 1
D-8042 Neuherberg
GERMANY

N. Parmentier
Département de Protection Sanitaire
Centre d'Etudes Nucléaires
BP 6
F-92260 Fontenay-aux-Roses
FRANCE

G. Patrick
Medical Research Council
Radiobiology Unit
Harwell, Didcot
Oxon OX11 ORD
ENGLAND

O. Pavlovski
Institute of Biophysics
Ministry of Public Health
Givopisnaya 46
Moscow D-182
RUSSIA

G. Premazzi
Commission of the European Communities
Joint Research Centre
Ispra Establishment
I-21020 Ispra
ITALY

V. Prodi
Department of Physics
University of Bo!ogna
Via Irnerio 46
I-40126 Bologna
ITALY

O. Ravera
Commission of the European Communities, C.C.R.
I-21020 Ispra (Varese)
ITALY

REP Institutes TNO
TNO Division of Health Research Library
P.O. Box 5815
151 Lange Kleiweg
2280 HV Rijswijk
THE NETHERLANDS

Reports Librarian
Harwell Laboratory,
Building 465
UKAEA
Harwell, Didcot
Oxon OX11 ORB
ENGLAND

P. J. A. Rombout
Inhalation Toxicology Department
National Institute of Public Health and Environmental Protection
P.O. Box 1
NL-3720 BA Bilthoven
THE NETHERLANDS

M. Roy
Institut de Protection et de Sûreté Nucléaire
Département de Protection Sanitaire
Service d'Etudes Appliquées de Protection Sanitaire
BP 6
F-92260 Fontenay-aux-Roses
FRANCE

F. A. Sacherer
PharmaTec
Am Römerhof 35
60486 Frankfurt/M
GERMANY

W. Seelentag, Chief Medical Officer
Radiation Health Unit
World Health Organization
CH-1211 Geneva 27
SWITZERLAND

J. Sinnaeve
Biology, Radiation Protection Medical Research
Commission of the European Communities
200 Rue de la Loi
B-1049 Brussels
BELGIUM

H. Smith
International Commission on Radiological Protection
P.O. Box 35
Didcot
Oxon OX11 ORJ
ENGLAND

J. W. Stather
National Radiological Protection Board
Building 383
Chilton, Didcot
Oxon OX11 ORQ
ENGLAND

M. J. Suess
Regional Officer for Environmental Hazards
World Health Organization
8, Scherfigsvej
DK-2100 Copenhagen
DENMARK

Sun Shi-quan, Head
Radiation-Medicine Department
North China Institute of Radiation Protection, MNI
P.O. Box 120
Tai-yuan, Shan-Xi
PEOPLE'S REPUBLIC OF CHINA

G. Tarroni
EHEA-AMB-BIO-FITS
Viale G. B. Ercolani 8
I-40138 Bologna
ITALY

D. M. Taylor
5 Branwen Close
The Sanctuary
Culverhouse Cross
Cardiff CF5 4NE
ENGLAND

K. H. Tempel
Institut für Pharmakologie,
Toxikologie und Pharmazie
Fachbereich Tiermedizin der
Universität München
Veterinärstraße 13
D-8000 München 22
GERMANY

J. T. Triffitt
MRC Bone Research
Laboratory
Nuffield Orthopaedic Centre
Oxford OX3 7LD
ENGLAND

United Nations Scientific
Committee on the Effects of
Atomic Radiation
Vienna International Center
P.O. Box 500
A-1400 Vienna
AUSTRIA

D. Van As
Atomic Energy Corporation
P.O. Box 582
Pretoria 0001
REPUBLIC OF SOUTH
AFRICA

J. Vennart
Bardon, Ickleton Road,
Wantage
Oxon OX12 9OA
ENGLAND

Vienna International Centre
Library
Gifts and Exchange
P.O. Box 100
A-1400 Vienna
AUSTRIA

V. Velf
Kernforschungzentrum
Karlsruhe
Institut für Genetik und
Toxikologie von Spaltstoffen
Postfach 3640
D-7500 Karlsruhe 1
GERMANY

G. Walinder
Unit of Radiological Oncology
University of Agricultural
Sciences
P.O. Box 7031
S-750 07 Uppsala
SWEDEN

Wang Hengde
North China Institute of
Radiation Protection
P.O. Box 120
Tai-yuan, Shan-Xi
PEOPLE'S REPUBLIC OF
CHINA

Wang Renzhi
Institute of Radiation Medicine
27# Tai Ping Road
Beijing 100850
PEOPLE'S REPUBLIC OF
CHINA

Wang Ruifa, Associate Director
Laboratory of Industrial
Hygiene
Ministry of Public Health
2 Xinkang Street
P.O. Box 8018
Deshengmenwai, Beijing
100088
PEOPLE'S REPUBLIC OF
CHINA

Wang Yibing
North China Institute of
Radiation Protection
P.O. Box 120
Tai-yuan, Shan-Xi
PEOPLE'S REPUBLIC OF
CHINA

Wei Lü-Xin
Laboratory of Industrial Hygiene
Ministry of Public Health
2 Xinkang Street
Deshengmenwai, Beijing
100088
PEOPLE'S REPUBLIC OF CHINA

J. Wells
Radiobiology Laboratory
Radiation Biophysics
Nuclear Electric
Berkeley Nuclear Laboratories
Berkeley
Gloucestershire GL 13 9PB
ENGLAND

B. C. Winkler, Director of Licensing
Raad Op Atomic
Atoomkrag Energy Board
Privaatsk X 256
Pretoria 0001
REPUBLIC OF SOUTH AFRICA

Wu De-Chang
Institute of Radiation Medicine
27# Tai Ping Road
Beijing
PEOPLE'S REPUBLIC OF CHINA

Yao Jiaxiang
Laboratory of Industrial Hygiene
2 Xinkang Street
Deshengmenwai, Beijing
100088
PEOPLE'S REPUBLIC OF CHINA

Kenjiro Yokoro, Director
Research Institute for Nuclear Medicine & Biology
Hiroshima University
Kasumi 1-2-3, Minami-ku
Hiroshima 734
JAPAN

V. Zeleny
Institute of Experimental Biology
and Genetics
Czechoslovak Academy of Sciences
Bidekpvocla 1-83, Prague 4
CZECHOSLOVAKIA

Zhu Zhixian
China Research Institute of Radiation Protection
Ministry of Nuclear Industry
P.O. Box 120
Tai-yuan, Shan-Xi
PEOPLES REPUBLIC OF CHINA

ON-SITE

DOE Richland Operations Office (4)
D. D. Green K8-50
P. W. Kruger K8-50
D. R. Segna K8-50
Public Reading Room A1-65

WSU Tri-Cities University Center
H. R. Gover, Librarian H2-52

Hanford Environmental Health Foundation (3)
S. E. Dietert H2-52
R. L. Kathren H2-52
T. Henn H1-01

Westinghouse Hanford Co.
D. E. Simpson B3-55

Pacific Northwest Laboratory (182)
R. R. Adee P8-13
R. C. Adams K8-09
L. E. Anderson K4-28
R. W. Baalman K1-50 (20)
J. F. Bagley K1-66
W. J. Bair K1-50 (2)
L. A. Braby P8-47
A. L. Brooks P7-53
J. A. Buchanan P7-82
R. L. Buschbom P7-82
T. D. Chikalla P7-75
B. J. Chou K4-10

PNL-9000, Pt. 1
UC-408

J. M. Christensen P7-58 (2)
T. T. Claudson K1-66
J. A. Creim K4-28
F. T. Cross K4-13
G. E. Dagle P7-53
J. R. Decker K4-16
H. S. DeFord K4-16
J. A. Dill K4-16
R. J. Douthart K4-13
S. L. Downs K2-05
R. D. DuBois P8-47
C. G. Edmonds P8-19
C. E. Elderkin K6-11
J. J. Evanoff K6-65
D. R. Fisher K3-53
L. G. Florek K4-16
W. C. Forsythe K4-16
A. F. Fuciarelli P7-56
K. M. Gideon K4-10
R. A. Gies K4-13
A. W. Gieschen K4-16
E. S. Gilbert P7-82
M. F. Gillis K1-50
W. A. Glass K3-53
B. J. Greenspan K4-16
D. K. Hammerberg P8-29
B. K. Hayden K4-16
J. M. Heineman P7-50
L. A. Holmes K1-29
M. G. Horstman K4-10
V. G. Horstman P7-58
T. E. Hui K3-70
A. C. James K3-51
A. E. Jarrell K4-12
J. R. Johnson K3-57
R. F. Jostes K4-13
M. T. Karagianes P7-58
M. Knotek K1-48
E. G. Kuffel K4-16
W. W. Laity K2-50
K. E. Lauhala P7-58
F. C. Leung K4-13
M. K. Lien P8-47
E. K. Ligotke P7-82
C. C. Lumetta P7-58 (5)
J. A. Mahaffey P7-82
D. D. Mahlum P7-56
E. M. Maloney K1-51
D. B. Mann P7-50
T. J. Mast K4-10
J. C. McDonald P7-03
P. W. Mellick K4-10
D. L. Miller P7-53
J. H. Miller P8-47
M. C. Miller P7-41
R. A. Miller K4-10
C. E. Mitchell P7-53
J. E. Morris P7-53
D. A. Nelson P8-38
J. M. Nelson P8-47
J. F. Park P7-52 (20)
M. A. Parkhurst K3-55
R. W. Perkins K6-48
J. T. Pierce K4-10
J. C. Prather K1-85
H. A. Ragan K4-13
R. A. Renne K4-10
D. N. Rommereim P7-55
R. L. Rommereim K4-10
C. O. Romsos K4-10
E. J. Rossignol K4-16
S. E. Rowe K4-13
P. S. Ruemmler K4-10
J. L. Ryan P7-25
L. B. Sasser P7-53
G. F. Schiefelbein P8-38
J. E. Schmaltz K7-22
L. C. Schmid K1-34
R. P. Schneider P7-56
L. E. Sever BSRC
B. D. Shipp K8-28
M. R. Sikov P7-53
E. C. Sisk P7-56
L. G. Smith K4-16
S. K. Smith P7-82
D. L. Springer P7-56
J. G. Stephan K6-84
R. G. Stevens P7-82
D. L. Stewart K6-96
L. C. Stillwell P7-56
G. M. Stokes K1-74
K. L. Swinth K3-53
W. L. Templeton K1-30
T. S. Tenforde K1-50 (10)
G.S. Thomas K7-22
R. M. Thomas P7-53
R. C. Thompson P7-58
B. D. Thrall P7-56
K. D. Thrall K3-57
H. R. Udseth P8-19
B. E. Vaughan K1-66
R. A. Walters K1-50
C. R. Watson P7-82
R. J. Weigel K4-16
R. E. Weller P7-52
R. B. Westerberg K4-16
R. E. Wildung P7-54
W. E. Wilson P8-47
Health Physics Department Library
Life Sciences Library (2)
Publishing Coordination
Technical Report Files (5)

DATE
FILMED
5/12/94
END